

Entwicklung eines physikalischen Modells der im Windpark  
generierten Turbulenz

Development of a physical model for calculation of the turbulence  
inside wind farms

Von der Fakultät für Mathematik und Naturwissenschaften der Carl von Ossietzky  
Universität Oldenburg zur Erlangung des Grades und des Titels eines  
Doktors der Naturwissenschaften (Dr. rer. nat)

angenommene Dissertation

von Herrn Arne Wessel

geboren am 25.06.1975 in Bremen

2

Gutachter Prof. Dr. Joachim Peinke  
Zweitgutachter Prof. Dr. Jürgen Parisi

Tag der Disputation: 27.10.2008

## Acknowledgement/Danksagung

An dieser Stelle möchte ich allen danken die mich bei meiner Doktorarbeit unterstützt haben.

Besonderen Dank gilt meinen beiden Mentoren Prof. Dr. Joachim Peinke und Dr. Bernhard Lange.

Prof. Dr. Joachim Peinke hat mich gelehrt wissenschaftlich zu arbeiten und die auftauchenden Fragestellungen in den physikalischen Kontext einzuordnen.

Dr. Bernhard Lange hat mir die angewandte Seite der Windenergieforschung näher gebracht. Seine Erfahrungen mit dem Themengebieten der Windenergie und Meteorologie brachten mich in Diskussionen immer ein Stück weiter.

Vielen Dank an Prof. Dr. Jürgen Parisi, der mir bei der Struktur der Arbeit erheblich weitergeholfen hat.

Ein großen Dank auch an meinen langjährigen Bürokollegen Jethro Betcke. Es war immer eine Freude mit ihm im selben Zimmer zu sitzen und diverse Fragestellungen physikalischer und weltlicher Art zu diskutieren. Oft half auch eine schnelle Rückmeldung von ihm bei neuen Ideen mich auf den richtigen Weg zu bringen.

Vielen Dank auch an Detlev Heinemann, der mir immer wieder bei Anträgen und internen Fragestellungen weitergeholfen hat.

Danke auch an Abha Sood mit der ich immer wieder einige Fragestellungen diskutieren konnte und die mich in der Zielgeraden unterstützt hat.

Dem gesamten Team von ForWind spreche ich meinen Dank aus, die Atmosphäre war sehr angenehm und ich habe mich immer wieder gefreut dort zu arbeiten.

Einen ganz großen Dank auch an meinen Schwager Christoph Kleefeld, der mich in der englischen Sprache unterstützt hat.

Vielen Dank an meine Eltern die mich immer wieder moralisch unterstützt haben und mir meine Laufbahn als Physiker überhaupt erst ermöglicht haben.

Vielen Dank auch an Katja, die es immer wieder geschafft hat mir auch in Zeiten größter Hektik die innere Ruhe wiederzugeben.

Für die finanzielle Unterstützung möchte ich der Deutschen Bundesstiftung Umwelt (DBU) und der EWE-Stiftung danken. Die DBU hat mich im Rahmen eines Doktorandenstipendiumprogrammes drei Jahre lang gefördert und die EWE-Stiftung hat mich das letzte halbe Jahr in der Zielgeraden unterstützt.

## Zusammenfassung

Für eine bessere Nutzung der Landschaft, eine bessere Anbindung an die Infrastruktur (Anbindung an das elektrische Netz, Zufahrtswege für die Wartung) werden Windkraftanlagen als Windparks gruppiert.

Neben diesen Vorteilen gibt es zwei Nachteile bei der Installation von Windparks: Abschattungseffekte durch die Windkraftanlagen untereinander reduzieren ihre Effizienz und eine verstärkte Turbulenz innerhalb der Windparks, die höhere Lasten an den Windkraftanlagen generiert.

Eine im Wind stehende Windkraftanlage hat einen Bereich im Abwind, den sie abschattet. Dieser Bereich wird als Nachlauf der Windkraftanlage bezeichnet. In dem Nachlauf ist die Windgeschwindigkeit reduziert, was zu niedrigeren Windgeschwindigkeiten an den Windkraftanlagen im Abwind und damit zu einer niedrigeren Leistungsproduktion führt. Im Vergleich zu einer einzeln stehenden Windkraftanlage ist die Effizienz reduziert. Dieser Effekt hängt von einer Reihe von Parametern ab, wobei die Hauptparameter das Layout des Windparks und die Windrichtung sind. In den letzten 25 Jahren wurden große Anstrengungen in der Forschung unternommen um verlässliche Berechnungen zu erstellen um gerade bei der Planungsphase von Windparks bessere Prognosen der Parkeffizienz berechnen zu können.

Im Allgemeinen ist die Turbulenz in der Windströmung innerhalb eines Windparks erhöht. Diese Erhöhung entsteht zum einen durch Turbulenz, die vom Rotor erzeugt wird und zum Anderen durch Windscheerung in der Nachlaufströmung.

Die einfachste Beschreibung der Turbulenz ist die Turbulenzintensität  $I$ , definiert als Standardabweichung der Windgeschwindigkeit  $\sigma$  dividiert durch die mittlere Windgeschwindigkeit  $u$ .

Die Größe Turbulenzintensität wird für unterschiedliche Anwendungen in der Planungsphase von Windparks verwendet, z.B. für die Optimierung des Layout des Windparks, so dass die Sicherheit erhöht und die Lebensdauer verlängert wird indem die Lasten an den Windkraftanlagen reduziert werden. Dies geschieht über die Optimierung der Abstände der Windkraftanlagen in Hinblick auf die Windrichtung und die Windgeschwindigkeitsverteilungen.

Im Rahmen dieser Doktorarbeit wurde eine Methode entwickelt um die Turbulenzintensität innerhalb eines Windparks zu parametrisieren. In der Planungsphase von neuen Projekten erlaubt diese Methode die potentielle Erhöhung der Turbulenzintensität durch die Windkraftanlagen. Diese Methode benutzt nur die typischen zur Verfügung stehenden Eingangsparameter und kommt mit kurzen Rechenzeiten aus, wodurch sie ideal für Gutachter von Windparkprojekten ist.

Der wichtigste Parameter für die Beschreibung der Turbulenz im Windpark ist das Turbulenzintensitätsprofil in der Nachlaufströmung der Windkraftanlage. Dessen Entwicklung mit der Entfernung hinter der Windkraftanlagen ist ein Hauptanliegen dieser Arbeit.

Vor der Untersuchung der Turbulenzintensitätsprofile in der Nachlaufströmung müssen einige Voraussetzungen überprüft werden. Es muss gezeigt werden, dass die Turbulenzintensität ein geeigneter Parameter zur Beschreibung der Turbulenz in der Nachlaufströmung einer Windkraftanlage ist. Deshalb beginnt diese Doktorarbeit mit einer Untersuchung der Turbulenz in der Nachlaufströmung gegenüber der Situation in der freien Strömung. Um sicherzugehen, dass unterschiedliche Messmethoden zu denselben Ergebnissen führen, der Einfluss der Messfrequenz, der gemessenen Windkomponenten, als auch das Entfernen eines linearen Trends werden untersucht. Normalerweise werden die Turbulenzintensitätsprofile aus Mittelwerten der Windgeschwindigkeit und den dazugehörigen Standardabweichungen berechnet. Die Mittelungszeit variiert dabei zwischen ein und zehn Minuten, je nach Messung. Unterschiedliche Mittelungszeiten führen dabei zu unterschiedlichen Turbulenzintensitätsprofilen. Eine Methode um die Turbulenzintensitätsprofile auf eine gemeinsame Mittelungszeit umzurechnen wird vorgestellt.

Eine typische Eigenschaft von Nachlaufströmungen im Allgemeinen ist die Ähnlichkeit von Windgeschwindigkeitsprofilen und Turbulenzintensitätsprofilen bei unterschiedlichen Abständen von dem Objekt. Messungen der Profile in den Nachlaufströmungen von Kugeln und Zylindern zeigen bei großen Distanzen hinter dem Objekt dieselbe Form der Profile für unterschiedliche Distanzen, d.h. die Profile können ineinander überführt werden indem die Höhe und Breite skaliert wird. Die Frage ist dabei, ist diese Ähnlichkeit bei den Nachlaufströmungen von Windkraftanlagen vorhanden und ist es möglich die Turbulenzintensitätsprofile mit einfach bestimmbar Parametern zu skalieren. Diese wurde an Messergebnissen von Windkraftanlagen von zwei unterschiedlichen Windfarmen untersucht. In diesem Zusammenhang war es notwendig eine Methode einzuführen um die Änderung der Form der Turbulenzintensitätsprofile hinter der Windkraftanlage mit zunehmender Distanz zu der Windkraftanlage zu beschreiben.

Basierend auf den durch die Skalierung gewonnen Daten wurde ein Modell entwickelt um die Turbulenzintensitätsprofile zu skalieren. Ein weiteres, bestehendes Modell von Magnusson wurde weiter verbessert, da die resultierende Turbulenzintensität von dem Originalmodell zu schnell mit zunehmender Distanz abnimmt. Beide Modelle (das Alte und das Neue) werden mit Turbulenzintensitätsprofilen von drei Windfarmen validiert und die Verbesserungen diskutiert. Um die Anwendung der Modelle zu zeigen, wurden die Modelle mit den Messungen der Turbulenzintensität von einem kompletten Windpark verglichen.

Bei den Ergebnissen konnte gezeigt werden, dass die Turbulenzintensität als erste Näherung ein adäquater Weg ist um die Stärke der Turbulenz in der Nachlaufströmung zu messen, da die Turbulenz in der Nachlaufströmung ähnliche Strukturen zu der Turbulenz in der freien Strömung aufweist.

Die Wahl der Messfrequenz hat nahezu keinen Einfluss auf die Turbulenzintensitätsprofile. Das Entfernen eines linearen Trends aus den Messdaten zeigt große Auswirkungen bei Mittelungszeiten von 1 Minute. Bei höheren Mittelungszeiten ist der Unterschied ver-

nachlässigbar. Die Verwendung des absoluten Windvektors gegenüber den Schwankungen in Richtung des mittleren Windgeschwindigkeitsvektors, welches der Hauptunterschied zwischen Cup- und Ultraschallanemometer ist, zeigt nur kleine Abweichungen. Signifikante Unterschiede in den gemessenen Werten tauchen bei unterschiedlichen Mittelungszeiten auf, wo die gemessene Turbulenzintensität logarithmisch mit der Mittelungszeit ansteigt. Generell ist es möglich Turbulenzintensitätsprofile zwischen unterschiedlichen Mittelungszeiten zu konvertieren, solange die Mittelungszeit 10 Minuten nicht übersteigt.

Es ist möglich die Windgeschwindigkeitsprofile aus unterschiedlichen Entfernungen hinter der Windkraftanlage von den zwei untersuchten Windparks zu skalieren. Eine als Gaußförmig angenommene Form der Profile stimmt gut mit den Messungen überein. Die Turbulenzintensitätsprofile sind nicht so einfach zu skalieren, denn sie weichen von einer Gaußverteilung bei größeren Distanzen ab und bei näheren Abständen weisen sie ein Plateau in der Mitte des Profiles auf. Unabhängig davon kann die Breite der Profile mit der Breite der Windgeschwindigkeitsprofile skaliert werden und gute Erfahrungen wurden mit der Skalierung der Höhe der Profile mit der Ableitung des Windgeschwindigkeitsprofils gemacht. Die Form der Turbulenzintensitätsprofile kann gut mit der Superposition von zwei Gaußverteilungen beschrieben werden. Vor der Skalierung muß die Umgebungsturbulenzintensität von den Profilen subtrahiert werden.

Basierend auf diesen Resultaten wurde eine Methode entwickelt, die auf dem Modell zur Beschreibung der Windgeschwindigkeitsprofile von Ainslie aufbaut, um die Turbulenzintensitätsprofile zu skalieren und um die Form der Turbulenzintensitätsprofile zu berechnen (Skalierungsmodell). Ein anderer Weg war die Weiterentwicklung des Modells from Magnusson et al.: Dieses Modell wurde mit den Windgeschwindigkeitsprofilen des Ainslie Modells kombiniert und der Einfluss der einzelnen Terme wurde neu formuliert (Scherungsmodell)

Die neuen Methoden wurden mit Erfolg an drei Windfarmen validiert. Sie können die Turbulenzintensität bei unterschiedlichen Abständen und Überlagerungen von Nachlaufströmungen gut beschreiben. Das Modell, das auf dem Skalierungsansatz beruht, tendiert zu einer Unterschätzung der Turbulenzintensitätsprofile, das erweiterte Magnussonmodell zeigt nur eine leichte Unterschätzung. Im Vergleich mit dem kompletten Windpark Middelgrund prognostiziert das Scherungsmodell die Turbulenzintensität an den einzelnen Windkraftanlagen gut. Das Skalierungsmodell tendiert zu einer Unterschätzung der Turbulenzintensitätswerte.

Beide Modelle zeigen gute Ergebnisse, die Genauigkeit der Vorhersage hängt im Allgemeinen von den Windgeschwindigkeitsprofilen ab. Eine verbesserte Berechnung der Windgeschwindigkeitsprofile kann die Genauigkeit der Turbulenzintensitätsprofile erhöhen.

Für die Parametrisierung des Skalierungsmodells werden in Zukunft noch mehr Messungen benötigt. In der Vergangenheit wurden nur wenige Messungen hinter Windkraftanlagen mit unterschiedlichen Abständen veröffentlicht. Hier besteht noch Bedarf.

## Abstract

Wind turbines are concentrated in wind farms for a better utilization of available space as well as joint use of infrastructure elements, like connections to an electrical grid or maintenance roads to the wind turbines.

Apart from these benefits, there are two main disadvantages associated with the installation of wind farms. Shading effects caused by the wind turbines of the wind farm will reduce its efficiency. Also, higher turbulence inside the wind farm will induce higher loads on the wind turbines.

A wind turbine located within the wind flow has a shaded area downwind of the rotor, called wake. In the wake, the wind speed is reduced, resulting in lower wind speeds at the wind turbines further downwind and therefore in a lower power production. Compared to single placed wind turbines, the efficiency is reduced. This effect is depending on a number of parameters, with the main parameters being the layout of the wind farm and the wind direction. For the last 25 years, major research has been undertaken into reliable calculations in support of the planning phase of a wind farm. Different models were developed to calculate the farm effects, most widespread are the models from [Jensen, 1993], [Ainslie, 1988].

In general, the turbulence of the wind flow increases inside a wind farm. This increase is a result of rotor generated turbulence as well as turbulence due to the wind shear in the wake. Especially in offshore wind farms the turbulence plays an important role, because the difference between the turbulence inside and outside of wind farm is higher than in the onshore counterpart.

The simplest description of the turbulence is the turbulence intensity  $I$ , defined as the standard deviation of the wind speed  $\sigma$  divided by the mean wind speed  $u$ .

The value of the turbulence intensity is used for different applications during the planning stage of wind farms, for example:

- Input parameter for models of the mechanical loads at wind turbines - the load models for wind turbines use a generated wind field as input for the load calculations. The turbulence intensity is one of the main input parameters for the wind field calculation.
- The layout of wind farms can be optimized for structural safety and lifetime – in order to reduce the loads at the wind turbines, the distances between the wind turbines can be optimized in respect of the main wind direction and the wind speed distributions.

In the course of this PhD thesis, a method has been developed to parameterize the turbulence intensity inside a wind farm. During the planning stages of new projects, this method allows the calculation of a potential increase in turbulence intensity caused by the wind turbines.

The method depends on typically available parameters and requires only a short calculation time, facilitating its easy use by consultants for wind farm projects.

The crucial parameters for the description of the turbulence in a wind farm, the turbulence intensity profiles in the wake of a wind turbine. Their development with distance behind the wind turbine are the main focus of this work.

Prior to investigating the turbulence intensity profiles in the wake, some preconditions have to be tested. It has to be shown, that turbulence intensity is a suitable parameter for describing the turbulence in the wake of a wind turbine. Therefore this thesis begins with an assessment of the turbulence in the wake compared to free stream situations. In order to ensure that different measurement methods lead to similar results, the influence of sampling frequency, measured wind component as well as possible effects of removing a linear trend from the data are investigated. Usually, turbulence intensity profiles are calculated from average values of mean wind speed and associated standard deviations. Often the averaging times differ, between about one and ten minutes. Varying averaging times lead to differences in the resulting profiles. A way of converting turbulence intensity profiles of different averaging times to a common averaging time basis is presented.

A typical feature of wakes in general is the similarity of the wind speed profiles and the turbulence intensity profiles at different distances from the object. Measurements in the wake at large distances behind spheres and cylinders show the same shape of the profiles, i.e. the profiles can be aligned by scaling only their width and height. The question is, if similarity is present in the wake of wind turbines and if it is possible to scale the turbulence intensity profiles with parameters gained from the wind speed profile. This has been studied at the wakes from wind turbines off two different wind farms. In this context it was necessary to introduce a technique to calculate the change in shape of the turbulence intensity profiles behind the wind turbine with increasing distance to the wind turbine.

Based on the resulting data from the scaling of the measured profiles, a model was developed to describe the turbulence intensity profiles. A recent model from Magnusson was further improved, since the resulting turbulence intensity of the original model declined too fast with increasing distance inside the wake. Both models (the old and the new one) are validated against turbulence intensity profiles from three wind farms and modeling improvements are demonstrated. For application purposes, both models were compared with measurements of turbulence intensity at a complete wind farm.

As results could be shown that the turbulence intensity is as first approximation an adequate way for measuring the amount of turbulence in the wake, as the turbulence in the wake compared to the free stream has similar structures.

Regarding the results, the choice of sampling frequency has nearly no influence on the turbulence intensity profiles. The removing of a linear trend effects the profiles at an averaging time of 1min significant, at higher averaging times the difference is negligible. The use of



the absolute wind speed vector instead of the fluctuations in the directions of the mean wind speed, which is the one of the main differences between cup and ultrasonic anemometer, show only small differences. Significant change in the measured values occur with different averaging times, where the increase in measured turbulence intensity goes logarithmic with increasing averaging time. Generally it is possible to convert the turbulence intensity profiles between different averaging times as long, as the time does not exceed 10 minutes.

It is possible to scale the wind speed profiles from different distances behind the wind turbine from the two investigated wind farms. An assumed Gaussian shape agrees well with the profiles. The turbulence intensity profiles are not simply to scale, because they exhibit a Gaussian profile at further distance and at nearer a plateau in the center of the profile. Nevertheless the width can be scaled with the wake width of the wind speed profiles and good results were estimated in scaling the height of the profiles with the derivation of the wind speed profile at the wake half width. The shape of the turbulence intensity profiles can be described well with the superposition of two Gaussian profiles. Before scaling, the ambient turbulence intensity has to be subtracted from the profiles.

Based on this results a method was developed which base on the model for the wind speed profile developed by Ainslie to scale and calculate the shape of the turbulence intensity profile (Scale model). Following another way, the model from Magnusson et al. was developed further on: It was combined with the wind speed profile from the Ainslie model and the influence of the different terms was formulated different (Shear model).

The new methods were validated with success with three wind farms. They can predict the turbulence intensity at the different distances and in case of multiple wake situations well. The model base on the scaling approach tends to under predict the turbulence intensity profiles, the enhanced Magnusson shows only a slight under prediction. At the comparison with the whole wind farm Middelgrund, the shear model predict the turbulence intensity at the wind turbines well. The scale model tends to too low predicted values of the turbulence intensity.

Both models show good results, the accuracy of the predictions depends i.e. on the wind speed profile. A better calculation of the wind speed profiles can enhance the accuracy of the turbulence intensity profiles.

For the parametrization of the Scale model, more measurements are needed in future. In the past only few measurements behind wind turbines at different distances were published. There is further need.



# Contents

<b>1</b>	<b>Introduction</b>	<b>17</b>
<b>2</b>	<b>Characterization of the turbulence in the wake</b>	<b>21</b>
2.1	Introduction . . . . .	21
2.2	Theory of the flow behind a wind turbine . . . . .	22
2.2.1	General structure of a wake . . . . .	22
2.2.2	Effects of real atmospheric flows . . . . .	24
2.2.3	Definition of turbulence intensity . . . . .	26
2.3	Measurements at the wind farm Elisenhof . . . . .	27
2.3.1	Description of the wind farm . . . . .	27
2.3.2	Measurement instrumentation . . . . .	28
2.4	Measured wake profiles . . . . .	30
2.5	Turbulence spectra in the Wake . . . . .	33
2.5.1	Calculation of Spectra . . . . .	33
2.5.2	Estimated power spectra . . . . .	34
2.6	Increment analysis of the flow in the wake . . . . .	35
2.7	Conclusion . . . . .	38
<b>3</b>	<b>Uncertainties in measuring turbulence intensity profiles</b>	<b>41</b>
3.1	Introduction . . . . .	41
3.2	Vindeby . . . . .	42
3.3	Influence of measuring with cup or ultrasonic anemometer . . . . .	44
3.4	Influence of the sampling frequency . . . . .	46

3.5	Influence of different averaging times . . . . .	47
3.6	Effects of Detrending on turbulence intensity profiles . . . . .	50
3.7	Conclusion . . . . .	52
<b>4</b>	<b>Scaling properties of the turbulence intensity in the wake</b>	<b>55</b>
4.1	Introduction . . . . .	55
4.2	Theory . . . . .	56
4.2.1	Error definition . . . . .	57
4.2.2	Scaling of wind speed profiles . . . . .	57
4.2.3	Scaling of turbulence intensity profiles . . . . .	58
4.2.4	Superposition of wake and ambient turbulence intensity . . . . .	60
4.2.5	Describing turbulence intensity profiles with a double Gaussian function . . . . .	60
4.3	Description of the measurements . . . . .	61
4.3.1	Experimental site Nibe . . . . .	62
4.3.2	Wind Farm Sexbierum . . . . .	63
4.4	Scaling of wind speed profiles . . . . .	65
4.4.1	Wind speed profiles from Nibe wind farm . . . . .	66
4.4.2	Sexbierum wind speed profiles . . . . .	68
4.4.3	Comparing the estimated parameters from both wind farms . . . . .	69
4.4.4	Conclusion . . . . .	71
4.5	Scaling of turbulence intensity profiles . . . . .	71
4.5.1	Nibe wind farm . . . . .	72
4.5.2	Sexbierum wind farm . . . . .	78
4.6	Fit of double Gaussian profile to standard deviation profile . . . . .	80
4.6.1	Nibe wind farm . . . . .	81
4.7	Conclusion . . . . .	83

<i>CONTENTS</i>	13
<b>5 Describing the turbulence intensity in the wake of a wind turbine</b>	<b>85</b>
5.1 Introduction . . . . .	85
5.2 Wind speed wake models . . . . .	86
5.2.1 Analytical model after Magnusson . . . . .	86
5.2.2 Model after Ainslie . . . . .	87
5.2.3 Ainslie in the Farm Layout Program (FLaP) . . . . .	90
5.3 Models of turbulence intensity in the wake . . . . .	90
5.3.1 Quarton formula . . . . .	91
5.3.2 Empirical formula by Crespo . . . . .	91
5.3.3 Approach from Frandsen and Thogersen . . . . .	92
5.3.4 Comparison of Quarton, Crespo and Frandsen model to Nibe measurements . . . . .	93
5.3.5 Magnusson and the dependency on the traveling time . . . . .	94
5.3.6 Calculation of turbulence intensity from the eddy viscosity . . . . .	94
5.4 The Shear-stress model . . . . .	95
5.4.1 Description of the shear-stress model . . . . .	95
5.4.2 Model parameters . . . . .	97
5.5 Scaling approach . . . . .	97
5.5.1 Introduction . . . . .	97
5.5.2 Description of Scaling approach . . . . .	98
5.5.3 Parametrization . . . . .	99
5.6 Superimposition of wakes . . . . .	99
5.7 Conclusion . . . . .	101
<b>6 Verification of models</b>	<b>103</b>
6.1 Introduction . . . . .	103
6.2 Single wake measurements at Nibe wind farm . . . . .	104
6.3 Sexbierum single wake . . . . .	107
6.4 Sexbierum double wake . . . . .	112
6.5 Vindeby double and quintuple wake . . . . .	113
6.6 Conclusion . . . . .	115

<b>7</b>	<b>Application of the model</b>	<b>117</b>
7.1	Description of the wind farm Middelgrund . . . . .	117
7.2	Turbulence intensity estimated from power fluctuations . . . . .	118
7.3	Turbulence intensity from wind turbine measurements . . . . .	119
7.4	Application of the turbulence models to the wind farm Middelgrund . . . . .	121
7.5	Conclusion . . . . .	123
<b>8</b>	<b>Conclusion</b>	<b>125</b>
<b>A</b>	<b>Technical data of the Metek Ultrasonic Anemometer</b>	<b>127</b>
A.1	Offline head correction for Metek anemometers . . . . .	127
<b>B</b>	<b>Conversion of Averaging time</b>	<b>129</b>
<b>C</b>	<b>Calculation of angle to horizontal distance</b>	<b>131</b>
<b>D</b>	<b>Additional information about the wind farms</b>	<b>133</b>
D.1	Elisenhof wind farm . . . . .	134
D.2	Middelgrund . . . . .	136
D.3	Nibe wind farm . . . . .	137
D.4	Sexbierum wind farm . . . . .	139
D.5	Vindeby . . . . .	141
	Bibliography . . . . .	142

## Nomenclature

$c_t$	thrust coefficient
$D$	rotor diameter [m]
$H$	hub height [m]
$h$	height above ground [m]
$I$	turbulence intensity [%]
$k$	turbulent kinetic energy [ $m^2/s^2$ ]
$P$	turbine electrical power [kW]
$R$	rotor radius [m]
$r$	absolut distance from wake centerline [m]
$U$	wind speed component along the undisturbed wind [m/s]
$u$	mean wind speed [m/s]
$u_{cent}$	mean wind speed deficit at the centerline [m/s]
$u'$	fluctuating part of $U$ [m/s]
$u^*$	friction velocity [m/s]
$V$	wind speed perpendicular to the undisturbed wind direction [m/s]
$W$	vertical wind speed component [m/s]
$x$	distance downwind from wind turbine [m]
$x_n$	end of the near wake [m]
$y$	horizontal distance from wind turbine centerline [m]
$z$	vertical distance from wind turbine centerline [m]
$z_0$	roughness length [m]
$\beta$	wake width [m]
$\varepsilon$	eddy viscosity [ $m^2/s$ ]
$\sigma_p$	standard deviation of electrical power [kW]
$\sigma_{u,v,w}$	standard deviation of wind speed in direction of u,v,w [m/s]
$\theta$	wind direction [ $^\circ$ ]

### suffix

amb	ambient / undisturbed conditions
add	additional values due to wake conditions
wake	wake condition
u,v,w	value in the corresponding direction

Symbols marked with a tilde, e.g.  $\tilde{\beta}$ , means that values are normalized. Unless otherwise noted, distances are normalized with the rotor diameter  $D$  and velocities with the ambient wind speed  $u_{amb}$ .





# Chapter 1

## Introduction

Wind turbines are concentrated in wind farms for a better utilization of available space as well as joint use of infrastructure elements, like connections to an electrical grid or maintenance roads to the wind turbines.

Apart from these benefits, there are two main disadvantages associated with the installation of wind farms. Shading effects caused by the wind turbines of the wind farm will reduce its efficiency. Also, higher turbulence inside the wind farm will induce higher loads on the wind turbines.

A wind turbine located within the wind flow has a shaded area downwind of the rotor, called wake. In the wake, the wind speed is reduced, resulting in lower wind speeds at the wind turbines further downwind and therefore in a lower power production. Compared to single placed wind turbines, the efficiency is reduced. This effect is depending on a number of parameters, with the main parameters being the layout of the wind farm and the wind direction. For the last 25 years, major research has been undertaken into reliable calculations in support of the planning phase of a wind farm. Different models were developed to calculate the farm effects, most widespread are the models from [Jensen, 1993], [Ainslie, 1988].

In general, the turbulence of the wind flow increases inside a wind farm. This increase is a result of rotor generated turbulence as well as turbulence due to the wind shear in the wake. Especially in offshore wind farms the turbulence plays an important role, because the difference between the turbulence inside and outside of wind farm is higher than in the onshore counterpart.

The simplest description of the turbulence is the turbulence intensity  $I$ , defined as the standard deviation of the wind speed  $\sigma$  divided by the mean wind speed  $u$ .

The value of the turbulence intensity is used for different applications during the planning stage of wind farms:

- Input parameter for models of the mechanical loads at wind turbines - the load models for wind turbines use a generated wind field as input for the load calculations. The turbulence intensity is one of the main input parameters for the wind field calculation.
- The layout of wind farms can be optimized for structural safety and lifetime – in order to reduce the loads at the wind turbines, the distances between the wind turbines can be optimized in respect of the main wind direction and the wind speed distributions.
- Calculation of increase in turbulence intensity in case of new wind turbines being placed adjacent to already existing ones. – In legal terms, in Germany turbulence can be handled as an imission, that is, the owner of existing wind turbines can indict the owner of newly build wind turbines if the distance between the wind turbines is too small, resulting in a potential decline in equipment lifetime due to the higher impact of turbulence.

In the course of this PhD thesis, a method has been developed to parameterize the turbulence intensity inside a wind farm. During the planning stages of new projects, this method allows the calculation of a potential increase in turbulence intensity caused by the wind turbines. The method depends on typically available parameters and requires only a short calculation time, facilitating its easy use by consultants for wind farm projects.

The crucial parameters for the description of the turbulence in a wind farm are the turbulence intensity profiles in the wake of a wind turbine. Their development with distance behind the wind turbine are the main focus of this work.

Prior to investigating the turbulence intensity profiles in the wake, some preconditions have to be tested. It has to be shown, that turbulence intensity is a suitable parameter for describing the turbulence in the wake of a wind turbine. Therefore this thesis begins with an assessment of the turbulence in the wake compared to free stream situations. In order to ensure that different measurement methods lead to similar results, the influence of sampling frequency, measured wind component as well as possible effects of removing a linear trend from the data are investigated. Usually, turbulence intensity profiles are calculated from average values of mean wind speed and associated standard deviations. Often the averaging times differ, between about one and ten minutes. Varying averaging times lead to differences in the resulting profiles. A way of converting turbulence intensity profiles of different averaging times to a common averaging time basis is presented.

A typical feature of wakes in general is the similarity of the wind speed profiles and the turbulence intensity profiles at different distances from the object. Measurements in the wake at large distances behind spheres and cylinders show the same shape of the profiles, i.e. the profiles can be aligned by scaling only their width and height. The question is, if similarity is present in the wake of wind turbines and if it is possible to scale the turbulence intensity profiles with parameters gained from the wind speed profile. This has been studied

at the wakes from wind turbines off two different wind farms. In this context it was necessary to introduce a technique to calculate the change in shape of the turbulence intensity profiles behind the wind turbine with increasing distance to the wind turbine.

Based on the resulting data from the scaling of the measured profiles, a model was developed to describe the turbulence intensity profiles. A recent model from Magnusson was further improved, since the resulting turbulence intensity of the original model declined too fast with increasing distance inside the wake. Both models (the old and the new one) are validated against turbulence intensity profiles from three wind farms and modeling improvements are demonstrated. For application purposes, both models were compared with measurements of turbulence intensity at a complete wind farm.

The thesis begins with a chapter about the characterization of turbulence in the wake. In the subsequent chapter the influences of measurements on the turbulence intensity profiles is investigated. Afterwards, the similarity of wind speed profiles and the similarity of turbulence intensity profiles have been assessed based on measurement examples from two wind farms. It followed an overview of existing models and a description of the two new models, which have been developed in course of this thesis. The next chapter gives a comparison of the two new models with measurements from three wind farms. In a subsequent chapter, the comparison will be extended to data sets of an entire wind farm. The thesis finishes off with the conclusion.



# Chapter 2

## Characterization of the turbulence in the wake

### 2.1 Introduction

The wind flow over the landscape in the boundary layer is turbulent. Higher turbulence increases the loads on the wind turbines. An increase of turbulence can result for example from a distinct orography or large obstacles. Wind turbines produce additional turbulence in the wake. If wind turbines are placed as a wind farm, often some wind turbines stand in the wake of other turbines, depending on the wind direction. Wind turbines in wind farms experience a higher turbulence than individual placed wind turbines and therefore higher loads. The load depends on the amount and the frequency of turbulent imission. The object is to orient the wind turbines in a wind farm optimal in respect to the load situation induced by the wakes. Influencing parameters are the probability of wind direction and wind speed, the distance between the wind turbines and the heights. In the scope of this thesis an approach was developed in chapter 5 to estimate the amount of turbulence at the wind turbines in a wind farm.

Turbulence is a complex phenomena. A quantity is needed, which reduces the turbulence to a measurable and comparable value. Therefore the parameter turbulence intensity is used. The turbulence intensity is defined by the fraction of the standard deviation of the wind speed  $\sigma_u$  and the mean wind speed  $u$ , i.e.  $I = \sigma_u/u$ . The standard deviation is a measure for the amount of turbulence in a stream, which is normalized with the wind speed.

The disadvantage of the turbulence intensity is that this quantity is non-ambiguous for different kind of turbulence, e.g. a sinus signal can result in the same turbulence intensity value as atmospheric turbulence. No statement can be made with the turbulence intensity concerning the different scales present in the flow, i.e. the amount of turbulence at different frequencies. To make sure that the loads at the wind turbines, created by turbulence, depend not on the

source of turbulence, i.e. the incoming free stream or wake flow, but only on the amount of turbulence intensity, the atmospheric flow in- and outside the wake is compared. Therefore high resolution time series of wind speed from a meteorological mast at the wind farm Elisenhof were measured. The measurements include free stream and wake conditions, as well. The power density spectra and the wind speed increments from both situation are compared if they show the same type of turbulence and which effects occur through the influence of the wind turbine.

The aim of this chapter is to give an introduction over the flow in the wake of a wind turbine and a preliminary investigation of the wake flow. It should be clarified if the turbulence intensity can be used as sufficient measure for turbulence in a stream in respect of the loads at wind turbines. Therefore the influence of the wind turbine on the energy spectra and the wind speed increments is investigated at the example of the wake flow of a single wind turbine.

The chapter begins with a description of the flow in the wake of a wind turbine, the effects of the ambient wind flow on the wind turbine and the definition of the turbulence intensity. Afterwards, measurements at the wind farm Elisenhof are described briefly. The wind speed and turbulence intensity profiles of the wake are investigated, followed by the power density spectra and the increment analysis for free stream and wake situations. The chapter finishes off with the conclusion.

## 2.2 Theory of the flow behind a wind turbine

### 2.2.1 General structure of a wake

Energy is taken from the incoming flow by the rotor and transformed to electric energy by the generator. This results in a momentum deficit behind the rotor and therefore a reduction in wind speed and a drop in pressure. Energy is reintroduced to the wake flow from the surrounding flow, the wake flow try to regain equilibrium with the surrounding flow, the wake develops. According to [Vermeulen, 1980], the wake can be split in three different regions: initial (near wake), transition (intermediate wake) and fully-developed region (far wake) (see fig. 2.1).

Due to the extraction of power from the flow, a force is induced on the rotor. This drag force on the rotor is called "thrust". A drag coefficient  $c_t$  can be defined, which is the ratio between the momentum acting on the rotor and the total momentum in the wind. It can be expressed with the drag force, resulting in the following equation [Sforza et al., 1979]:

$$c_t = \frac{\text{momentum force on the rotor}}{\text{max. momentum in wind}} = \frac{mv}{\rho t \frac{\pi}{4} D^2 u_{amb}^2} = \frac{2F_t}{\rho \frac{\pi}{4} D^2 u_{amb}^2}, \quad (2.1)$$

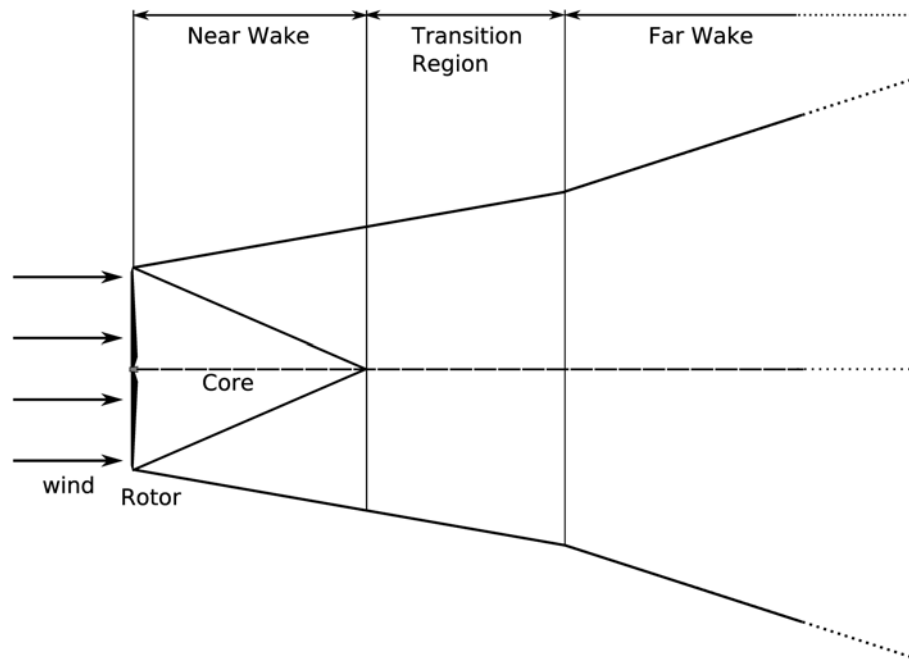


Figure 2.1: Schematic geometry of the wake. The widening of the wake border has been exaggerated for clarity [Vermeulen, 1980].

with the thrust force  $F_t$ , the density of air  $\rho$ , the rotor diameter  $D$  and the mean ambient wind speed  $u_{amb}$ . The thrust coefficient can be directly related to the deficit in momentum caused by the rotor. Therefore, the coefficient determines the initial conditions of the wake. The momentum is conserved and affects so the complete structure of the wind speed profile in the wake.

Directly behind the rotor a low speed region exists, where the flow can be assumed to have a constant velocity over the wake area [Vermeulen, 1980]. For a high efficiency of the wind turbine, the energy extraction is nearly homogeneous over the rotor area. This results in a constant deficit in momentum and therefore a region of a constant velocity deficit of the stationary wind profile. This region of constant velocity directly behind the rotor is called the inner core. The difference between the low wind speed in the inner core and the higher ambient wind speed lead to the development of a shear layer. The inner core fades away with increasing distance due to turbulence mixing from the shear layer. Direct behind the rotor the pressure drops down. The region from the rotor to the point where the inner core is faded away and the pressure regained equilibrium is called the near wake region and is up to a distance of about 2-3  $D$  (rotor diameter) behind the wind turbine.

In the intermediate region the wake is still growing with increasing distance by turbulent mixing at the edge. The stationary wake profile changes its shape from the profile with a plateau in the middle to a shape, which is often assumed to be a gaussian distribution

[Waldl, 1997].

In the far wake a wind speed deficit profile has developed, which shows self-similarity, e.g. the cross stream profiles show the same shape at different stream wise locations, but its width and velocity deficit vary.

In the core region the vortex produced by the rotor dominates the production of turbulence. In the far wake region turbulent mixing occurs at positions with local mean flow instabilities, mainly at positions near high shear in the mean wind speed profile. On the other hand, the turbulence mixing reduces the mean shear by mean momentum transfer. In situations of higher ambient turbulence intensity, the regaining of the equilibrium is expected to be faster. Higher mixing occurs and more exchange in momentum between wake and ambient flow occurs, the wake width increases faster with increasing distance than in situations with lower ambient turbulence intensity. This results in lower wind speed deficits in the wake. Medici [Medici, 2004] observed this phenomenon at wind tunnel measurements behind a small two bladed wind turbine. The turbulent velocities are small compared to the mean velocity and therefore transverse transfer of stream wise mean momentum is slow. The transport of turbulence downstream is therefore much faster than the development of the mean velocity profile sideways.

In the far wake, the shear stress can be related to the derivation of the wind speed profile as done by the one equation closure of the Reynolds equation. If the shear stress is assumed to be a measure of turbulence in the wake, the turbulence is directly related to the shape of the wind speed profile in the wake. With a proportional factor, the eddy viscosity  $\varepsilon$ , the relation can be formulated as:

$$-\overline{u'v'} = \varepsilon \frac{\partial u}{\partial r}. \quad (2.2)$$

In the equation is  $u$  the mean wind speed,  $u', v'$  are the fluctuations of wind speed in direction of  $u$  and perpendicular to  $u$ , assuming a rotational symmetric coordinate system. The distance from the wake centerline is expressed by  $r$  normalized by the rotor diameter.

The tips of the rotor produce small vortices. These are generated by the pressure difference between under and above the wing. At the tip, the pressure differences compensates over the edge of the tip and forming vortices with a low pressure region inside, which are moving downstream along the flow. The vortices are not very stable, so they are dissolved at a distance of about 3 to 4 rotor diameter as shown in CFD simulations by [Troldborg et al., 2006].

## 2.2.2 Effects of real atmospheric flows

In real atmospheric flows many different effects determine the wake of a wind turbine. In Fig. 2.2 a selection of different effects is shown: The condition of the incoming flow with the wind profile due to the influence of the boundary layer, the effects of terrain and density.



Downstream of the wind turbine the influence on the ambient flow from the rotor and tower generated wake is shown.

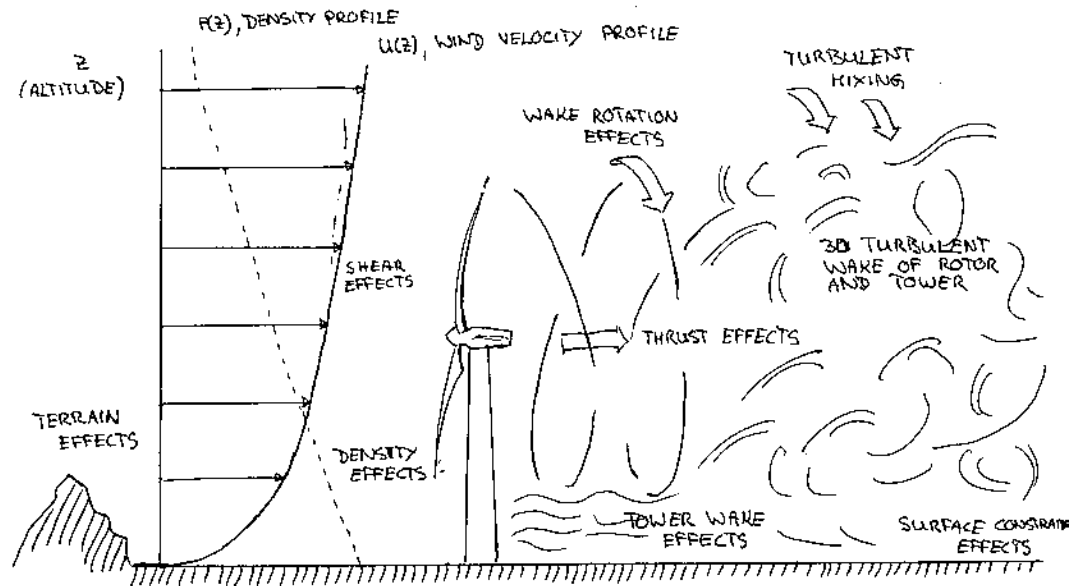


Figure 2.2: Wind effects on a wind turbine in ambient conditions. Redrawn from [Sforza et al., 1979]

The higher complexity starts with the ambient conditions for the wind turbine. Due to the atmospheric boundary layer, i.e. the interaction between the wind flow and the ground, the wind speed in the lower atmosphere has a vertical wind speed profile with low wind speed at the ground and higher wind speeds with increasing heights. In a neutral stratification, the profile can be assumed to be logarithmic and depends mainly on the roughness of the landscape. Including other thermal stratifications, the profile changes to a logarithmic linear wind profile. The vertical wind profile leads to different wind speeds over the rotor area, expressing as wind shear on the rotor. The incoming wind speed is often referred to the wind speed at hub height.

The same incoming wind speed at hub height might result from different vertical wind speed profiles, depending strongly on the wind profile and therefore on the roughness of the landscape and the thermal stratification. Therefore the mean wind speed has only a limited informational value about the wind speed distribution over the rotor area.

Behind the rotor in the wake of the wind turbine the wind profile continues and adds to the wake profile created by the rotor.

Depending on the terrain the turbulence changes: In a more complex landscape, the gradient of the vertical wind speed profile is larger, the wind shear increases. This results in a higher turbulence. The higher turbulence changes the power curve and, as already referred in the previous section, to a different development of the wake structure.

The density of air is related to the pressure and temperature in the atmosphere. Due to the changing ambient conditions the density changes with height and time. The air density influences the power production of the wind turbine, e.g. a higher density results in a higher power production at the same incoming wind speed.

The listed effects influences directly the rotor and therefore indirectly the structure of the wake. For simplicity, in many turbulence intensity models the parameters are reduced on the wind speed, the roughness and the ambient turbulence intensity.

Behind the wind turbine, the rotor and the tower of the wind turbine produce the wake structure. Beneath the already described development of the wake structure, the continues change in wind direction and in wind speed over time leads to a constant change of the wake structure. Due to the changes in wind direction, the wind speed profile in the wake moves with the wind direction changes and meanders. For a fixed point behind the wind turbine this meandering results in a change in wind speed and can have similar effects as turbulence on the downwind turbines.

Beneath the effects of the logarithmic wind profile and the meandering on the wake of a wind turbine, the nacelle and the tower produce their own wakes which contribute to the wake of the wind turbine. wind speed even turbulence intensity can be assumed to be axis symmetric in the wake. Additionally, from the torque produced by the rotor a rotation of the whole wake structure around the centerline results.

### 2.2.3 Definition of turbulence intensity

The amount of turbulence in a flow can be expressed by the value turbulence intensity  $I$ . It is defined as the standard deviation of the wind speed  $\sigma$  divided through the mean wind speed  $u$ .

$$I_i = \frac{\sigma_i}{u} \quad (2.3)$$

Where  $i$  stands for the spatial component  $i = x, y, z$  of the wind speed vector and  $u$  for the magnitude of mean wind speed in the mean wind direction. In the following only the longitudinal component  $i=x$  is used, i.e. the turbulence of the component in the mean wind direction.

The averaging time is normally ten minutes, but deviates sometimes, when for example more samples are needed and the time of the measurement campaign was restricted, shorter averaging times of 1min or 3min were used.

The standard deviation of wind speed can be normalized in two different ways resulting in two definitions of the turbulence intensity. It is possible to normalize the standard deviation of the wind speed with the wind speed locally measured at the same point or using the ambient wind speed  $u_{amb}$ . The standard deviation of wind speed has to be seen in relation to the wind speed, where these fluctuations occur, to judge the effects on the loads of the wind

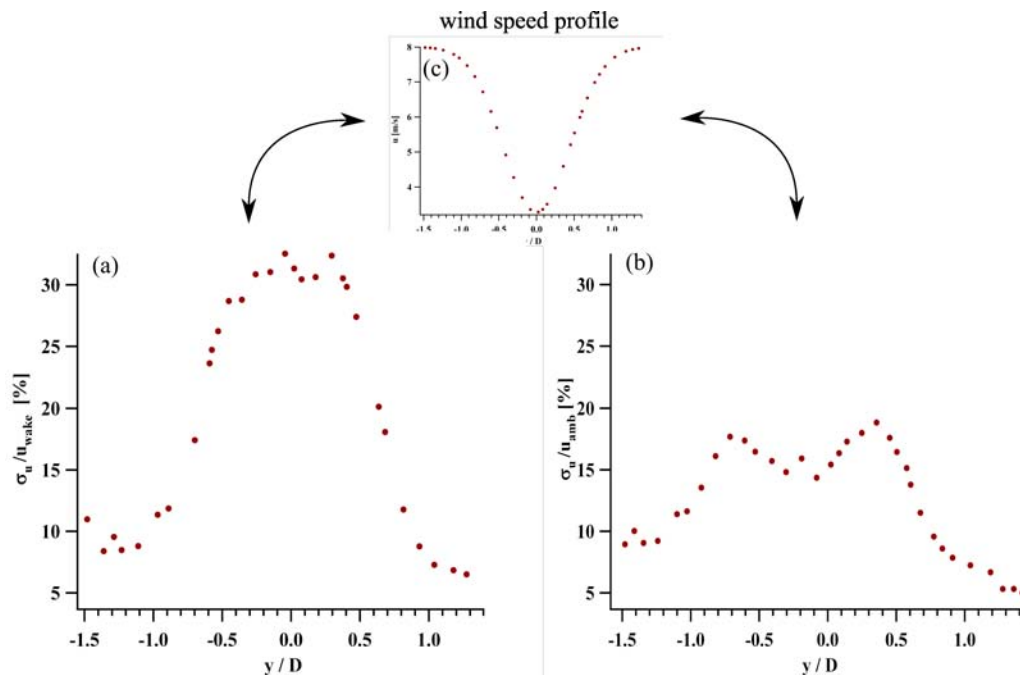


Figure 2.3: Interrelation between the two definitions of turbulence intensity: Turbulence intensity normalized with wind speed in the wake (a) and normalized with the ambient wind speed (b). Both definitions are related with each other by the wind speed profile in the wake (c).

turbine. Therefore in this thesis the normalization with the mean wind speed, measured at the same point as the standard deviation of the wind speed  $I = \sigma_u / u_{wake}$ , is used in the following.

In fig. 2.3 the interrelation between the turbulence intensity profiles in the wake of a wind turbine resulting from the two different ways of normalization. They are related over the wind speed profile in the wake. The profile normalized with ambient wind speed shows a wide double peak structure, whereas the turbulence intensity profile has a plateau in the middle.

## 2.3 Measurements at the wind farm Elisenhof

### 2.3.1 Description of the wind farm

The wind farm area Sintfeld consists of four wind farms: Elisenhof, Eilerberg (Helmern), Meerhof and Wohlbedacht. It consists of 43 wind turbines. At the western end of this area near the wind farm Elisenhof the University of Oldenburg operated a meteorological mast near an Enercon E-66 wind turbine. The layout of the wind turbines can be seen in fig. D.2 in the appendix.

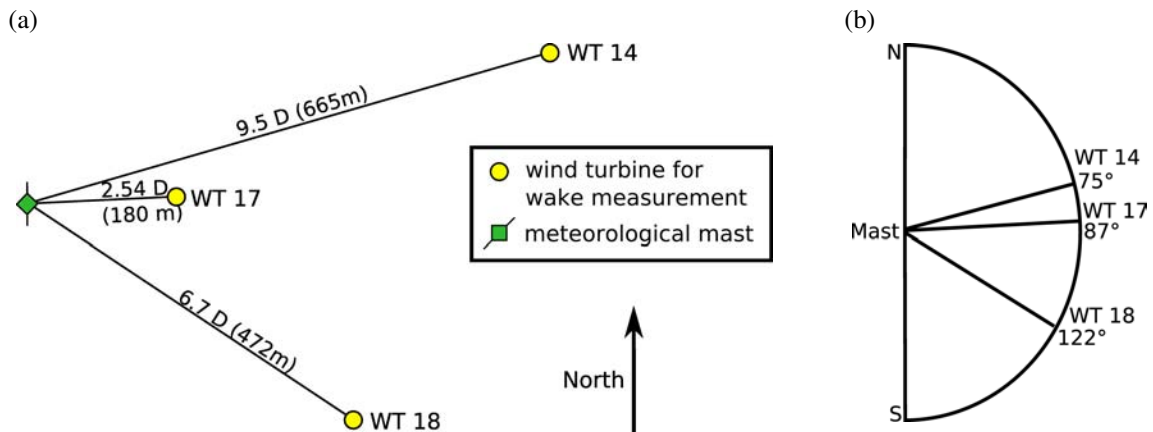


Figure 2.4: Map of the meteorological mast together with the three nearest wind turbines(a) and directions of the wind turbines relative to the mast(b).

The wind farm is sited in farm land south of Paderborn near a small village called Meerhof. It spreads over an area of about  $5\text{km}^2$ . In the North-South direction the dimension is about 1.75 km and in West-East direction of 2.75 km.

The investigated Enercon wind turbine WT 17 has a rotor diameter of  $D = 70\text{m}$  at a hub height of  $H = 98\text{m}$ . Power production from the wind turbine was logged with a sampling frequency of 1 Hz. Power and thrust curve can be found in the appendix D.1.

### 2.3.2 Measurement instrumentation

A meteorological mast was placed 2.54 D to the west of the Enercon wind turbine, which can be seen in Fig. 2.4. The mast was extensively equipped with two ultrasonic anemometers (from Metek and Gill) at nearly hub height (95m) and one from Metek at 65m. Cup anemometers were mounted at the heights 12m, 35m, 50m, 63m, 80.5 and 98m and wind vanes at the heights of 10m, 35m, 61m and 98m. The sampling frequency of the ultrasonic anemometer was 50Hz, all other devices worked with a sampling frequency of 1Hz. The measurements were stored as raw time series data. For a sketch of the meteorological mast see fig. D.1 in the appendix D.1.

Data was collected without interruption from Oktober 1995 to April 1996. Time series of simple wake situations were used to analyze the properties of the turbulence in the wake of the wind turbine 17.

For the current work the ultrasonic anemometer from Metek at hub height was used. Due to a software error, one horizontal wind speed component was missing in the data set of the Gill anemometer. For data validation the cup anemometer at the height of 63m was used,

as no calibration was available for the cup anemometer in 98m. The wind vane at 61m has a wrong calibration and a misalignment, data from the wind vane in a height of 35m were taken.

The ultrasonic anemometer at hub height was validated with the wind speed measurements from the cup anemometer at a height of 63m and the wind direction with the wind vane at 35m. Measurements of mean wind speed and wind direction were compared and show a linear dependency. Wind direction depending profiles of mean wind speed and standard deviation of wind speed show similar structures from cup and ultrasonic anemometers.

The booms at hub height were aligned in North-South direction. The Metek was mounted at the northern boom at a distance of 2.2m from the mast. The mast diameter at this height is approximately 0.2m. This results in a distance of 11D between mast and ultrasonic anemometer. The cup anemometer at the height of 63m was mounted on a boom in the direction of  $330^\circ$  at a distance of 2m (10D). Only small influences of the mast on the wind speed measurements at wind direction from and towards the wind turbine are expected.

One wake situation is investigated with the meteorological mast in particular: From Enercon E-66 wind turbine 17 with a distance of 2.54D (180m) in a direction of  $87^\circ$  see Fig. 2.4. Two additional wind turbines, WT 18 at 6.7D (472m) in direction of  $122^\circ$  and WT 14 in the direction of  $75^\circ$  at a distance of 9.5D (665m), are sited upwind of wind turbine 17. Nearly no data is available from the wind direction of the wind turbine 14, whereas a wind speed reduction was measured from WT 17. Upwind from these wind turbines the complete wind farm is sited and might have additional influence on the wakes.

### **Calibration of the ultrasonic anemometer**

The Metek ultrasonic anemometer consists of a center post surrounded by the three transponder pairs (see Fig. 2.5). The measured data was corrected for 2-dimensional flows, supplied by the manufacturer (see ref [Met, 2004]). According to the manufacturer a 3-dimensional correction algorithm should only be applied for a vertical wind speed component with wind speeds higher than 10 % from the mean flow, which was not the case.

The ultrasonic anemometer measures provides wind speeds in a stationary rectangular coordinate system. The components X,Y,Z for the North-South, East-West and the vertical component are used. To receive information about the components relative to the main wind direction and therefore a frame of reference is introduced, which is always in the mean wind direction. The new wind speed components are U,V,W (with  $U = u + u'$ ,  $V = v + v'$ , where  $u,v$  are mean values and  $u',v'$  the fluctuating parts) with  $u$  along the mean wind direction in horizontal and the assumption that the horizontal perpendicular component  $v$  is zero in the mean:  $v = 0$ . For the vertical component  $w$  it was assumed that  $w = 0$ . A right handed frame of reference was used. The mean values were estimated for an averaging time of 1 min and 10 min.



Figure 2.5: Photograph of a Metek ultrasonic anemometer.

## 2.4 Measured wake profiles

A first sight on the structure of the wake of a wind turbine can be done by looking at the wind speed profiles and the turbulence intensity profiles at different ambient wind speeds.

The ambient wind speed was estimated from the power measurements at the wind turbine 17 and converted to wind speed with the inverse power curve  $u(P)$  from the Enercon E-66. The power curve from the manufacturer (taken from the database in the software WindPro [Energi- Og Miljødata (EMD), 2004]) was used to estimate the wind speed at the wind turbine (see App. D.1).

The wake profiles for wind turbine 17 were calculated by bin-averaging the time series of the mean values for a wind direction range with steps of  $3^\circ$  and for the wind speed ranges with a bin size of 2 m/s. The averaging time used for this purpose was set to 1min. Due to the small amount of data, the 1min averages guaranteed at least 40 data points per bin and 400 at maximum.

Figure 2.6(a) shows the normalized wind speed  $\tilde{u} = u/u_{amb}$  of the ultrasonic anemometer as a function of wind direction measured in the wake. The error bars mark one standard deviation of the values averaged of each bin. The wind speed classes are between 5 m/s and 11 m/s.

Two wake structures can be seen: the wake of wind turbine 17 in a wind direction range of 57 to 108 degrees in a distance of  $2.54D$  to the ultrasonic anemometer and the wake structure from the wind turbine 18,  $6.7 D$  away from the ultrasonic anemometer, in a wind direction between 108 and 129 degree. Effects from the wind turbine 14 can not be observed. The wind turbine 15 is placed at a distance of  $11.4 D$  in line with the measurement mast and wind turbine 17, upwind from wind turbine 17 (see map D.2). At distances of about  $12 D$ , the wind speed deficit from the turbine should be negligible, but the turbulence from

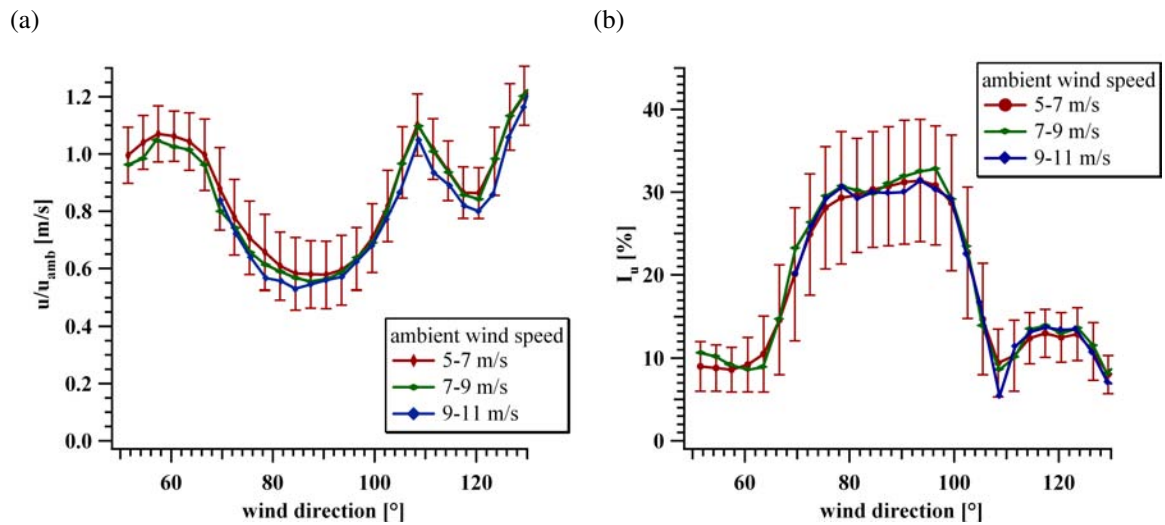


Figure 2.6: Normalized wind speed (a) and turbulence intensity (b) as function of the wind direction in the wake.

the wind turbine is still present, but with very low values, as observed by Hogström et. al [Högström et al., 1988]. So it might affect wind turbine 17 with a higher ambient turbulence intensity.

The figure shows that the profiles of normalized wind speed  $\tilde{u}$  are almost equal in shape for the depicted wind speed classes. This can be explained by the fact that the thrust coefficient varies only by about 12% in this range, which is responsible for the wind speed profile in the wake as explained in section 2.2.1.

The wind speed in the wake centerline reaches a minimum of about 0.53. At the margin of the wake, values larger than unity were measured. Upwind from the wind turbine 17, more wind turbines were sited, which affect the wind measurements of wind turbine 17, but have no influence on the measurement at the meteorological mast. For example at a wind direction of 60°, the wind turbine 17 is biased by the wake of wind turbine 14, whereas the measurement mast is in free stream conditions. This results in a measurement of a lower ambient wind speed by the wind turbine than by the meteorological mast and therefore normalized wind speed outside the wake larger than unity.

The profile of the normalized wind speed reminds more to a mirrored parabola. This is the result of the measurement in the transition zone of the wake, where the change of the profile with constant wind speed to the Gaussian profile occurs, as described in section 2.2.1.

Figure 2.6(b) shows the turbulence intensity of the horizontal wind component in direction of  $u$ . For the wind speed class 9 to 11 m/s insufficient number of data points were available for the wind direction below 70°, so the wake at this wind speed bin is incomplete. The turbulence intensity increases towards the center of the wake at 86°. There, the turbulence is

at a maximum:  $I \approx 32\%$ , compared with an undisturbed value of  $I_{amb} \approx 10\%$ . The profiles show a plateau in the center for wind directions between 75 and 100 degree. This is usually observed at wake measurements in the transition area of the wake (see chapter 4).

Additionally the correlation term between  $u$  and  $v$  in the horizontal plane  $\overline{u'v'}$  also called the shear was calculated for different wind directions.

In fig. 2.7 the wake profile of the shear stress can be seen. According to the relation 2.2 the derivation of the wind speed profile was added. The shear stress profile shows the typical structure with a minimum and a maximum as observed in previous measurements at Sexbierum wind farm [Clijne, 1993]. The derivation of the wind speed profile has the same shape as the shear stress profile, but the minimum and the maximum are narrower.

The closure assume a stationary profiles where the Reynolds stress is proportional to the derivation of the wind speed profile. It assumes that the shear created by the wind speed profile is directly transferred to the shear stress. The real situation is non stationary, meaning the shear from the mean wind speed profiles creates the shear stress. This process can assumed to be successive: A wind speed profile at a certain distance behind the wind turbine affects the shear stress profile at a larger distance. Therefore measuring wind speed profile and shear stress profile at the same distance behind the wind turbine might result in a narrower shear stress profile than the wind speed profile, because it is related to a mean wind speed profile upwind from the measurement site.

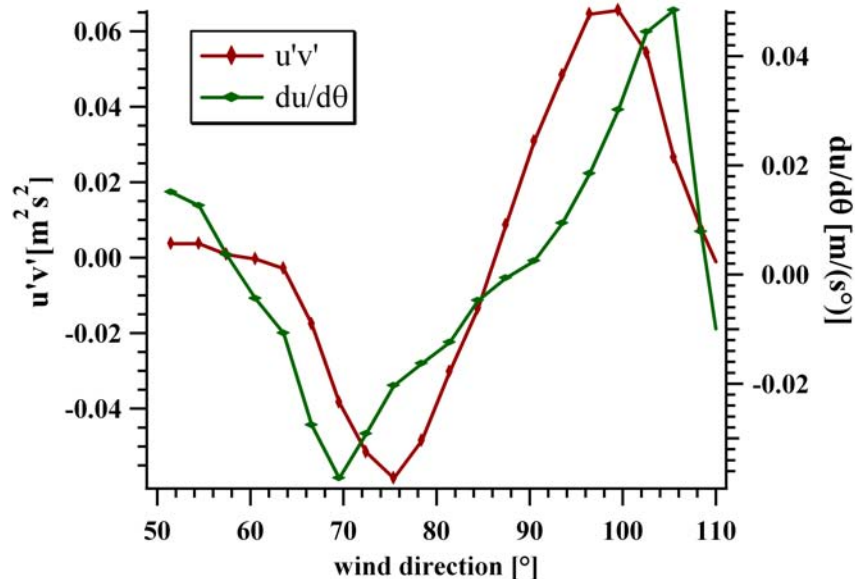


Figure 2.7: Profile of shear stress and derivation of the wind speed profile against the wind direction, measured at the wake situation of the wind farm Elisenhof.



## 2.5 Turbulence spectra in the Wake

As previously remarked, different type of signals can results in the same values of standard deviation. To compare the turbulence intensity values in and outside the wake, the signals of both situations should show similar structures and not be completely different. The power density spectrum provide a practicable way to compare the structures of the wind speed time series of both situations.

Turbulence in the atmosphere occurs at different length scales. Comparing the wake situation to the free stream conditions, additional turbulence is generated by the wind turbine and by the wind shear in the wake. The power density spectra  $S(n)$ , in the dependence of the frequency  $n$  and calculated according to Bendat and Piersol [Bendat and Piersol, 1971], is used to compare the processes in the wake with the free stream.

The standard deviation of the wind speed can be expressed with the integral over the power density spectrum:

$$\sigma_u^2 = \int_0^{\infty} S(n)dn \quad (2.4)$$

By that the turbulence intensity is directly related to the power density spectra.

### 2.5.1 Calculation of Spectra

High resolution data from the ultrasonic anemometer at hub height were taken to calculate the power density spectra  $S(n)$ .

Before the Fourier transformation, the time segment was tapered with a Cosine taper, so that the start and the end of the time series trend to zero. The taper was used at the first and last ten percent of the time series. For a block length of 10 min,  $N=32768$  points were used for the Fourier transformation. The resulting spectrum was divided in 39 frequency bands with a nearly logarithmic spacing, ranging from 0.0015 Hz to 23.4 Hz. The values from the spectra were averaged for each frequency band, also called frequency smoothing [Kaimal and Finnigan, 1994]. The result are 39 values of power density, each for one frequency band.

For the graphical representation, composite spectra from several measurement blocks were used. In this way, measurements uncertainties can be reduced. Therefore the spectra were bin averaged for a free wind situation in the wind direction of  $220^\circ - 240^\circ$  and a wake situations of  $74^\circ - 94^\circ$  for an incoming wind speed of 5–7 m/s measured at the ultrasonic anemometer.

Before averaging the spectra  $S$  were multiplied with the frequency  $n$  to archive  $nS(n)$ , which is of the same dimension of the standard deviation  $\sigma_{u,v,w}^2$ .

## 2.5.2 Estimated power spectra

Power spectra at hub height measured at free stream and wake conditions are shown in Fig. 2.8(a) and Fig. 2.8(b), for the  $u$  and  $w$  component of the wind speed respectively. The  $v$ -component is not plotted, as it differs not significantly from the spectrum of the  $u$ -component.

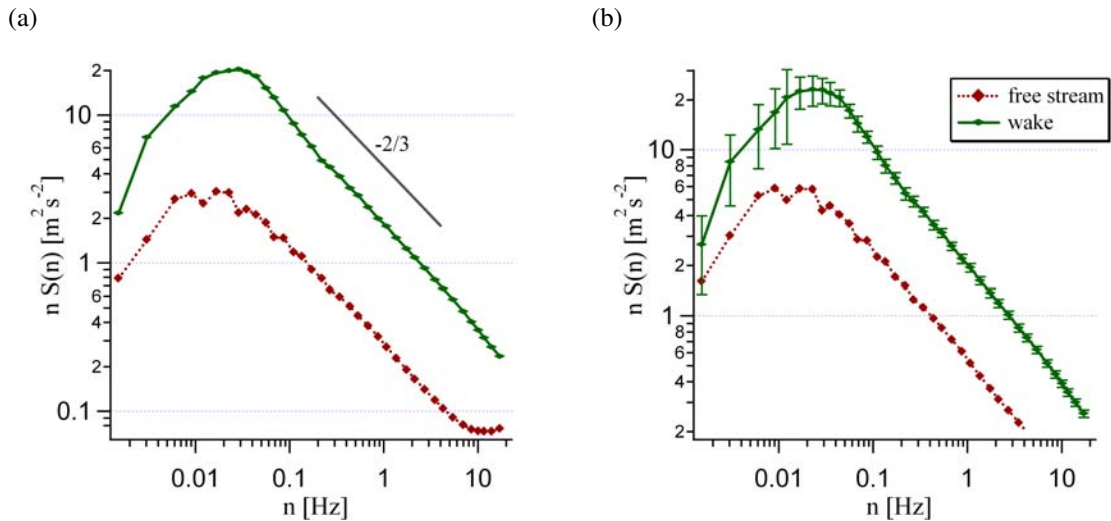


Figure 2.8: Turbulence spectra at hub height in wake condition and free stream situation for the wind speed component  $u$  (a) and  $w$  (b).

The wake spectra show a similar broad band form to the free stream curve, but shifted to higher values of energy over the complete frequency range. This is related to the higher production of turbulent kinetic energy, which also can be seen by the higher turbulence intensity in the wake. Based on equation (2.4), the standard deviation relates to the integral over the spectra.

The peaks of the spectra from the wake situations are slightly shifted to higher frequencies against the ones from free stream situations. The wind turbine is assumed to produce additional turbulence by shear in the wake and shed the ambient turbulence to smaller eddies. As a result, the energy peak is shifted to higher frequencies.

This might result from the decomposing of larger eddies to smaller ones by the rotor resulting in a shift of the peak in the spectra.

At high frequencies, turbulence spectra show a cascade in the decrease in energy from lower to higher frequencies. The larger swirling eddies decompose to smaller eddies until they dissipate into heat. This process is represented by a potential law with the exponent of  $-2/3$ . The free stream and wake conditions show the same  $n \cdot S(n) \propto n^{-2/3}$  behavior at a frequency higher than 0.04 Hz, indicating a well developed inertial subrange. The cascade process is

working the same way in atmospheric as in wake conditions. The slope of both situations (u-component, fit range 0.2 ... 5.47 Hz) is the same with a value of 0.61 ( $-2/3 \sim 0.66$ ).

The free stream spectrum of the w-component has higher energy values than the u-component. The shape of the spectrum in the wake for all components are very similar, which shows that the flow is more similar in the wake. Due to the rotor and the wind shear in the wake, higher mixing occurs, which can result in a more isotropic flow inside the wake than in free stream conditions.

The spectra from free stream conditions behave unusual at high frequencies, they rise again at the end of the spectra. This effect can result from the noise created by the ultrasonic anemometer [Kaimal and Finnigan, 1994]. The ambient wind speed has lower fluctuations than the fluctuations in the wake. When the signal drops below the noise threshold, high frequency distortions are produced.

In Fig. 2.8(a) can be seen, that the increased turbulence in the wake leads to a shift of the complete spectra to higher energies. Beneath this increase in energy of the whole spectra, at certain frequencies an additional displacement of the energies occur. To investigate this effect, both spectra were normalized with the standard deviation of the wind speed and the difference is calculated (see Fig. 2.9). In that way the effects of the wake on the different frequencies of the spectra become visible. At lower energies the difference becomes negative, so the energy in the lower frequencies of the normalized wake spectra is lower than the spectra from the free stream situation with a minimum at 0.006 Hz. This corresponds to a scale of 1000m at an assumed mean wind speed of 6 m/s. At higher frequencies of 0.01 Hz to 0.17 Hz (600m to 35m at a wind speed of 6m/s) the normalized wake spectra shows an increase in energy. The maxima is at 0.03 Hz, which corresponds to a scale of 200m. Due to the larger measurement error in the spectra, as can be seen in Fig. 2.8(b), this values are only a rough estimate and can easily vary around a hundred meters.

## 2.6 Increment analysis of the flow in the wake

The power density spectra shows a change in turbulence inside the wake, the peak moving towards the higher frequencies. With the help of the increment analysis additional characterizations over the wind speed fluctuations at different scales can be gained.

The increments of the wind speed are the difference of the velocities at different locations measured at the same time. If the locations are closer together, smaller eddies are resolved, if they are further apart the focus lies on the larger eddies. Due to the lack of two measurement locations, which distance has to be changed for the different length scales, the Taylor hypothesis of frozen turbulence is used. It assumes that the turbulence is frozen and moves with the average mean wind speed  $u$  downwind from the wind turbine. The wind speed is measured at a fixed point and the gusts pass the anemometer with the mean wind speed. The distance

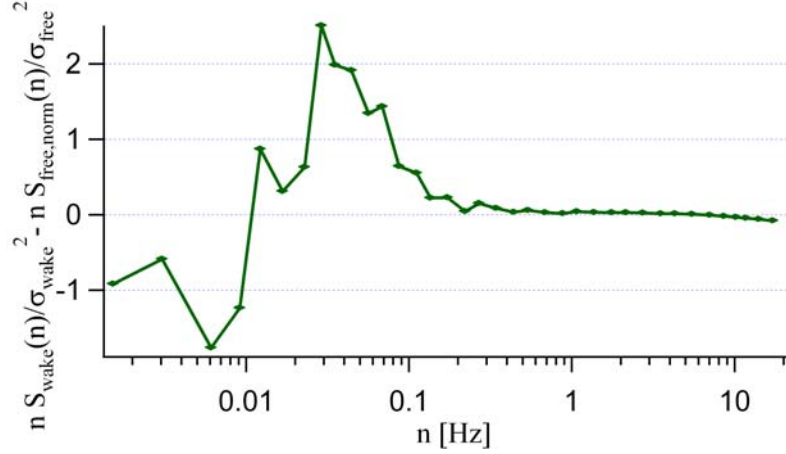


Figure 2.9: Difference between the normalized wake and free stream spectra for the  $u$ -component of the velocity

between the measurement points is defined over the time step  $\tau$  between the measurements. The velocity increment is defined as:

$$\delta U_\tau = U(t + \tau) - U(\tau), \quad (2.5)$$

The increments are analyzed by plotting the probability density function (PDF)  $p(U_\tau)$  of the values. If large changes in the signal occur more recently, the distribution changes from a Gaussian shape to a distinct peak around the mean value and fat tails with the occurrence of large velocity fluctuations in this scale. The distribution becomes intermittent.

A measure of the intermittence of a distribution can be defined with the Castaing formula [Castaing et al., 1990]. Castaing developed an equation to describe an intermittent distribution by the superposition of Gaussian distributions  $p(U_\tau|\sigma)$  with different standard deviations  $\sigma$ . The distribution of the standard deviation is based on a lognormal distribution  $f(\sigma)$ . The resulting distribution can be formulated by the convolution of both distributions  $p(u_\tau|\sigma)$  and  $f(\sigma)$ :

$$p(U_\tau) = \int_0^\infty p(U_\tau|\sigma) \cdot f(\sigma) \quad (2.6)$$

$$= \int_0^\infty \frac{1}{\sigma\sqrt{2\pi}} \exp\left[-\frac{U_\tau^2}{2\sigma^2}\right] \cdot \frac{1}{\lambda\sqrt{2\pi}} \exp\left[-\frac{\ln(\sigma/\sigma_0)}{2\lambda^2}\right] \frac{d\sigma}{\sigma} \quad (2.7)$$

The  $\sigma_0$  is the median value of the lognormal distribution. The grade of intermittence is determined by the form parameter  $\lambda^2$ . A large value of  $\lambda^2$  contributes to a broad lognormal distribution and therefore an intermittent distribution of  $p(U_\tau)$ . If  $\lambda^2$  goes against zero, the lognormal distribution has its boundary values as delta function  $\delta(\sigma - \sigma_0)$  resulting in a Gaussian distribution of  $p(U_\tau)$  with the variance  $\sigma_0^2$ .

The Castaing distribution can be fitted to the probability density functions produced from measured data for the different time steps  $\tau$ . The form parameter in dependence of the time  $\tau$  gives the information how different the deviation of the investigated from a Gaussian distribution is and therefore how intermittent the distribution is.

The free stream and wake situation of the flow at wind farm Elisenhof is investigated. The measured time series was divided in segments of 1min. Subsequent segments with wind speed mean value in the range of 5–7 m/s and wind direction in wake ( $74^\circ$ - $94^\circ$ ) or free stream ( $220^\circ$ - $240^\circ$ ) situation were connected to blocks. The increment analysis was applied on these blocks. The distributions for the free stream and wake situations are shown in Fig. 2.10. The PDFs are plotted against the wind speed increments normalized with the standard deviation of the wind speed increments.

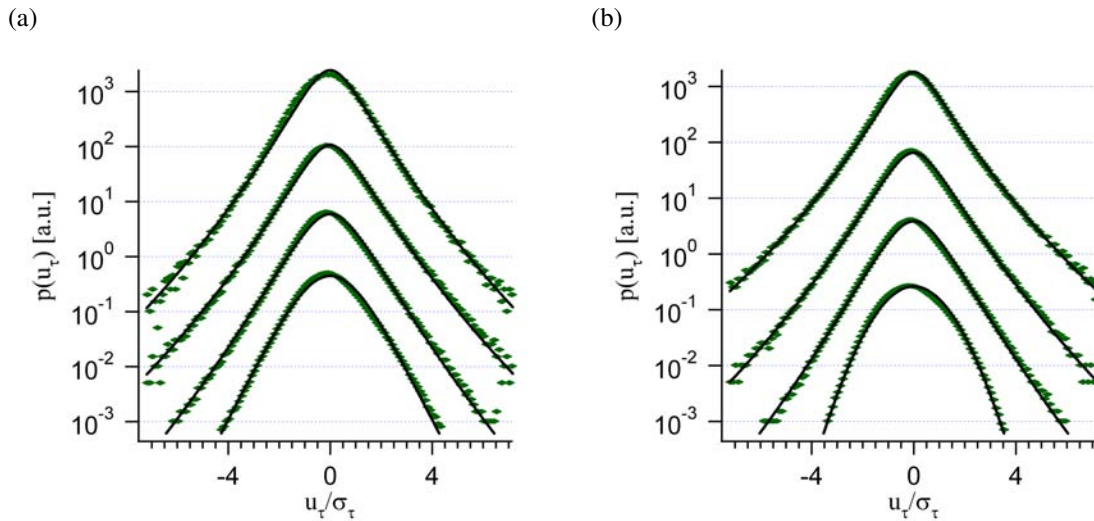


Figure 2.10: The increments of the wind speed for the free stream (a) and wake situation (b) are shown. The increments are calculated for different time steps  $\tau$  from top to bottom of 0.02, 0.16, 0.6 and 10.2s. For clarity, the distribution are shifted against each other.

The distributions look similar at low time steps  $\tau$  at both situations. At longer time steps the distributions from the free stream situation stay intermittent, whereas the distributions from the wake situation changes to a more Gaussian shape.

Regarding the form factor  $\lambda^2$  for the free stream and wake situation. The form factor is plotted in dependence of the time step  $\tau$  in double logarithmic plot in Fig. 2.11. As could be seen at small time steps, both values for  $\lambda^2$  have similar values between 0.15 and 0.2. The value estimated from the free stream measurement decreases slowly on the logarithmic scale with increasing time step, whereas the form factor from the wake situation show a significant decrease at time steps from  $\tau=1$ s to 10s. From 10s on the form factor remains at values of around  $10^{-4}$ .

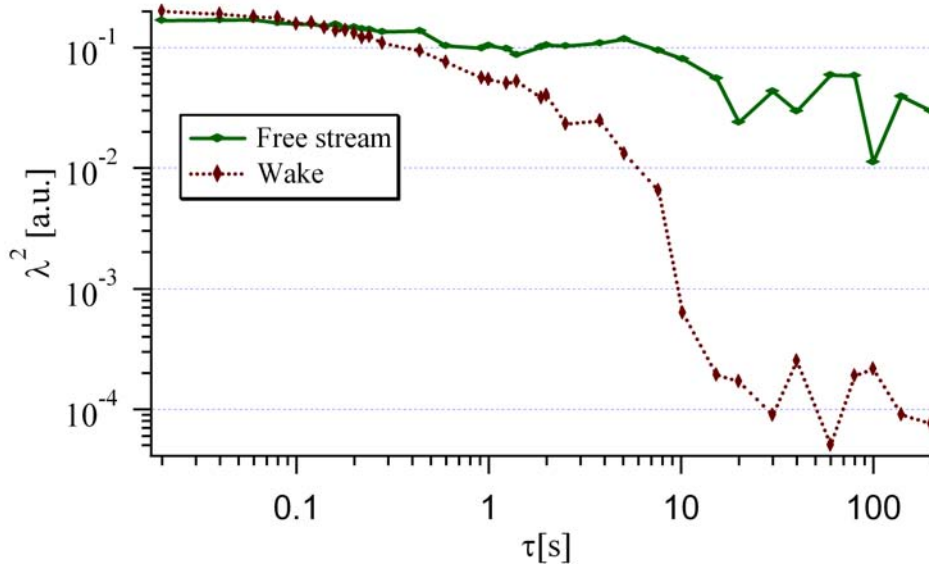


Figure 2.11: Form parameter  $\lambda^2$  plotted against the time step for the PDFs in free stream and wake situation.

An increase of the form factor at large time steps (200s) could not be observed. Larger time steps could not be realized due to a lack of data. For the processing of the increments, continuous time series in the given wind speed class and wind direction are needed. The continuous time series must have at least 100000 data elements for time steps larger than 200s. In the case of 400s, only an amount of 85 998 data points remain for the wake situation: The tails at large increments are not present any more, the form factor can not be estimated with reasonable accuracy.

The increment distributions are intermittent at short time steps for the free stream and wake situation. The PDF from the free stream condition stays intermittent at larger time steps for the measurement, but the PDF of the wake situation changes from a time step  $\tau$  of 1s to a gaussian shape in the case of the wake situation.

It can be concluded, that at time scales larger than 10s, large wind speed fluctuation or gusts in the size of 60m not present in the wake anymore. At smaller time steps the gusts appear in the wake situation as in free stream situation.

## 2.7 Conclusion

The wake of a wind turbine downwind of a large wind farm was investigated. Measurements of the velocity in the wake with an ultrasonic anemometer mounted at hub height at a distance of 2.49 D were analyzed.

The turbulence intensity profiles show an increase from 10% of 30% in turbulence intensity inside the wake. Neither the normalized wind speed nor the turbulence intensity profiles seem to be affected by the ambient wind speed. The turbulence intensity normalized with the wind speed in the wake show nearly no influence by the ambient wind speed.

The profile of the Reynolds stress was estimated and compared to the derivation of the wind speed profile and found to be narrower. With the eddy viscosity closure, both profiles are related by a constant, the eddy viscosity. A possible explanation is that the Reynolds stress depends on the wind speed profile. Due to the dependency, a delay between the development of the Reynolds stress profile and the wind speed profile would be expected, which cause the different width of the profiles. This delay is not considered in the eddy viscosity closure.

The power density spectrum shows an increase of turbulent kinetic energy in the wake at all frequencies opposite to the free stream conditions. Beneath this increase, at two parts of the spectrum the energy is redistributed. At scales of 200m the spectra has a maximum and at larger scales a decrease occurs opposite to the free stream measurements.

The increments of the wind speed show a decrease of intermittence at the stream in the wake in scales larger than the rotor diameter, whereas the free stream wind stays nearly intermittent up to time steps of 100s and more.

Comparing the turbulence in the wake and free stream situation in respect on the value turbulence intensity it can concluded: The shapes of the power density spectra in free stream and wake situations are similar at frequencies higher than 0.1Hz, despite the offset caused by the higher amount of turbulence in the wake. The increment distributions are similar for timescales smaller than 10s. Therefore the turbulence at scales up to the order of the rotor diameter shows similar structures in- and outside the wake. At larger scales, the turbulence structures deviate in the wake from the free stream situations. In case of the spectra the differences are up to a factor of two. The turbulence intensity can only be a first approximation for the description in- and outside of the wake.





# Chapter 3

## Uncertainties in measuring turbulence intensity profiles

### 3.1 Introduction

The measurement of the wind speed is normally done with meteorological masts equipped with anemometers at different heights. In recent years, cup anemometers were used and are more and more replaced by ultrasonic anemometers. The goal is for the measurement of the standard deviation of the wind speed, as also for other measurements, to achieve the "real" value. As already described in the previous chapter, the standard deviation depends not only on the amount of fluctuations, but also on the type of signal. Additionally errors occur by the used anemometer, the averaging time, the sampling frequency and the post-processing of the data. Quite often the post-processing is done inside a locally installed data logger and no raw data is available.

Mostly used at meteorological masts are cup and ultrasonic anemometers. Beside the fact that the ultrasonic anemometer operates with a higher sampling frequency, a main difference is that the ultrasonic anemometer measures both horizontal components  $U, V$  and the vertical component  $W$  of the wind speed and the cup anemometer only the norm of the components  $U, V$ . The effect of the different ways of measuring the turbulence intensity profiles is shown exemplarily with measurements from single wakes at wind farm Elisenhof. There, high resolution data in time was recorded with an ultrasonic anemometer, which gave the possibility for different scenarios.

Wind speed data measured at meteorological masts is often averaged on the fly and stored as mean values with additional standard deviation. The averaging period according to IEC standards [IEC, 2005] is normally ten minutes, but due to high fluctuation in wind directions often shorter averaging periods were used in recent measurements [Clijne, 1993],[Taylor, 1990]. The different averaging time has a minor influence on the

measured mean wind speed at wake measurements, but affects the standard deviation of the wind speed and therefore the turbulence intensity. The possibility of scaling turbulence intensity profiles measured with different averaging times is investigated at the example of Vindeby wind farm. The Vindeby data benefit from a long term measurement and therefore enough data points to compare different averaging times.

Trends in the wind speed data are not eliminated by linear detrending or filtering, when data is processed directly in the data logger. With the measurements from wind farm Elisendhof, the influence of a linear detrending of the data is compared to the normal averaging procedure.

The difference between the estimated values from the different methods is expressed in the root mean square error (RMSE), which is defined as:

$$RMSE = \sqrt{\frac{1}{N-1} \sum_{i=0}^N [I_1 - I_2]^2}. \quad (3.1)$$

$N$  gives the number of wind direction sectors and  $I_1$  and  $I_2$  the turbulence intensity from the different methods.

The chapter starts with a short description of the wind farm Vindeby (the wind farm is previously described in chap. 2), followed by the comparison of the measurement method of cup anemometer against the ultrasonic anemometer and the effects of changes in the sampling frequency. The influence of different averaging times on the turbulence intensity profiles and the influence of detrending on the turbulence intensity profiles are discussed. At the end the conclusion is presented.

## 3.2 Vindeby

Vindeby wind farm is the world first offshore wind farm [Vin, 2004]. It consists of 11 wind turbines. Three meteorological masts were build to measure the wind conditions around the wind farm. Two were build near the wind farm and one at the nearby coast. The 11 Bonus 450 kW turbines are arranged in two rows as shown in fig. 3.1.

The Vindeby offshore wind farm is located off the northwestern coast of the island of Lolland, Denmark. To the west and north there is open sea fetch and land fetch to the south in a distance of 1270m to the southern meteorological mast.

The installed Bonus wind turbines have a rotor diameter of  $D = 37\text{m}$  and a hub height of  $H = 35\text{m}$  [Barthelmie et al., 1994] and are stall regulated.

Outside the wind farm the two measurement masts SMS and SMW are installed. Both masts are equipped with Risø cup anemometers in the heights: 48, 43, 37.5, 29, 20, 15, 7m and

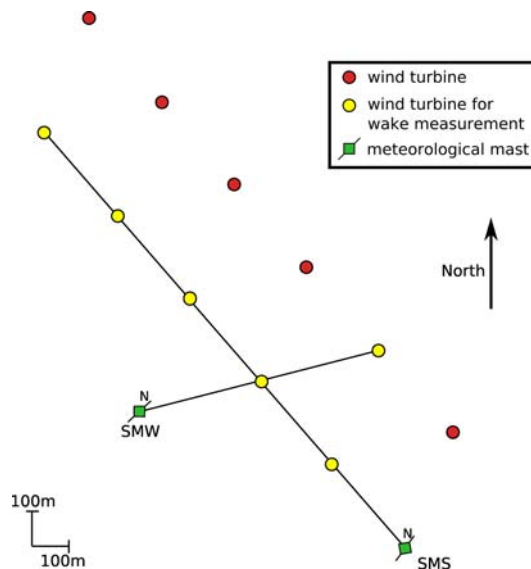


Figure 3.1: Layout of Vindeby wind farm. The position of the wind turbines and the two meteorological masts SMW and SMS are shown.

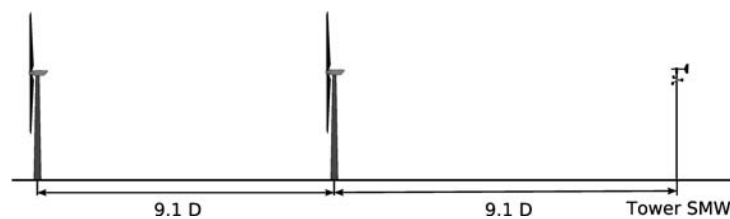


Figure 3.2: Vindeby wind farm: Double wake situation

wind vanes in the heights 43m and 20m. The mast SMW and SMS are equipped with two cup anemometers at the height of 37.5m, where the booms are oriented in the direction  $46^\circ$ - $226^\circ$ . The booms at the southern mast SMS is oriented in direction of  $173^\circ$  and  $353^\circ$ .

The sampling frequency was 20Hz stored as 1min averaged data. Data was available in the time between 2.5.1994 to 1.10.1995. For the estimation of the wind speed and turbulence intensity profiles the cup anemometers at 37m (nearly hub height) and the wind vanes at 43m were used.

The double wake situation occurs for a wind direction of  $75^\circ$  for mast SMW and the quintuple wake for mast SMS at a wind direction of  $320^\circ$ . The setup along the axis of the wind turbines is shown in fig 3.2 for the double wake and fig 3.3 for the quintuple wake situation. For the wake measurements always one measurement mast in free stream condition and one in the wake was used.

The profiles were derived from 1min averaged time series averaged to 10min time series,

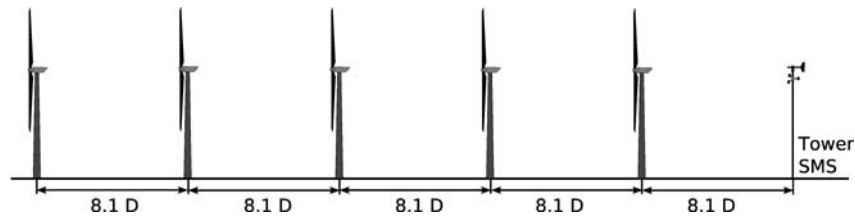


Figure 3.3: Vindeby wind farm: Quintuple wake situation

where a running average was used (see Appendix B). The ambient turbulence intensity at the free mast ranges from 5% to 7%.

### 3.3 Influence of measuring with cup or ultrasonic anemometer

At former measurements cup anemometers were used to estimate the mean wind speed and the turbulence intensity in the wake of a wind turbine. Only in the last years the more expensive ultrasonic anemometer have been installed at meteorological masts.

The interest is to measure the turbulence intensity componentwise, divided in the components U,V,W, where U is in mean wind direction, V right angled to U and W the vertical direction in a right hand coordinate system. The ultrasonic anemometer and propeller anemometers can measure each component separately, whereas a cup anemometer measures the total horizontal wind speed. The difference between calculating the turbulence intensity only from the u-component or using the absolut wind speed  $k$  in the horizontal plane is investigated.

As described in the previous chapter, the turbulence intensity in U-direction  $I_u$  is calculated with a frame of reference according to the mean wind direction. There the standard deviation in direction of u  $\sigma_u$  is calculated and divided through the vector mean of the wind speed, so a true vector average is used for u:  $u = \sqrt{\bar{U}^2 + \bar{V}^2}$ .

When measuring with the cup anemometer an absolut turbulence intensity is measured derived from the standard deviation  $\sigma_k$  from the absolut wind speed  $K = \sqrt{U^2 + V^2}$  divided through the absolut mean wind speed  $k_{cup}$ . The calculation of the mean wind speed  $k_{cup}$  is independent from the wind direction, it is a scalar average, resulting from the possibility to only measure the absolute amount of wind speed independent from wind direction:  $k_{cup} = \sqrt{\bar{U}^2 + \bar{V}^2}$ .

To compare this effect, the high resolution data from the ultrasonic anemometer at the meteorological mast at wind farm Elisenhof is used. The use of the ultrasonic anemometer for

### 3.3. INFLUENCE OF MEASURING WITH CUP OR ULTRASONIC ANEMOMETER<sup>45</sup>

both components has the benefit, that only this investigated effect will be investigated and additional effects like the turbulence dependency of the cup anemometer does not influences the results.

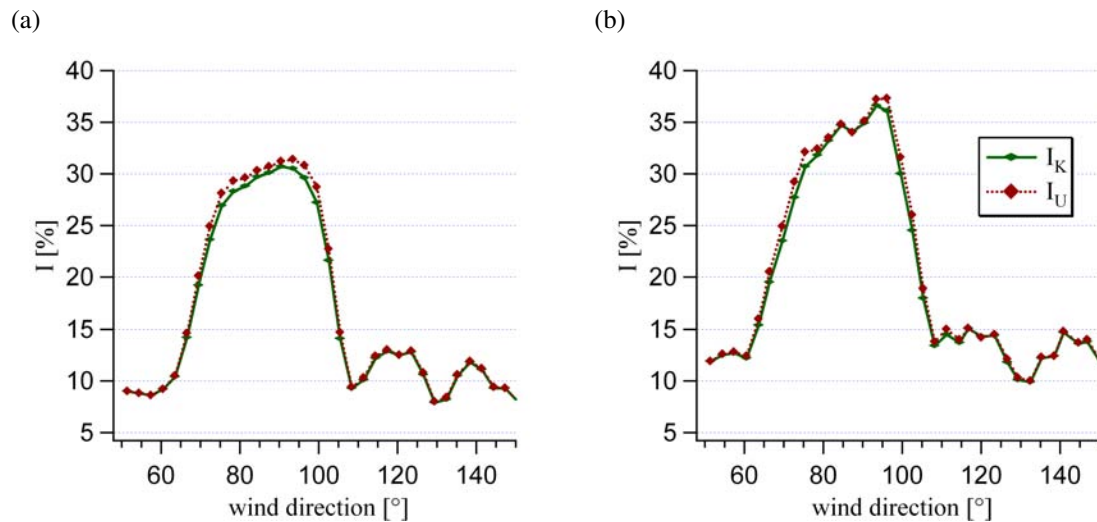


Figure 3.4: Turbulence intensity profile from the two wakes at wind farm Elisenhof. The turbulence intensity from the wind component u and from the combined component k was used. The averaging time of 1min (a) and an averaging time 10 min (b)

In fig. 3.4(a) and 3.4(b) the two turbulence intensity profiles for the u- and k-component can be seen for the different averaging times of one and ten minutes. The turbulence intensity profiles created with one minute averaged values show a higher slope at the wake half width and the shape is smoother, than the 10-minutes averaged profile. The maximum turbulence intensity at 10 min averaging time is about 16 % higher than with the turbulence intensity profiles from 1 min averages.

Regarding the difference between the u- and k-component at both figures, outside the wake nearly no difference can be seen. Inside the wake the turbulence intensity from the u-component is slightly higher. Overall the values at both averaging times show an RMSE of 0.7 %.

The difference between the turbulence intensity profiles from the horizontal absolute wind speed to the u component is rather small. Cup anemometers differentiate to ultrasonic anemometers in additional ways. The effects like overspeeding, the sampling rate and the effects of turbulence on the cup anemometer are not regarded in this comparison. The effect of the different sampling frequencies will be evaluated in the next section. A high error occurs due to the effects on ambient turbulence on the measurements, as shown by Deiss [Deiss et al., 2001] with measurements inside a wind channel. The error was in the range of up to 5.9 % comparing zero turbulence intensity to a level of 6 %.

### 3.4 Influence of the sampling frequency

Due to the different type of construction of anemometers, the measurement is often limited to a typical sampling frequency. Cup anemometer are normally sampled not higher than 5 Hz, whereas ultrasonic anemometer could have rates up to 50 Hz. The sampling frequency reached by the cup anemometers is often quite lower, as the cups have a high idleness. Based on the time series with the different sampling frequencies, the average values are estimated by the data logger.

The effect of different sampling frequencies is compared exemplarily by reducing the sampling frequency of a time series by averaging. For this a time series from the ultrasonic anemometer at hub height from wind farm Elisenhof was used. This time series was sampled with a frequency of 50 Hz. An additional time series with a sampling frequency of 5 Hz was generated: Every ten values from the original time series were averaged to one new value. Both time series were binned for the wind directions and an ambient wind speed of 5–7 m/s with averaging times of 1min and 10min. The resulting profiles can be seen in Fig. 3.5(a) and 3.5(b).

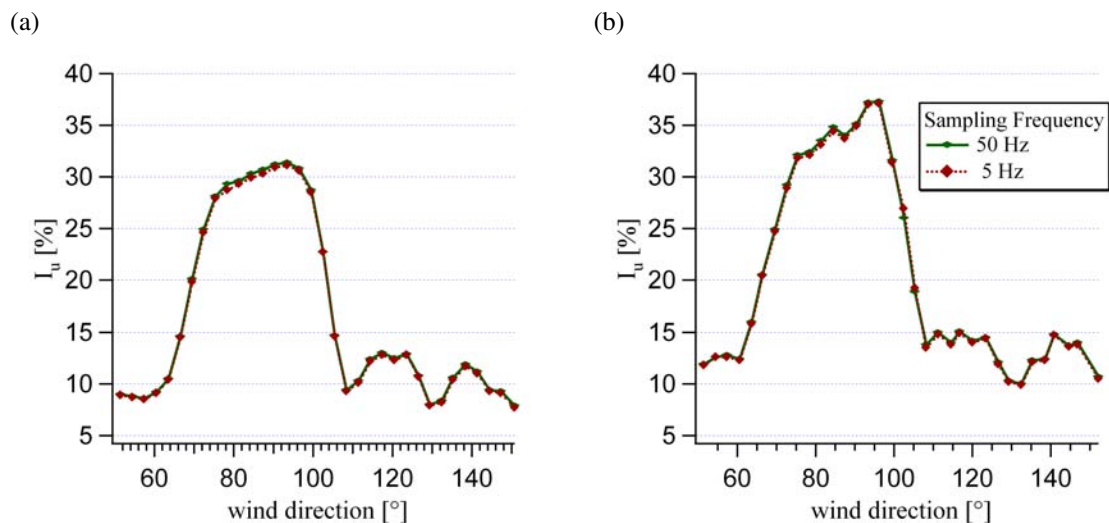


Figure 3.5: Turbulence intensity profiles estimated from time series with two different sampling frequencies: 5 Hz and 50 Hz. The averaging time of 1min (a) and an averaging time 10 min (b)

In wake condition the turbulence intensity profile from the time series with a higher sampling frequency are slightly higher than the profiles from the slower sampled time series. The RMSE for the averaging time of 1 min is 0.23 % and for 10 min 0.27 %. The effect of the sampling frequency is negligible in the case of wind farm Elisenhof.

### 3.5 Influence of different averaging times

For comparison of turbulence intensity profiles with different averaging times the double wake situation at the wind farm Vindeby is used. Time series with an averaging time  $T$  of 1, 2, 3, 5, 10, 15 and 30 min were produced from the original data and bin averaged for an ambient wind speed  $u_{amb} = 8 - 10 \text{ m/s}$  from the meteorological mast in free stream condition and with horizontal steps of  $1^\circ$  degree. The result are wind speed and turbulence intensity profiles for the seven different averaging periods. The results were applied to the turbulence intensity profiles from wind farm Elisenhof.

Two ways for transforming the turbulence intensity profiles from shorter averaging times to longer ones are evaluated: On the one hand, the profiles are multiplied with a scaling factor  $S$  and on the other hand, the profiles are shifted with an over the width of the profile constant offset  $I_{off}$ . The idea of the scaling of the turbulence intensity profiles is based on the assumption that all the profiles show a similarity. A constant offset can be explained if one imagine several segments of wind speed measurements, each with its own turbulence intensity value. For a longer averaging time, several segments will be connected. Normally these segments will not have the same mean value of wind speed, as they are also influenced by wind speed fluctuations of larger scales. These slower wind speed fluctuations add an additional turbulence intensity to the turbulence intensity values of the single segments. If transforming 1 to 10min values, these fluctuations would be in the length scale of about 400m (e.g. at a wind speed of 7 m/s and the time of 1min) and therefore expected to be larger than the wind turbine diameter. It can be assumed that they appear in the ambient and in the wake measurements as well: The constant offset affect the complete turbulence intensity profile.

The scaling factor  $S$  is calculated from the ratio of the ambient turbulence intensities from different averaging times (for example for 1 and 10min averaging:  $S = I_{amb,1}/I_{amb,10}$ ) and the offset from the mean value of the difference between the profiles  $I_{off} = I_{10} - I_1$ .

A selection of turbulence intensity profiles for different averaging times is plotted in fig. 3.6. For the averaging times 1min and 10min the standard deviation from the binning process is shown additionally.

As can be seen the level of turbulence increases over the whole profile with increasing averaging time. Additionally at longer averaging times larger than 15 min the width of the turbulence intensity profiles increasing with increasing averaging time. Longer averaging times include a higher range of wind direction fluctuations in the averaging block. A broadening of the wake structure and a decrease in the turbulence intensity maximum in the wake is the consequence.

The wind speed deficit profiles were used to estimate the half width of the wake  $\beta$  with a Gaussian fit, the point where the wind speed is reduced from the maximum deficit in the wake to half of the deficit. The maximum turbulence  $I_{max}$  intensity and the turbulence

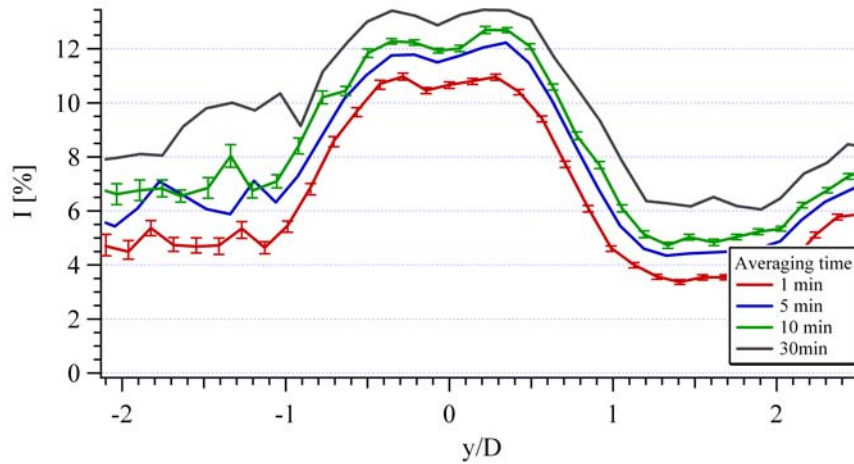


Figure 3.6: Horizontal double wake turbulence intensity profiles from time series which averaging times from 1 to 30 minutes. The error bars, exemplarily shown at the 1 min. and 10 min. averaged profile, show the standard deviation from the mean value in the certain bin.

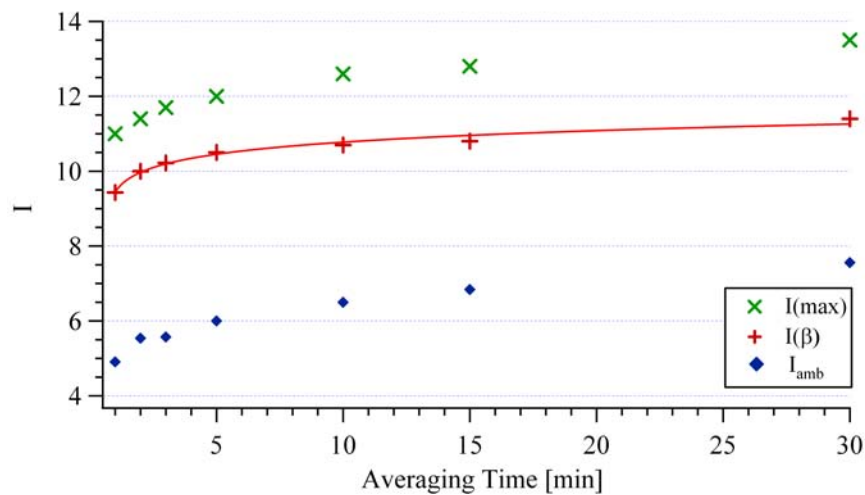


Figure 3.7: Maximum turbulence intensity, turbulence intensity at the half width of the wake  $\beta$  and the ambient turbulence intensity from the double wake turbulence intensity profiles versus the averaging time  $T$ .

intensity values at the distance of the wind deficit wake half width  $x = \beta I_\beta$  were estimated for the different averaging times  $T$ . The turbulence intensity values at the points  $I_{max}$ ,  $I_\beta$  and  $I_{amb}$  are shown in Fig. 3.7 in dependency of the averaging time. As can be seen, the turbulence intensity increases fast at low averaging times and stagnates at longer averaging times. The fitted curve is based on an logarithmic profile.

For the scaling of the turbulence intensity profiles from 1 to 10min a scaling factor  $S$  of 1.44 is estimated and from 3 to 10 min of 1.16. In Fig. 3.8 the turbulence intensity profiles are



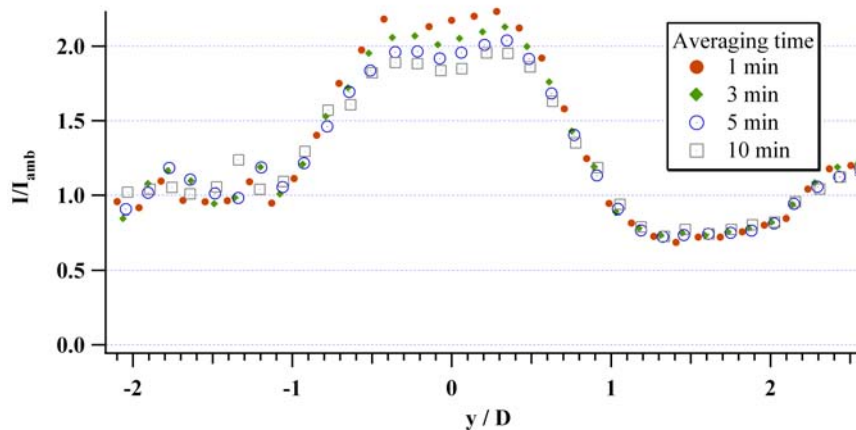


Figure 3.8: Turbulence intensity profiles from different averaging times  $T$  scaled with the ambient turbulence intensity.

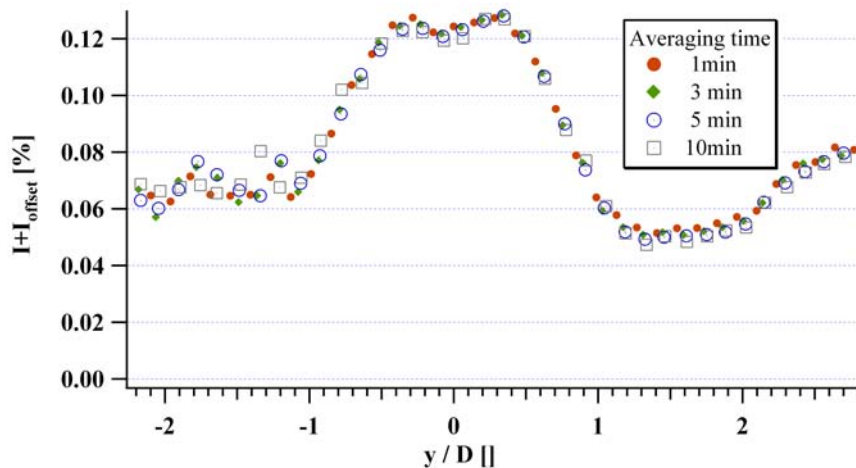


Figure 3.9: Turbulence intensity profiles from different averaging times shifted by a constant value to match the turbulence intensity profile from an averaging time of 10min.

scaled with the measured ambient turbulence intensity  $I_{amb}$  in the range of 1min to 10min. It could be seen that the turbulence intensity outside the wake is scaled correctly, whereas the wake maximum turbulence intensity increases with increasing averaging time. A broadening of the wake could at this averaging times not be observed. The RMSE is about 7.3 % for the transformation from 1min to 10 min values.

The calculated offset  $I_{off}$  between the profiles is 1.77 % for the shift from 1min averaged to the 10min averaged profiles and 0.28 % from the 3min to the 10min values. The shifted profiles together with the 10min average profile can be seen in Fig. 3.9. The RMSE is 0.41 % (1 to 10min) and 0.43 % (3 to 10min).

In Fig. 3.10  $I_{off}$  is shown in dependence of the normalized distance to the wake center

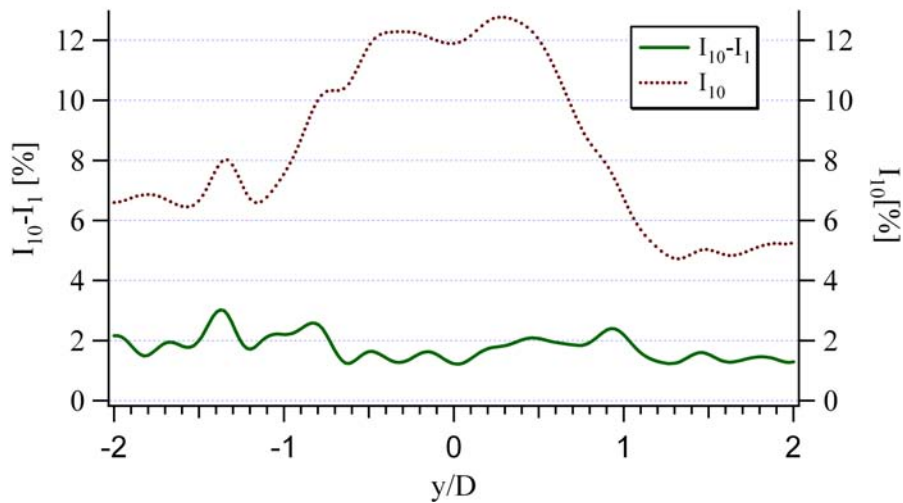


Figure 3.10: Difference  $I_{off}$  between the turbulence intensity profile with an averaging time of 1 and 10 min in dependence of the normalized distance from the wake center. It can be seen that the offset between the profile  $I_{10}$  and  $I_1$  fluctuates around 2 percentage points and has no explicit dependence from the position in the wake. Additionally the turbulence intensity profile from 10min average is shown.

$\tilde{y} = y/D$ . Also the turbulence intensity profile from the 10min average time series is added to the figure. The values  $I_{off}$  show no difference between wake and non wake situation.

The transformation with a constant offset of the turbulence intensity profiles from 1 min to 10 min average time can be seen in Fig. 3.11 for the wake measurement from wind farm Elisenhof. Here an offset of 3.5 % was estimated with an RMSE of 1.45%.

The comparison of the two ways of transforming shows that the use of a constant offset lead to a significant lower error than the scaling with a constant factor. It is recommended to use this method to transform turbulence intensity profiles between different averaging times. As the mean value of the offset is independent of the wake or free stream situation it can be estimated directly from free stream measurements and no information about the wake structure at different averaging times is needed.

### 3.6 Effects of Detrending on turbulence intensity profiles

Mean wind speed statistics is done from averaging blocks of 1 to 10 min. In this time ranges the "mean" wind speed does not remains constant, like inside wind channels, but changing slowly. To separate the effect of the trend of the "mean" wind speed from the fluctuating part, a method called detrending is used. In the present case linear detrend is used. A linear

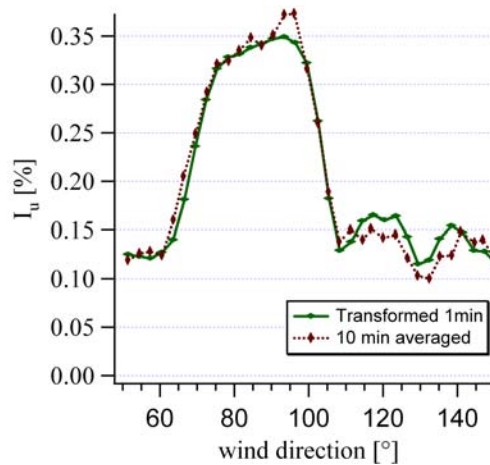


Figure 3.11: Transformation of turbulence intensity profiles from 1min averaged time series to 10min averaged values by adding a constant factor. The transformed turbulence intensity profile is shown and the original turbulence intensity profile from 10 min averaged time series as well.

fit is applied to the data and this fitted line is subtracted from the data before the calculation of standard deviation or correlations [Hansen and Larsen, 2003].

Data loggers at measurement masts often calculate the mean values and statistics locally and discard the raw data. Often the mean value is used to estimate the standard deviation and no detrending was done.

The influence of the linear detrending of the raw data on the turbulence intensity profiles is shown at the example of the measured wakes at wind farm Elisenhof. In Fig. 3.12(a) and 3.12(b) with the different averaging times of one and 10 minutes. Here, bin averaged turbulence intensity profiles from the wind vector in u-direction from the single wake measurements at wind farm Elisenhof are shown with and without removing of a linear trend. The effects of detrending is extremely visible at the shorter averaging time, which results in a lower turbulence intensity of the detrended values. The 10 min averaged values does not show such a high deviation between the profiles. The largest difference can be observed in the middle of the wake, whereas outside the wake there is only a small change. This results from the different wind speed in and outside the wake, which affect the turbulence intensity. The change in standard deviation in and outside the wake is the same, only the mean wind speed changes, which results in a different large deviation of the turbulence intensity profiles in and outside the wake.

The estimated RMSE for the 1 min averaged values is 2.5 % and for the ten minutes averaged values 1.2 %.

The detrending of measured data lower the resulting values of turbulence intensity. The effects increase with shorter averaging time: in shorter time intervals, the detrending removes

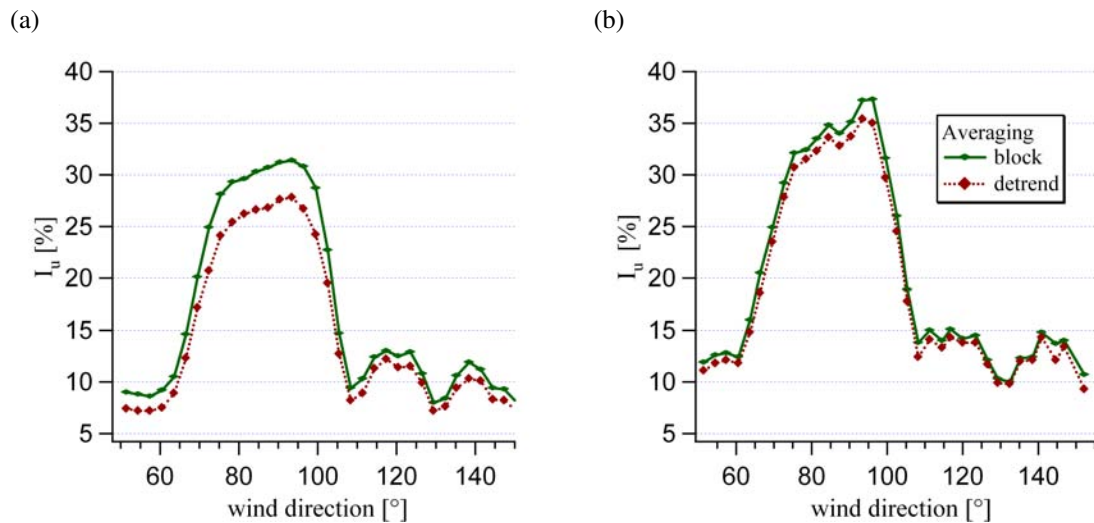


Figure 3.12: Turbulence intensity profiles calculated with block averaged and linear de-trended data. The profiles were estimated from one minute averaged values in Fig.(a) and ten minutes averaged in Fig.(b) from ultrasonic anemometer measurements at wind farm Elisenhof.

fluctuations on a smaller scale, which seems to fluctuate higher than the long term trend at the ten minutes data.

### 3.7 Conclusion

Different uncertainties occurring in the estimation of turbulence intensity profiles are compared. Thereby it was analyzed if a conversion of turbulence intensity profiles estimated from time series with different averaging times is possible.

The main difference errors occur with the use of the detrending at averaging times of 1min. There the RMSE is about 2.5 %. As source of this large fluctuations causing this error the averaging time of 1min is assumed. At an averaging time of 10min the error reduces to 1.2 %. A sign that in the time scale of 10min the fluctuations which are compensated by the linear fit are not so large as in the case of the averaging time of 1min.

For the transformation of the turbulence intensity profiles from different averaging times, a way is found, which enables a conversion with a small error. Thereby a constant offset over the width of the profile is added/subtracted to the turbulence intensity profile. This transformation work with multiple wakes as in the case of Vindeby as well as the wake measurements at wind farm Elisenhof. The RMSE caused by the transformation of 1min to 10min averaged profiles is 0.41 % for Vindeby and 1.45 % for Elisenhof.

The error from different averaging time and the difference between the measurements of the absolute wind speed (as in the case of the cup anemometer) and the vectorial wind components (as measured by the ultrasonic anemometer) are small with 0.27 % and 0.7% at an averaging time of 10 min.

The determined errors are summarized in table 3.7.

Comparisson	1 min average	10 min average
Cup/Sonic	0.63 %	0.7 %
Detrend	2.5 %	1.2 %
Sampling frequ.	0.23 %	0.27 %
Scaling of 1min to 10min	1.45 %	

Table 3.1: Comparison of the uncertainties in estimating turbulence intensity. The root mean square error is listed.



# Chapter 4

## Scaling properties of the turbulence intensity in the wake

### 4.1 Introduction

Wind tunnel measurements from flows behind spheres and in jets show a similarity of the wind speed and turbulence intensity profiles, when measured in the intermediate and far zone. So far, the profiles could be scaled by using factors for the amplitude and the width of the profile, as known from basic fluid dynamics.

The factors for the scaling were estimated from the turbulence intensity and wind speed profiles themselves. The maximum value of the profiles in the wake and at special positions is used to scale the height, and the half width of the profiles. For calculating the scaling parameters for turbulence intensity profiles only a few ways were proposed. Harsha et al. [Harsha and Lee, 1970] showed that turbulence intensity in the wake could be scaled using the Reynolds stress. This idea was picked up from Zelazny [Zelazny, 1972], who analyzed jets and the wake flows behind spheres and developed a model to scale turbulence intensity profiles with parameters from the wind speed profile. His aim was to calculate the irradiation of noise behind the turbine of a rocket from the turbulence intensity. For the calculation of the wind speed profile, an existing eddy viscosity approach was enhanced.

In the current chapter the possibilities of the scaling of turbulence intensity profiles based on wake measurements from wind turbines at two different wind farms will be presented.

The wake of a wind turbine is in many ways quite different from a jet or the wake of a solid body. Wind channel measurements behind bodies were mainly realized in a laminar surrounding stream. The wake of a wind turbine differs in many ways:

- The flow incident on the wind turbine is turbulent.

- The wind direction over the averaging time is not steady and the ambient wind speed not constant.
- The rotor produces additional turbulence.
- The rotor is not solid and produces therefore a coflowing stream to the surrounding wind. Energy is taken from the wind by the rotor, correspondingly the velocity in the wake is lower.

In previous works, different ways to calculate the maximum turbulence intensity in the wake were developed as described in the next chapter. No investigations of the scaling of wind turbine turbulence intensity profiles were done so far. The aim of this investigation is to find a way to scale the turbulence intensity profiles and calculate the scaling parameters from the wind speed profiles. In order to achieve different ways of scaling the turbulence intensity in the wake were evaluated: Scaling of the turbulence intensity profiles with values estimated at two different positions in the profile as well as two different ways of calculating a scaling parameter from parameters estimated from the wind speed deficit profiles.

The evaluation is done with measurements from wind turbines at the wind farms Nibe and Sexbierum, which provide wake measurements at different distances behind the wind turbine.

The theory section 4.2 introduces two methods to calculate the scaling parameters of the turbulence intensity. In the following section the wind speed profiles are scaled 4.4. Using the estimated parameters the scaling of the turbulence intensity profiles is evaluated in 4.5. The fit of a double Gaussian function to the profiles of the standard deviation of the wind speed is done in section 4.6 and the chapter finishes with the conclusion in section 4.7.

## 4.2 Theory

The section begins with a short remark on the definition of error. The scaling of wind speed profiles is described in the first section, followed by a description of the calculation of the scaling parameters for the turbulence intensity profiles. Then a way of extracting the ambient turbulence intensity from the turbulence intensity in the wake is described. The section ends with an approach describing the shape of turbulence intensity profiles with as a superposition of two Gaussian distributions.



### 4.2.1 Error definition

The linear least square fits, used in the following, use as an error measure the chi-square value of the modeled and measured profiles:

$$\tilde{\chi}^2 = \sum_{i=1}^N \frac{(y_{i,meas} - y_{i,fit})^2}{y_{i,meas}}, \quad (4.1)$$

where  $y_{i,meas}$  are the measured values,  $y_{i,fit}$  the fit results and  $\sigma_{i,fit}$  and N the number of measurements.

The error given at the fitted parameters is always one standard deviation. The confidence bar in the plots describes a confidence interval of 90 %.

### 4.2.2 Scaling of wind speed profiles

The wind speed in the wake is usually defined by the wind speed deficit  $u_{def}(r,x)$ , which describes the wind speed in the wake  $u(r)$  by the difference of wind speed  $u_{def}(r)$  to the ambient wind speed  $u_{amb}$  at the radial position r from the center of the wake and at the distance x to the wind turbine:

$$u(r,x) = u_{amb} - u_{def}(r,x) \quad (4.2)$$

The shape of the wind speed deficit profile in the wake is assumed to be Gaussian, according to Vermeulen [Vermeulen, 1980], who used the basic approach for a wake flow behind a body described in Abramovich [Abramovich, 1963]. The Gaussian shape was also found in results of the Ainslie model, an eddy viscosity solver, by Wald [Wald, 1997] (later described in chapter 5).

Therefore a normalized Gaussian wind speed deficit profile  $\tilde{u}(\tilde{r}) = u(\tilde{r})/u_{amb}$  was assumed. The wind speed profile is normalized to the ambient wind speed  $u_{amb}$  and to the distances with rotor diameter D. The normalized values are marked with a tilde. The Gaussian distribution is expressed in a way that the centerline deficit  $\tilde{u}_{cent}$  is the maximum of the distribution and  $\tilde{\beta}$  the half width, with a value of  $0.5\tilde{u}_{cent}$ , resulting in the normalization factor  $\ln(0.5)$ . The distribution is subtracted from the normalized ambient wind speed  $\tilde{u}_{amb}$ , per definition one, to receive the normalized wind speed profile in the wake:

$$\tilde{u}(\tilde{r}, \tilde{x}) = \tilde{u}_{amb} - \tilde{u}_{cent}(\tilde{x}) \exp\left(\ln(0.5) \frac{(\tilde{y} + \tilde{y}_0)^2}{\tilde{\beta}(\tilde{x})^2}\right), \quad (4.3)$$

where  $\tilde{y}$  is the horizontal distance from the centerline,  $\tilde{y}_0$  a correction of a horizontal shift, if a misalignment exists between wind turbine and measurement mast, and  $\tilde{\beta}$  the wake half width. In some cases, when there is an measurement offset of the anemometers between the incoming ambient wind speed and the wind speed measured in the wake, the value  $\tilde{u}_{amb}$  might have values different than one. In these cases, the ambient wind speed deficit  $\tilde{u}_{amb}$  is used to correct the wind speed offset.

### 4.2.3 Scaling of turbulence intensity profiles

#### Approach from Zelazny

Zelazny [Zelazny, 1972] formulated in his PhD thesis a way to calculate the turbulence intensity in a wake or in a jet. The approach consists of a relationship expressing the turbulence intensity in terms of eddy viscosity, of an assumption for the eddy viscosity and a correction term for high velocities. The equation was validated against wind channel data from a large number of measurements.

The equations based on the decomposition of the velocity in a stationary and a fluctuating part  $U = u + u'$  for all three dimensions  $U, V, W$  in cylindrical coordinates. The component  $U$  is in direction of the stream,  $V$  radial to the center in horizontal direction and  $W$  radial to the center in vertical direction. Zelazny approximates the flow in the wake as axisymmetric, whereas the  $W$  component is later expressed by the  $U$  and  $V$  components. The standard deviation of the components is noted as  $\sigma$ , for example  $\sigma_u = \sqrt{u'^2}$ .

Starting with the assumption of Harsha and Lee [Harsha and Lee, 1970], who related the Reynolds stress  $\overline{u'v'}$  to the turbulent kinetic energy at the half width  $\beta$  of the stream with the following equation:

$$\overline{u'v'} = 0.15\rho(\sigma_u^2 + \sigma_v^2 + \sigma_w^2), \quad (4.4)$$

where  $\rho$  is the density of the fluid.

Based on this equation, Zelazny combines eddy viscosity with the turbulence intensity. He treats the ratio  $v'/u'$  as constant in a first approximation and approximated it by its value at the velocity half width. A parametrization with measured data lead to the additional increase in the ration with increasing distance:

$$\frac{\sigma_v}{\sigma_u} = \sqrt{(0.5 + 0.005\tilde{x})} \quad (4.5)$$

The relation should be valid for distances  $\tilde{x} \leq 100$  and is used for substituting  $v'$  in equation (4.4).  $\tilde{x}$  is the distance to the wake producing object normalized to the diameter of the object. Additionally for axisymmetric flows  $\overline{v'} = \overline{w'}$  is set. This leads to:

$$\overline{u'v'} = 0.15(1 + 2(0.5 + 0.005\tilde{x}))\sigma_u^2. \quad (4.6)$$

Using the eddy viscosity approach, which relates the shear stress to the derivation of the stationary wind speed profile at the half width of the wake  $\beta$ :

$$\overline{u'v'}(\tilde{x}) = \varepsilon_\beta \left( \frac{\partial u(r, \tilde{x})}{\partial r} \right)_\beta. \quad (4.7)$$

A description of the eddy viscosity  $\varepsilon_\beta$ , originally from the Schetz model [Schetz, 1968] was improved with a correction term for high velocities:

$$\varepsilon_\beta(\tilde{x}) = 0.036 \frac{\int_0^\infty |\rho u(\tilde{r}, \tilde{x}) - \rho u_{amb}| \tilde{r} d\tilde{r}}{\tilde{\beta}^2 (1 + 0.6|M - M_{amb}|)}, \quad (4.8)$$

where  $M$  and  $M_{amb}$  are the Mach number inside and outside the stream. It is defined by the speed in the stream divided by the velocity of sound. The wind speed is much lower than the velocity of sound, therefore it is subsonic, resulting in  $M \ll 1$ . Combining equations (4.6) with (4.7) and including (4.8), a formulation for the standard deviation of velocity at the half width  $\beta$  of the stream could be found:

$$\sigma_{u,\beta}(\tilde{x}) = 0.49 \sqrt{\frac{\int_0^\infty |\rho u(\tilde{r}, \tilde{x}) - \rho u_{amb}| \tilde{r} d\tilde{r}}{\rho \beta (1 + 2(0.5 + 0.005\tilde{x})) (1 + 0.6|M - M_{amb}|)}} \left( \frac{\partial u(\tilde{r}, \tilde{x})}{\partial \tilde{r}} \right)_{\tilde{\beta}} \quad (4.9)$$

The shape of the turbulence intensity profile is described by Zelazny with an empirical function. The shape remains constant over the distance behind the body. The scaling is done at the wake half width  $\beta$  with equation (4.9).

The turbulence intensity profiles measured behind the wind turbine should be scaled with (4.9). Therefore a simplified version is used including the following assumptions:

- Because of velocities small against the Mach number, the air was assumed as incompressible and the density  $\rho$  was set to the same value inside and outside the wake.
- The term  $1 + 0.6|M_c - M_{amb}|$  describes the influence of the Mach number on the eddy viscosity, in the current case the difference between the mach number is smaller than 0.01 and the additive correction term therefore smaller than one percent. Therefore this term is set to one.

Based on a Gaussian shaped wind profile according to (4.3) and with the simplification, previously described, the formula (4.9) was evaluated. In this context the normalization previously described is used. The resulting term is:

$$S_{zelaz}(\tilde{x}) = \frac{u_c(\tilde{x})}{(1 - 0.5u_c(\tilde{x})) \sqrt{8(1 + 2(0.5 + 0.005\tilde{x}))} u_{\tilde{\beta}}(\tilde{x})} \propto \frac{\sigma_{u,\beta}}{u_{\tilde{\beta}}(\tilde{x})}, \quad (4.10)$$

which is proportional to the turbulence intensity at the position  $\beta$ .

### **Turbulence intensity related to shear**

The turbulence intensity in the wake could be directly related to the wind shear using Prandtl's mixing length approach [Abramovich, 1963]. Therefore the derivation of the wind speed profile is a direct measure of the amount of turbulence intensity in the wake. The standard deviation in the wake could be described by:

$$\sigma_u = l_u \frac{\partial u}{\partial r}, \quad (4.11)$$

where  $l_u$  is the mixing length.

For calculating the turbulence intensity at the half width of the wake  $\tilde{\beta}$ , the derivation of the normalized wind speed profile is used:

$$\left( \frac{\sigma_u(\tilde{x})}{u(\tilde{x})} \right)_{\tilde{\beta}} = L_u \left( \frac{\partial \tilde{u}(\tilde{x})}{\partial \tilde{r}} \right)_{\tilde{\beta}} \quad (4.12)$$

The mixing length is assumed to be inverse proportional to the product of the wind speed at the half width of the wake and the new introduced factor  $L_u$ :

$$l_u = \frac{1}{\tilde{u}_{\tilde{\beta}}(\tilde{x})} L_u, \quad (4.13)$$

As a first approach,  $L_u$  is assumed to be constant and the following scaling factor is used for the scaling of the turbulence intensity profiles:

$$S_{prandtl} = \left( \frac{\partial \tilde{u}(\tilde{x})}{\partial \tilde{r}} \right)_{\tilde{\beta}} \quad (4.14)$$

#### 4.2.4 Superposition of wake and ambient turbulence intensity

The turbulence intensity profiles include the ambient turbulence and the turbulence generated by the wake. To scale the profiles, it has to be differentiated between ambient turbulence intensity  $I_{amb}$  and the wake generated added turbulence intensity  $I_{add}$ . It was assumed that both turbulence intensities are directly additive as suggested by Magnusson as well [Magnusson, 1996], e.g.

$$I_{wake} = I_{amb} + I_{wake} \quad (4.15)$$

Other approaches, like the one from Quarton [Quarton and Ainslie, 1989], propose quadratic addition of the turbulence intensity, so that the turbulence intensity is squared and treated as energy, which could be directly added. This way of addition is investigated in section 4.5.1.

#### 4.2.5 Describing turbulence intensity profiles with a double Gaussian function

During wind tunnel measurements made by Medici [Medici, 2004] a double peak structure was discovered in the profiles of the standard deviation of the wind speed  $\sigma_u$  behind a model wind turbine in the far wake (see fig. 4.1). The structure evolves from four distinct peaks to two profiles broadening at the far wake at distances larger than 3D. The profiles of the standard deviation profiles behind large wind turbines from Nibe wind farm [Taylor, 1990] show the two peak structure in the intermediate wake. At a larger distance about 6D, the structure changes to a single peak.

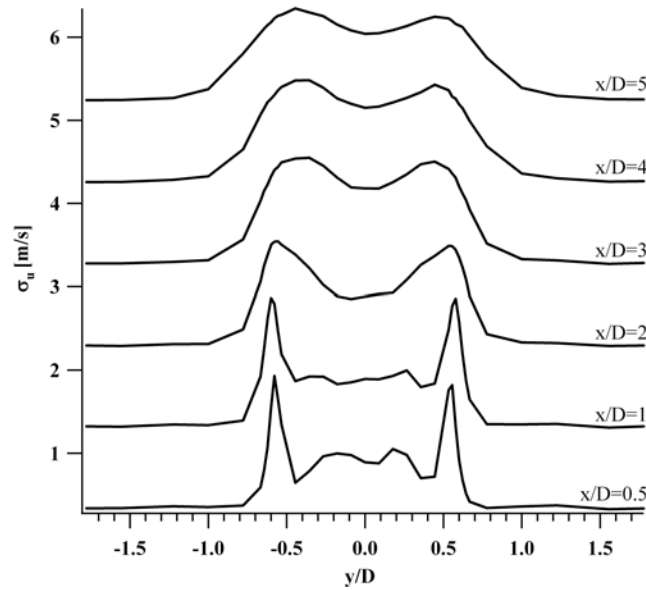


Figure 4.1: Profiles of the standard deviation of the wind speed ( $\sigma_u$ ) for  $x/D=0.5$  to  $x/D=5$  at an ambient wind speed of 5 m/s from wind channel measurements behind a model wind turbine. Redrawn from Medici [Medici, 2004]

Presented here is an approach to describe the standard deviation profiles with two superposed Gaussian profiles. The two profiles are horizontally displaced with the an displacement  $\tilde{y}_{disp}$  from the centerline. Here the displacement  $y$  is normalized by the rotor diameter  $D$  and therefore marked with a tilde. The width of the two profiles is described by the parameter  $\tilde{\alpha}$ :

$$G(\tilde{y}, \tilde{y}_0, \tilde{\alpha}, \tilde{y}_{disp}) = G_{max}(\tilde{x}) \left[ \exp\left(\ln(0.5) \frac{(\tilde{y} - \tilde{y}_{disp} + \tilde{y}_0)^2}{\tilde{\alpha}(\tilde{x})^2}\right) + \exp\left(\ln(0.5) \frac{(\tilde{y} + \tilde{y}_{disp} + \tilde{y}_0)^2}{\tilde{\alpha}(\tilde{x})^2}\right) \right]. \quad (4.16)$$

$G_{u,max}$  is the height of the profile. The development of the width and the offset of the profiles is investigated by fitting the equation to the measured profiles. The parameter  $\tilde{y}_0$  could be used to compensate for a vertical shift, which might be present in the measurements.

### 4.3 Description of the measurements

The development of the wake structure behind wind turbines should be investigated. Therefore wind speed and turbulence intensity profiles in the wake of a single wind turbine at different distances from the wind turbine are needed.

Data from wake measurements at different distances are rare. Pre-processed data exists from measurements from two wind farms sited located at Nibe and Sexbierum. They provide

single wake wind speed and turbulence intensity profiles at 4 and 3 different distances, respectively. The sites are described in the current section. The measured wind speed and turbulence intensity profiles were published in reports and are publicly accessible. These wind speed and turbulence intensity profiles from both sites are used in the following work.

The wake profiles were measured with meteorological masts at several distances behind the wind turbine. Horizontal wind speed and turbulence intensity profiles in the wake were measured with anemometers at different heights. Depending on the incoming wind direction, a horizontal profile of the wake can be derived.

Bin-averaging of wind direction, wind speed and wind speed standard deviation is used to obtain the horizontal wind speed and turbulence intensity profiles. The wind speed from a measurement mast in free stream condition is used for the bin averaging if available.

The horizontal distance from the wind turbine centerline is calculated as described in appendix C.

### 4.3.1 Experimental site Nibe

At the experimental Danish wind farm Nibe, single wake wind speed and turbulence intensity profiles at four different distances and at different heights were measured. The profiles were taken from the report [Taylor, 1990].

The wind farm Nibe is located at a coastal site in northern Jutland. In wake situations with southerly winds, the wind flows over flat, rough grassland with no significant obstacles. The estimated roughness length from measured vertical wind speed profiles are  $z_0=0.07-0.1m$  for the fetch over the rough grassland and  $z_0=10^{-4}m-10^{-2}m$  for westerly winds with the wind incident from the sea.

The site comprises two wind turbines aligned on the North-South axis (the true magnetic bearing is  $188^\circ$ ). The alignment of the wind turbines is parallel to the coast line with a distance of 150m to the west. The distance between the two turbines is 200m. The southern wind turbine is called 'B' and the northern 'A'. Two measurement masts were located between the wind turbines and two in a straight line behind wind turbine 'A' in a northern direction, as shown in Fig. 4.2.

The wind turbines used were Nibe experimental turbines with a rated power of 650 kW. The wind turbines had a rotor diameter of  $D = 40m$  and a hub height of  $H = 45m$ . The two wind turbines are three bladed with active yawing. In the appendix D.3 the power curve and thrust curve and an overview of the technical data of the wind turbines are presented.

Single wake measurements were performed behind wind turbine 'B', with wind turbine 'A' being switched off. The distances  $x$  of the wake profiles to the wind turbine 'B' are: 2.5D (100m), 4D (160m), 6D (240m) and 7.5D (300m), given in rotor diameters D.

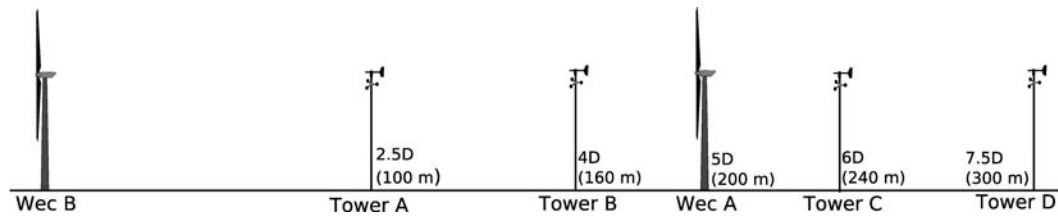


Figure 4.2: Schematic layout of the Nibe site. Wind profiles were taken at southern wind behind wind turbine 'B' from Taylor [Taylor, 1990]

The four meteorological masts were equipped with Risø cup anemometers and Risø wind vanes at the height of 45m. The data was measured with a sampling frequency of 2Hz and averaged over a period of 1min.

The measurement campaign was conducted in the period from January 1985 to July 1987. During this period 23866 records in wake situation with an averaging time of 1 min were recorded.

The horizontal wind speed and turbulence intensity profiles were measured at hub height. The profiles were bin averaged for an ambient wind speed  $u_{amb}$  of 8.0 to 9.1 m/s. The thrust coefficient of the wind turbine 'B' for this wind speed range is  $c_t=0.82$ .

Measurements of the ambient turbulence intensity were not available. For the current work the turbulence intensity was calculated as an average value from the wind direction sections in the turbulence intensity profiles which correspond to the free stream conditions. The resulting averaged values is  $I_{amb} = 9.3 \pm 0.2 \%$ .

### 4.3.2 Wind Farm Sexbierum

The measurements at wind farm Sexbierum provide single wake measurements at three different distances and a double wake measurements at one distance. The single wake measurements are used in this chapter for the scaling of profiles, whereas both single and double wake measurements are used later in this thesis for the validation of the turbulence intensity models.

The pre-processed wind speed and turbulence intensity profiles were taken from the report [Clijne, 1993].

The wind farm contains 18 wind turbines and seven meteorological masts scattered over the farm for measurements of ambient wind conditions. The wake measurements were done with mobile measurement masts, for measurements of ambient conditions the stationary mast M4 was used. The Fig. 4.3 shows the positions of the wind turbines, the mobile measurement masts and the stationary mast M4.

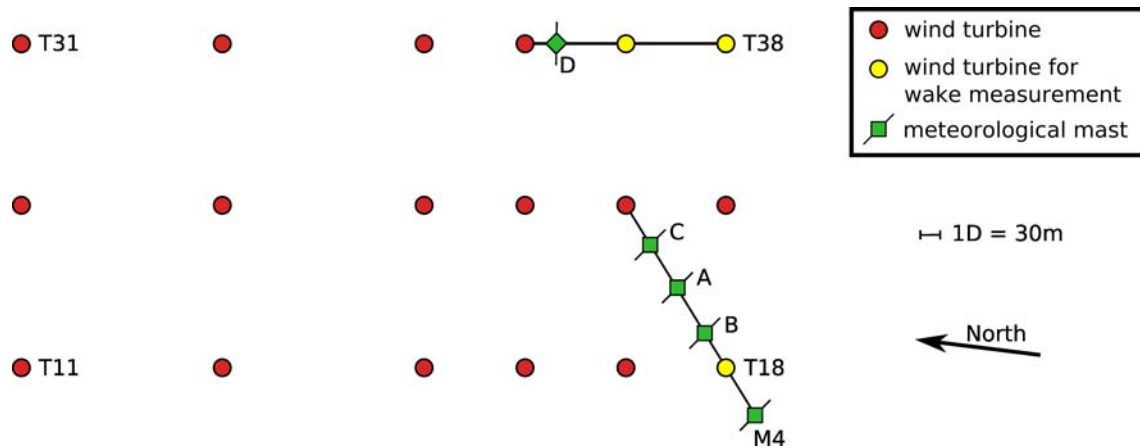


Figure 4.3: Layout of Sexbierum wind farm. The wind turbines are shown as circles. The rectangles mark the positions of the measurement masts. From the stationary masts only mast M4 is drawn.

The single wake measurements were performed behind turbine T18 at the three distances 2.5 D (75m), 5.5 D (165m) and 8 D (240m) behind the wind turbine T18 on the line T18 to T27 (see Fig. 4.4).

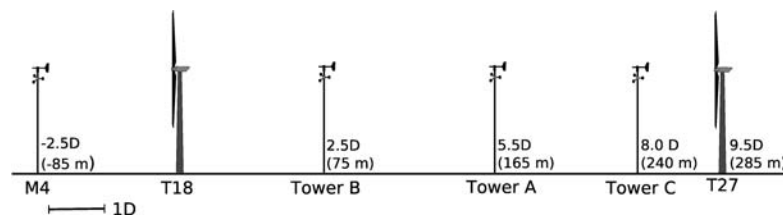


Figure 4.4: Arrangement for single wake situation at Sexbierum, the wind comes from the left. The drawing is only schematic, the distances do not comply with the rotor diameter of the drawn wind turbines.

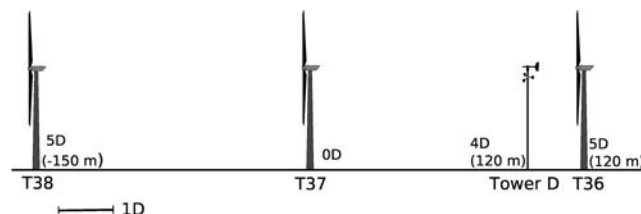


Figure 4.5: Arrangement for double wake situation at Sexbierum. The wind comes from the left.

The double wake measurements were carried out behind wind turbines T38 and T37 along



the line of T38 to T35. The meteorological mast was placed between wind turbine T36 and T37 (see Fig. 4.3)). The distance between the two turbines was  $5D$  and the mast was placed  $4D$  behind the downwind turbine (see Fig. 4.5). Wake condition exists for a wind direction of SSE.

Sexbierum is an experimental wind farm located in the Northern part of the Netherlands at approximately 4km distance to the shore. The landscape is farmland with a few scattered farm buildings as obstacles. The roughness length is about  $z_0 = 0.047m$ .

The wind turbines were three bladed HOLEC machines with a rotor diameter of  $D=30.1m$  at a hub height of  $H=35m$ . The rated power is 310kW. (For technical data see table D.4 in the appendix). The HOLEC machines have the rotor mounted downwind of the rotor.

The transportable masts were equipped with 3D-propeller anemometer at the heights of 47m, 35m and 23m at mast B and 35m (hub height) at mast A and C. The sampling frequency was 4 Hz and the averaging time 3 min.

The measurements were done between June and November 1992. The database used includes a total of 857 samples (3 min averaged) distributed over 5 wind speed bins, and is therefore rather small.

Horizontal profiles exist for the ambient wind speed bins  $u_0 = 6-7, 7-8, 8-9, 9-10$  and  $10-11$  m/s. A bin width of  $2.5^\circ$  for the wind direction was used. The wind speed vector was divided into a rectangular coordinate system  $u,v,w$ , calculated with a frame of reference where  $u$  is in the direction of the mean wind. The measured ambient turbulence intensity is  $I_{amb} = 9.5\%$ . Wind speed and turbulence intensity profiles exist for all three wind components.

In the current work only horizontal profiles at a hub height from the  $u$ -component were investigated.

The influence of the wind turbine T27 located downwind of tower 'C' might have created a retaining effect. No experiences and measurements of such effects at large scale wind turbines were measured yet and it is difficult to assess the effect on the profiles.

## 4.4 Scaling of wind speed profiles

The measured single wake wind speed profiles from Nibe and Sexbierum were investigated with respect to similarity. A Gaussian profile according to Eq. (4.3) was fitted to the wind speed deficit profiles at the different distances using least-square optimization. The resulting scaling parameters wake half width  $\tilde{\beta}$  and centerline deficit  $\tilde{u}_{cent}$  were used to scale these wind speed profiles. The scaling parameters are necessary for the scaling of turbulence intensity profiles, as discussed in the next section. A horizontal offset of the profiles is compensated with the parameter  $\tilde{y}_0$ .

Distance [D]	$\tilde{u}_{cent}$ [m/s]	$\tilde{\beta}$	$\tilde{y}_0$	ChiSquare	Points
2.5	$0.59 \pm 0.02$	$0.52 \pm 0.02$	$-0.18 \pm 0.02$	0.02	27
4	$0.32 \pm 0.02$	$0.58 \pm 0.02$	$-0.23 \pm 0.02$	0.01	37
6	$0.32 \pm 0.01$	$1.06 \pm 0.03$	$-0.40 \pm 0.03$	0.005	31
7.5	$0.20 \pm 0.02$	$0.90 \pm 0.07$	$-0.37 \pm 0.07$	0.005	30

Table 4.1: Estimated fit parameters for the Gaussian fit to Nibe wind speed profiles.

The offset of the normalized wind speed  $\tilde{u}_0$  is set to a constant value, usually assumed to be one, since at large  $\tilde{y}$  (e.g. outside the wake) no wind speed deficit is present. The normalized profiles of wind speed from Nibe wind farm show a wind speed outside the wake larger than unity. This would mean that the wind speed downwind of the wind turbine is higher than upwind. In the report no documentation about this phenomena is found. It will probably result from an offset in wind speed measured between the anemometers upwind and downwind of the wind turbine. The fit of the Gaussian profile will be affected in width and height, if not done at the baseline. Therefore the baseline will be corrected with the parameter  $\tilde{u}_0$ . The offset is calculated as a mean value, averaged over all intersections of wind speed profiles with free stream conditions. The average is based on the entire data sets of all towers.

After estimating the fit parameter, the wind speed deficit profiles  $\tilde{u}(\tilde{y}, \tilde{x})$  were scaled with the wake half width  $\tilde{\beta}$  in  $\tilde{y}$  direction as well as the wind speed deficit  $\tilde{u}_{def}(\tilde{y}, \tilde{x})$  with the centerline deficit  $\tilde{u}_{cent}$ . The shape of the wind speed profiles can be directly compared.

First the horizontal wind speeds from the Nibe wind farm are investigated, followed secondly by the profiles from Sexbierum.

#### 4.4.1 Wind speed profiles from Nibe wind farm

The four horizontal wind speed deficit profiles measured at hub height at the distances  $x = 2.5D, 4D, 6D$  and  $7.5D$  were used for scaling.

For the positive offset of the wind speed profiles towards higher values a value of  $\tilde{u}_0 = 1.03 \pm 0.03$  was estimated from the free stream conditions in the wake.

A Gaussian fit was applied to the wind speed profiles. The wind speed profiles are horizontal displaced from the assumed center of the wake. This might be a result from an offset in the wind direction measurements, which was not documented. The fitting algorithm corrects this offset with the parameter  $y_0$ . An example for the fit for tower B is shown in fig. 4.6. Only small differences between the fit and the wind speed profile can be seen. Table 4.1 gives an overview over the estimated fit parameter.

In Fig. 4.7 the normalized measured profiles from all four distances are given. The difference between the profiles is small and the low Chi-square show that the shape of the measured

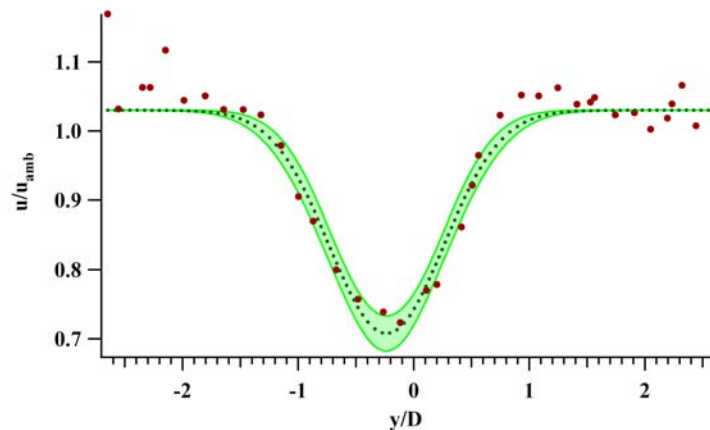


Figure 4.6: Gaussian fit to the normalized wind speed profile measured at the meteorological tower B. The wind speed is normalized with the ambient wind speed and the distance from the centerline with the rotor diameter.

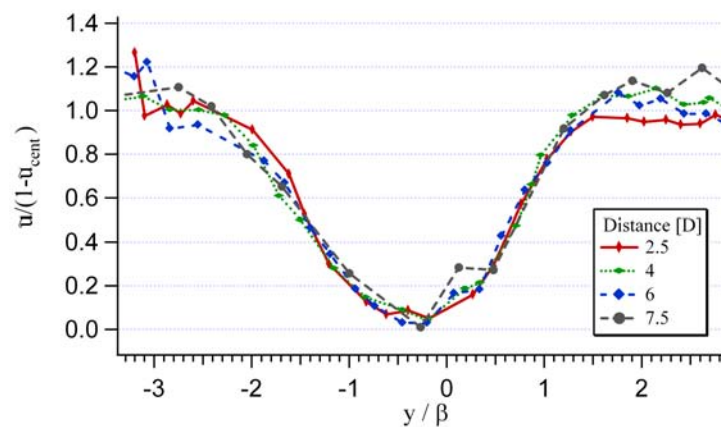


Figure 4.7: All four wind speed profiles from Nibe wind farm plotted with normalized axis. The distances between the measurement location and the wind turbine are listed in the box.

wind profiles is in good agreement with the shape of a Gaussian profile. The scaling with wind speed centerline deficit and wake half width works well.

As expected, the centerline deficit  $\tilde{u}_{cent}$  decreases with increasing distance, although no difference between the centerline deficit at  $4D$  and  $6D$  is present. The half width  $\beta$  of the wake shows a maximum at a distance of  $6D$  with a half width greater than one rotor diameter.

A maximum of the wake half width at an intermediate distance is unusual, as one would expect a continuous growing of the wake. A possible reason might be the location of wind turbine A between tower B at  $4D$  and tower C at  $6D$ . During the measurements, the wind turbine A was switched off. It might be possible that the flow around the nacelle affected the

measurements at tower C, since the nacelle was placed in a strait line between wind turbine B and the tower D during the centerline deficit measurements. The wake of the nacelle might decrease the wind speed at tower C noticeable. This explains why the centerline deficit shows almost no changes between the measurement in front of the wind turbine A and behind it. In a simulation with the Ainslie model, described in chapter 5, an increase of the centerline deficit of up to 20 % was observed, but not a widening of the wake profile.

#### 4.4.2 Sexbierum wind speed profiles

Single wake horizontal wind speed deficit profiles measured at the distances 2.5D, 5.5D and 8D were scaled. The profiles were estimated at hub height and an ambient wind speed bin  $u_{amb} = 9 - 10$  m/s. The wind speed profile (4.3) was fitted to the three wind speed deficit profiles.

Due to the large scatter of the wind speed profiles, a reliable estimation of the offset outside the wake could not be given. Therefore, the positive offset  $\tilde{u}_0$  was set to one. A slight horizontal displacement of the wind speed profiles occurred, which was taken into account with the parameter  $\tilde{y}_0$  in the data fit.

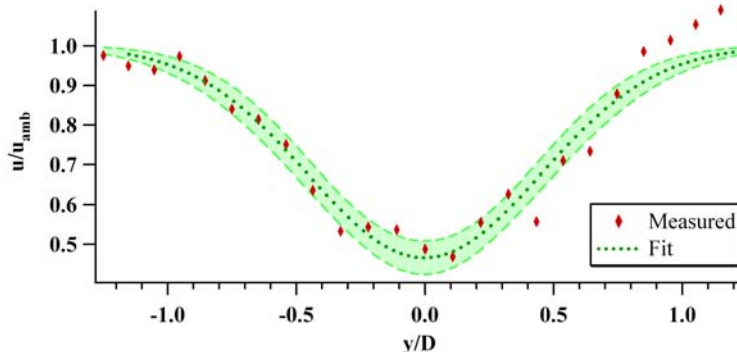


Figure 4.8: Gaussian fit performed on normalized wind profile measured at a distance of 2.5D behind the wind turbine at Sexbierum site.

An example fit is shown in fig. 4.8. The measured wind speed deficit profile follows the shape of the Gaussian profile, but shows a high scatter. The scatter results from a low number of measurements, as previously mentioned in the description of the wind farm. The results of the fit are listed in table 4.2.

The wake half width increases and the centerline deficit decreases continuously with increasing distance as expected. The Chi Square is two times higher than calculated for the Nibe wind farm, because of the high scatter in the wind speed deficit profiles.

Distance [D]	tower	$u_{cent}$ [m/s]	$\tilde{\beta}$	$\tilde{y}_0$	ChiSquare	Points
2.5	B	$0.53 \pm 0.03$	$0.53 \pm 0.03$	$-0.02 \pm 0.04$	0.01	21
5.5	A	$0.31 \pm 0.02$	$0.74 \pm 0.05$	$0.00 \pm 0.03$	0.07	16
8	C	$0.22 \pm 0.03$	$1.04 \pm 0.2$	$-0.03 \pm 0.2$	0.05	13

Table 4.2: Results of the fit of a Gaussian profile to the wind speed deficit profiles measured at wind farm Sexbierum.

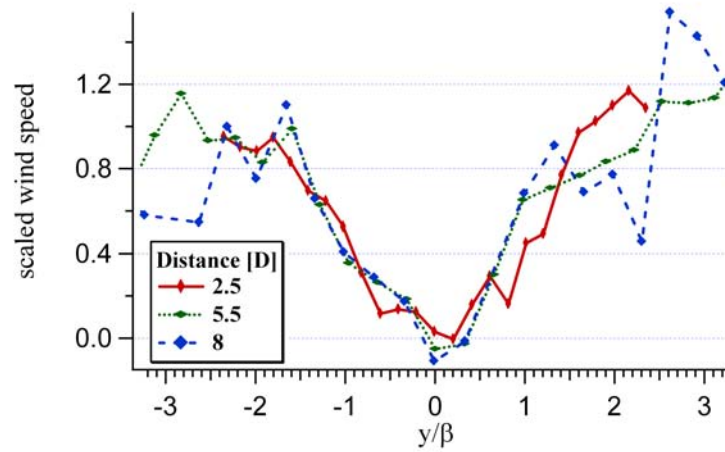


Figure 4.9: Scaled wind speed profiles from all three different distances behind the wind turbine at Sexbierum wind farm.

The wind speed is again scaled with the wind speed deficit  $\tilde{u}_{cent}$  and the normalized horizontal distance  $\tilde{y}$  with the wake half width  $\tilde{\beta}$ . The profiles of all three towers can be seen in fig. 4.9. Despite the high scatter, the wind speed profiles show a similar shape.

#### 4.4.3 Comparing the estimated parameters from both wind farms

The estimated values of the wake half width  $\tilde{\beta}$  and the centerline deficit  $\tilde{u}_{cent}$  from both wind farms were compared.

In Fig. 4.10(a) the centerline deficit is plotted against the distance behind the wind turbine in rotor diameters. The centerline deficits measured at Nibe wind farm are lower than the values measured at Sexbierum wind farm, except for the value at the third distance of 6D.

The wake half width plotted versus the distance can be seen in fig. (4.10(b)). The values measured at both wind farms increase in the same way except for the third measurement at Nibe wind farm, which shows a very broad wake half width.

Wind speed profiles from Nibe and Sexbierum measured at a distance of 2.5 D are shown in

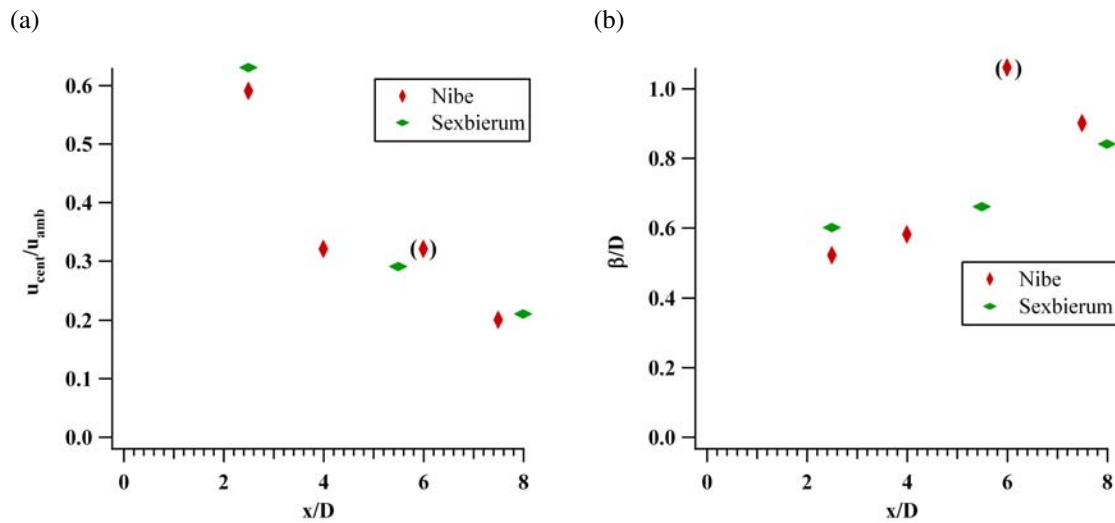


Figure 4.10: Estimated centerline wind speed deficit  $\tilde{u}_c$  from Nibe and Sexbierum wind farm versus the distance behind the wind turbine (a) and the wake half width  $\tilde{\beta}$  estimated from the wind speed deficit profiles from Nibe and Sexbierum versus the distance  $y/D$  (b).

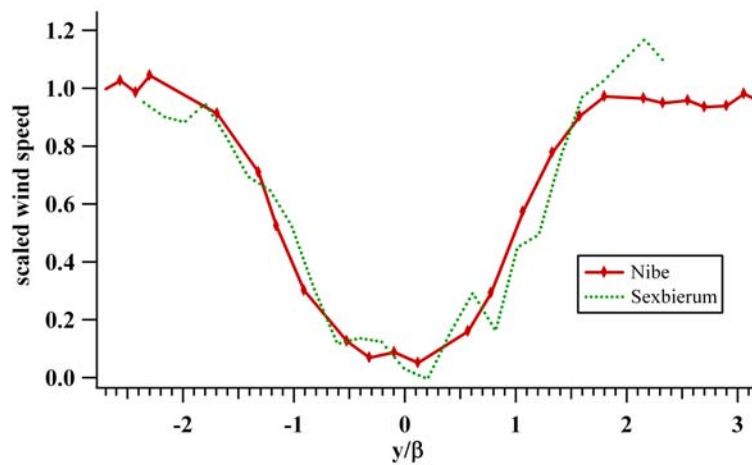


Figure 4.11: Normalized wind profiles measured at the wind farm Nibe and Sexbierum at a distance of  $2.5 D$  behind the wind turbine

fig. (4.11). Both profiles show the same shape. The Sexbierum profile has a higher amount of scatter.

The wake width and centerline wind speed deficit show a similar behavior and are in the same magnitude. An assessment of the development of both values with increasing distance could not be done due to a lack of data.

#### 4.4.4 Conclusion

The wind speed profiles measured at Nibe and Sexbierum wind farms can be described with a Gaussian profile. Even at the short distance of  $2.5D$ , where the profile is measured in the near wake, the Gaussian shape fits very well.

The scaling of the width of the profiles with the wake half width  $\tilde{\beta}$  and the wind speed deficit with the inverse centerline deficit  $\tilde{u}_{cent}$  works well.

A parametrization of the development of the centerline deficit and the wake half width with increasing distance could not be done, due to the low number of available distances. In recent wake models [Ainslie, 1988], the centerline deficit and the wake half width are related to the thrust coefficient and the ambient turbulence intensity. For the parametrization different combinations of these ambient conditions in conjunction with measurements at a minimum of four different distances behind the wind turbine are necessary in order to clearly identify a non linear behavior of the centerline deficit as well as the wake width with increasing distance. A non linear behavior can only be assumed given the present results.

### 4.5 Scaling of turbulence intensity profiles

The horizontal turbulence intensity profiles measured at the Nibe and Sexbierum wind farms were evaluated with different ways of scaling. A way to scale the turbulence intensity profiles for similarity should be identified.

Before scaling the turbulence intensity profile  $I_{wake}(\tilde{y})$ , the ambient turbulence intensity  $I_{amb}$  has to be removed from the turbulence intensity in the wake. Therefore the ambient turbulence is subtracted directly from the turbulence intensity profiles:  $I_{add} = I_{wake} - I_{amb}$ .

The ambient turbulence intensity was derived from averaging over the measured turbulence intensity at free stream conditions in the turbulence intensity profiles at Nibe wind farm. Measurements from a measurement mast in free stream conditions were used at Sexbierum wind farm.

The shape of the turbulence intensity profile in the wake depends on the distance behind the wind turbine. A distinct shape, as in the case of the wind speed profiles, the Gaussian profile, could not be found. For this reason a fit of certain profiles to the measured profiles can not be done, which makes the definition of a wake half width difficult. Therefore the width of the turbulence intensity profile is scaled with the half width of the wind speed profile  $\tilde{\beta}$ .

The turbulence intensity in the profiles is scaled in different ways: Scaling with two values estimated at different positions in the wake profile. Additionally, two ways of calculating the scaling parameter from the wind speed profile parameters were evaluated. These are in detail:

- The turbulence intensity at the position of the half width of the wind speed profile  $\beta$ :  $I_{add,\beta}$ .
- The maximum turbulence intensity  $I_{add,max}$
- The scaling parameter  $S_{zelaz}$  as proposed in the model from Zelazny in [Zelazny, 1972]
- The scaling parameter  $S_{prandtl}$  calculated from the derivation of the wind speed profile at position  $\tilde{\beta}$ , according to Prandtl's mixing length theory.

The average values of the turbulence intensity at the positions  $\pm\tilde{\beta}$  (the wake half width, estimated with the fit of the Gaussian profile to the wind speed profiles),  $I_{add,\beta}$ , and the maximum turbulence intensity  $I_{add,max}$  were estimated directly from the turbulence intensity profiles. For interpolation purposes a fit with a high order polynomial was applied to the turbulence intensity profiles and the maximum turbulence intensity  $I_{add,max}$  and  $I_{add,\beta}$  at the position  $\pm\tilde{\beta}$  were measured. After subtracting the ambient turbulence intensity both values are used for scaling of the turbulence intensity profiles.

The factor  $S_{zelaz}$  for scaling the turbulence intensity is calculated with equ. (4.10). For the calculation of the factor  $S_{prandtl}$ , the equation (4.14) is used. The required parameters  $\tilde{\beta}$  and  $\tilde{u}_c$  are taken from the results of the Gaussian fit to the measured wind speed profiles as described in the previous section. The scaling parameters were estimated for the turbulence intensity profiles at all distances behind the wind turbine. The scaling factors were applied to the profiles. For every scaling factor the turbulence intensity profiles from the different distances were plotted, where the turbulence intensity is scaled with the scaling factor and the width is scaled with the wake width  $\beta$ . The turbulence intensity profiles change their shape with increasing distance, therefore, the profiles could only be compared qualitatively.

The scaling factors  $I_{add,\beta}$ ,  $S_{zelaz}$  and  $S_{prandtl}$  are all estimated at the same position  $\beta$ . They can be directly compared and proportionality factors have been estimated  $L_{zelaz} = I_{add,\beta}/S_{zelaz}$  and  $L_{shear} = I_{add,\beta}/S_{prandtl}$ , when possible.

### 4.5.1 Nibe wind farm

The horizontal turbulence intensity profiles measured at Nibe wind farm were scaled in four different ways as described in the introduction. After calculation (of the four factors for the four different distances), the factors were applied to the turbulence intensity profiles.

The ambient turbulence intensity was calculated from the free stream conditions with  $I_{amb} = 9.3 \pm 0.2 \%$  which was subtracted from the values of turbulence intensity  $I_{add,\beta}$  and  $I_{add,max}$ .

The factors  $I_{add,\beta}$  and  $I_{add,max}$ , estimated from the turbulence intensity profiles, and the calculated scaling factors  $S_{zelaz}$  and  $S_{prandtl}$  from the wind speed profile parameters are listed in the Table 4.3.



Distance [D]	$I_{add,\beta}$ [%]	$I_{add,max}$ [%]	$S_{zelaz}$ [%]	$S_{prandtl}$ [%]
2.5	16.7	22.2	58.9	157.2
4	9.5	11.1	26.2	76.4
6	5.9	9.0	26.5	41.8
7.5	4.2	6.6	15.4	30.8

Table 4.3: Turbulence intensity scaling parameters for wake measurement from Nibe wind farm

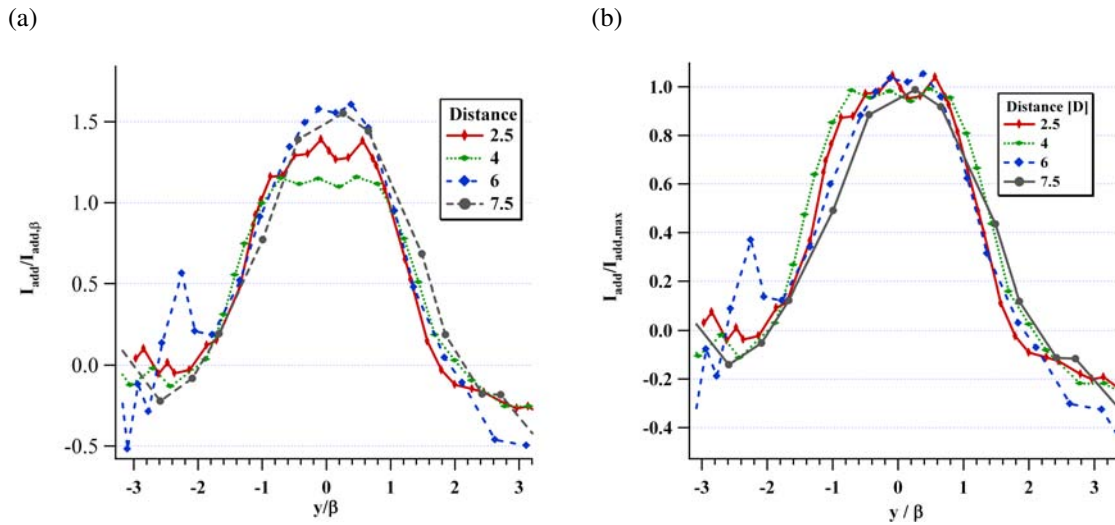


Figure 4.12: Scaled turbulence intensity profiles from Nibe wind farm. Turbulence intensity is scaled with the turbulence intensity estimated at  $\beta$ :  $I_{add,\beta}$  (a) and with the maximum turbulence intensity value  $I_{add,max}$  (b). The horizontal distance  $y$  is normalized with the wake half width  $\beta$  estimated from the wind speed profiles.

In Fig. 4.12(a) and 4.12(b), the turbulence intensity was scaled with  $I_{add,\beta}$  and  $I_{add,max}$ , respectively. In this and all following figures, the level of ambient turbulence intensity  $I_{amb}$  was already subtracted from the turbulence intensity profiles. The width of the profiles is scaled with the half width  $\beta$  of the wind speed profiles. The turbulence profiles show two distinct regimes: The profiles at the nearer distances of 2.5D and 4D show a plateau in the middle, whereas the plateau is not existent in the turbulence intensity profiles at 6D and 7.5D, the turbulence intensity profile approach a Gaussian shape.

The scaling of the distance  $\tilde{y}$  with the wind speed profile wake half width  $\tilde{\beta}$  results in nearly the same wake half widths at all four towers, when the height is scaled with  $I_{add,\beta}$ . Scaled with  $I_{add,max}$ , the width of the profiles differ slightly.

Scaling with  $I_{add,\beta}$ , all curves show nearly the same width at the turbulence intensity half value. The maxima are different in these cases: At the distances of 2.5D and 4D the plateaus

are lower than the maxima of the profiles at the farer distance, which agrees well with theory. The turbulence intensity profiles scaled with  $I_{add,max}$  have the same maxima, due to the definition of this scaling. At the turbulence intensity half value the width of the profiles differ more compared to the scaling with  $I_{add,\beta}$ .

A comparison of both scaling approaches requires the knowledge of the expected shape of the turbulence intensity profile. If one assumes that the main source of turbulence is the shear caused by the shear layer between the outer and the inner flow, the higher turbulence originates from the boundaries of the wake, where the wind shear occur first in the near wake of the wind turbine. This turbulence production will increase towards the center of the wake with increasing distance behind the wind turbine. The width of the turbulence intensity profile will not decrease in contrast to the width of the wind speed profile as in the case of the scaling with  $I_{add,max}$ . In this case the turbulence intensity profiles further downwind are smaller after scaling compared to the profiles nearer to the wind turbine. The turbulence intensity profiles scaled with  $I_{add,\beta}$  keep their width relative to the wind speed profile with increasing distance from the wind turbine, but increase the turbulence intensity towards the center. This results seems more reasonable and the scaling of the turbulence intensity profiles with  $I_{add,\beta}$  is preferred.

In Fig. 4.13(a) and 4.13(b) the calculated scaling factor  $S_{z_{elaz}}$  and  $S_{p_{randtl}}$  were applied to the turbulence intensity profiles. Large deviations exist between the turbulence intensity profiles scaled with  $S_{z_{elaz}}$ . The maxima do not show any trend with the distance of the profiles to the wind turbine. This is also reproduced in the width of the profiles at the half value of turbulence intensity, where the width of the profiles differ randomly. Scaling with  $I_{add,\beta}$  results in the two different patterns in the maxima, but the width of the profiles at the turbulence intensity half values match well, only the profile from the nearest distance is slightly too small.

In order to compare the calculated scaling values  $S_{z_{elaz}}$  and  $S_{p_{randtl}}$ , in Fig. 4.14 the ratios of  $S_{z_{elaz}}$  and  $S_{p_{randtl}}$  to  $I_{add,\beta}$  are plotted versus the distance behind the wind turbine. The values from  $L_{z_{elaz}} = I_{add,\beta}/S_{z_{elaz}}$  are highly fluctuating with distance, no distinct pattern is present. The ratio  $L_{p_{randtl}} = I_{add,\beta}/S_{p_{randtl}}$  shows a slight increase with increasing distance at the first three towers and a slight decrease at the furthest distance.

### Sensitivity analysis of the scaling

The sensitivity of the scaling of the turbulence intensity profiles is investigated in this section. The fit of wind speed deficit profiles with an offset deviating from unity, the effect of different ambient turbulence intensities and the approach of adding the ambient turbulence intensities are discussed with the example of the Nibe wake measurements .

For the scaling of the wind speed profiles, a Gaussian profile has been fitted to the measured wind speed profiles. Due to the high level of wind speed deficits larger than one, a parameter

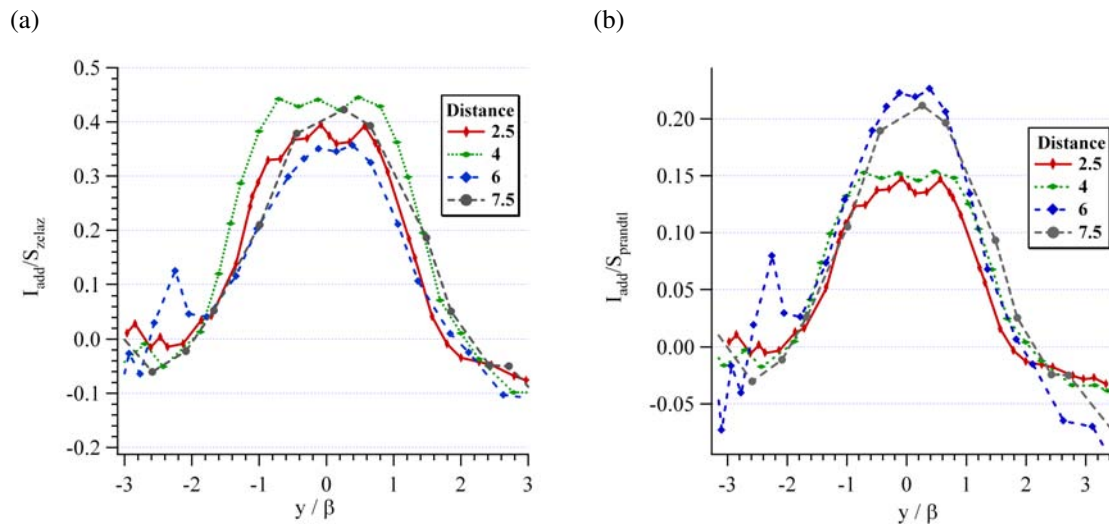


Figure 4.13: Turbulence intensity profiles from Nibe wind farm scaled with the approach from Zelazny (a) and with the mixing length approach from Prandtl (b).

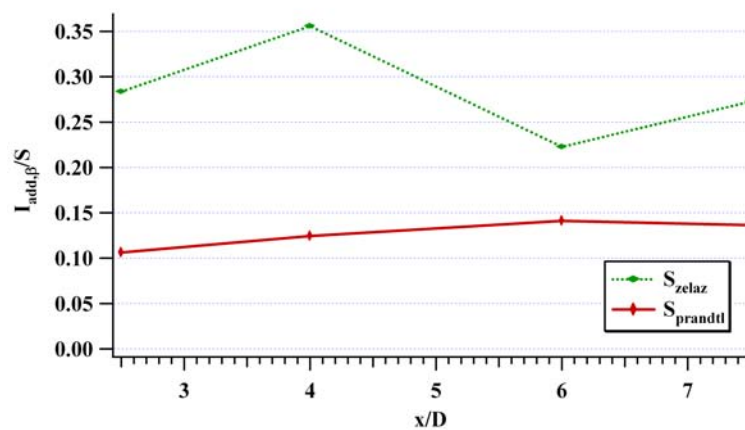


Figure 4.14: Ratio of scaling parameter between  $I_{add}(\beta)$  and scaling factor versus the distance  $D$

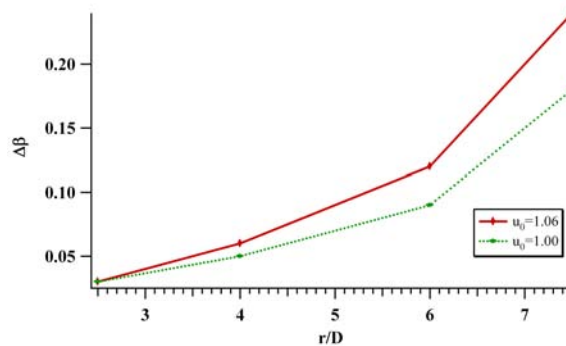


Figure 4.15: Deviation of the wake half width  $\beta$  between the estimated value at an offset of  $u_0=1.03$  and the fitted curves with  $u_0=1.00$  and  $u_0=1.06$

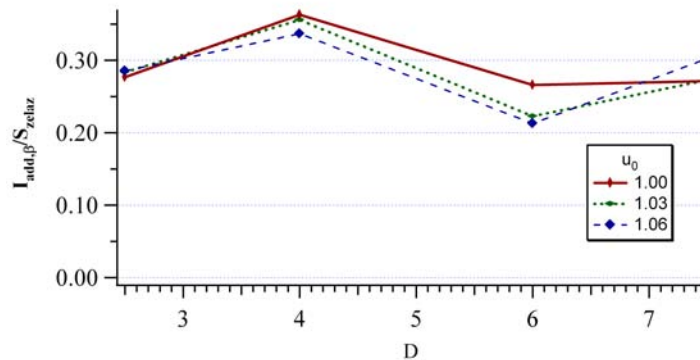


Figure 4.16: Ratio of  $I_{add,\beta}/I_{zelaz}$  vs the distance for three different values of  $u_0$ : 1.00, 1.03 and 1.06.

$u_0$  was introduced to correct these deviations. In the previous section this value was set to  $u_0=1.03$ . According to the estimated standard deviation of 0.03, the cases  $u_0=1.00$  and  $u_0=1.06$  were evaluated. The change in  $u_{cent}$  is directly related to the different  $u_0$  and change in the same way. It produces a constant offset. The difference between the wake half width  $\beta$  at  $u_0=1.00$  and  $u_0=1.06$  and the wake half width estimated with  $u_0=1.03$  increases with increasing distance (see fig. 4.15). The value increase according to a power law with an exponent of 3.3 to 3.5.

The different parameter sets of  $u_{cent}$  and  $\beta$  for  $u_0=1.00$  and  $u_0=1.06$  were used to estimate  $I_{add,\beta}$ ,  $S_{zelaz}$  and  $S_{prandtl}$ . For  $I_{add,\beta}$ , the upper and lower values of  $u_0$  induce a maximum deviation of  $I(\beta)$  of 8% to the value at  $u_0=1.03$ . The influence of the offset  $u_0$  on the calculation of the scaling factor  $S_{zelaz}$  from Zelazny is shown in fig. 4.16. At 2.5 D the value remains nearly constant, at larger distances there are deviations of 20% at a distance of 6 D and the value at  $u_0$  is 1.0.

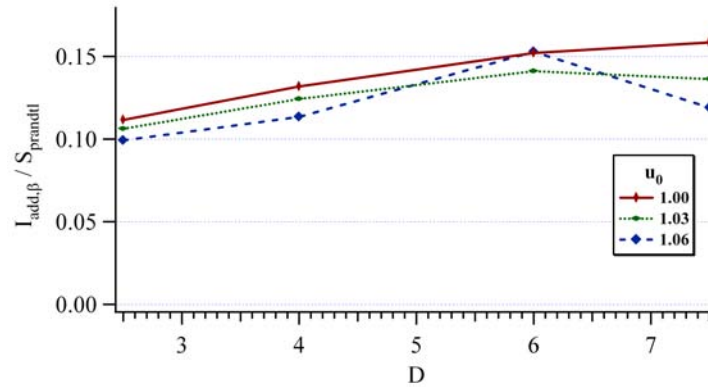


Figure 4.17: Ratio  $I_{add,\beta}/I_{shear}$  vs distance from the wind turbine for three different values of  $u_0$ : 1.00, 1.03 and 1.06.

The ratio of  $I_{add,\beta}/S_{prandtl}$  is plotted versus the distance from the wind turbine for all four towers and the three different  $u_0$  in fig. 4.17. The data points for the three different conditions are shifted to a higher ratio of  $S_{prandtl}$  with decreasing  $u_0$ , except for the value from  $u_0 = 1.06$  at distance 6.5 D, which is higher than the value of  $u_0=1.03$ . The maximum deviation of 8 % occurs at the distance 7.5 D. In contrast to the the deviation of  $\beta$  caused by the selection of  $u_0$ , the deviation of the ratio  $I_{add,\beta}/S_{prandtl}$  only amounts up to 8%, which results in the case of lower  $u_0 = 1.00$  in a constant shift of the scaling factor. This does not affect the scaling of the profiles.

Deviations in estimation of the values of ambient turbulence intensity influences the estimated ratios  $I_{add,\beta}/S$  with an offset. In case of direct added ambient turbulence intensity this offset could be written as:

$$L_{off} = \frac{I_{off}}{S}, \quad (4.17)$$

where  $I_{off}$  is the deviation of the turbulence intensity and  $S$  is the scaling factor depending on the used method. Therefore the offset in scaling of the profiles is strongly dependent on the scaling factor. An increase of 0.2 % of ambient turbulence intensity (standard deviation of ambient turbulence intensity) causes the values  $I_{add,\beta}$  to increase by 1 % at tower 1 and by 4 % at tower 4. The estimation of ambient turbulence intensity introduces an error of around 4 % at the margins of the standard deviation of the ambient turbulence intensity.

Based on the assumption that adding turbulence intensities is adding energies, ambient and added wake turbulence intensity can be added quadratically. The scaled turbulence intensity profiles (with  $I_{add,\beta}$ ) with quadratic addition can be seen in fig. 4.18. In the present case a quadratic addition of turbulence intensity does not lead to significant differences in scaling of turbulence intensity profiles compared to the linear addition of ambient turbulence intensity and therefore is not used further on.

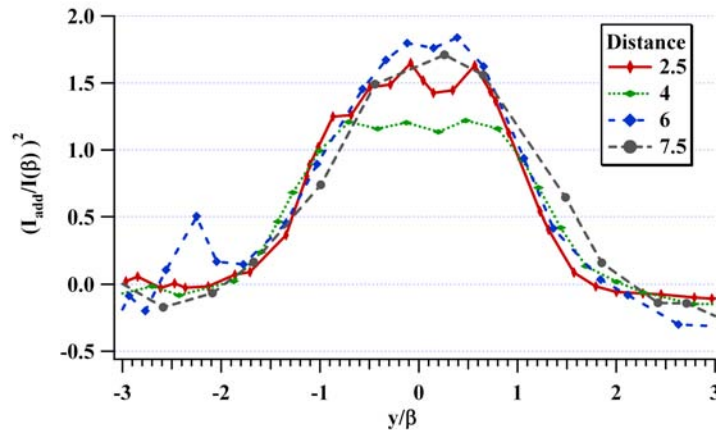


Figure 4.18: Scaled turbulence intensity profiles from Nibe wind farm. Scaling with  $I(\beta)$  and quadratic adding of ambient turbulence intensity

## Conclusion

The scaling of turbulence with  $I_{add,\beta}$  and  $I_{add,max}$  show different results. The former scaling gives a good agreement in the profile slopes at  $\beta$  and the latter shows a good agreement in the maximum turbulence intensity, as expected. Assuming that the main turbulence generation started at the borders of the wake and evolve to the center with increasing distance, it is not be expected that the turbulence intensity wake width decrease relative to the wake width of the wind speed profiles. Therefore a scaling with  $I_{add,\beta}$  is proposed for the scaling of the turbulence intensity profiles.

The scaling with  $S_{prandtl}$  show similar results to the scaling with  $I_{add,\beta}$ . As a first order approximation  $S_{prandtl}$  can be assumed to be proportional to  $I_{add,\beta}$ . A value of  $L_{shear} = 0.13 \pm 0.02$  has been calculated for the ratio  $I_{add,\beta}/S_{prandtl}$ . With the prandtl approach it is possible to calculate the scaling factors of the turbulence intensity profiles for the wind farm Nibe.

The ratio of  $I_{add,\beta}$  and  $S_{zelaz}$  varies between 0.22 and 0.36. No relationship seems to be present. In the case of the Nibe wind farm, the approach from Zelazny is not valid.

## 4.5.2 Sexbierum wind farm

The scaling of the turbulence intensity as done in the previous section with four different approaches is applied to the turbulence intensity profiles from Sexbierum wind farm. Due to the relative high scatter of the turbulence intensity profiles, only the estimated scaling parameters were compared. An example for the scaling with  $I_{add}$  is shown in fig. 4.19.

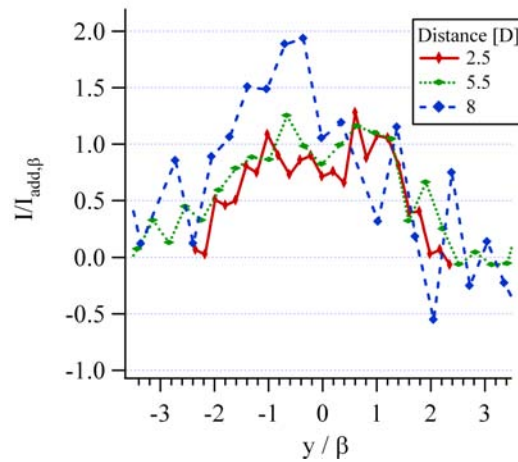


Figure 4.19: Sexbierum wind farm turbulence intensity profiles scaled with the turbulence intensity  $I_{add,\beta}$ . The distance  $y$  is scaled with the wind speed profile wake half width  $\beta$ .

The ambient turbulence intensity is estimated by measurements from a free standing measurement mast with a value of  $I_{amb} = 10.7\%$ .

As a result of the high scatter in the measurements, an estimation of the maximum turbulence intensity and the turbulence intensity at position  $\beta$  can not be achieved with a high accuracy. Therefore the resulting scaling factors are only listed  $I_{add,\beta}$ ,  $I_{add,max}$ ,  $S_{zelaz}$  and  $S_{prandtl}$  (see Table 4.4). Only the scaling factor  $I_{add,\beta}$  is plotted in Fig. 4.19.

Distance [D]	$I_{add,\beta}$ [%]	$I_{add,max}$ [%]	$S_{zelaz}$ [%]	$S_{prandtl}$ [%]
2.5	16.3	16.5	25.6	138.6
5.5	8.5	8.8	50.6	58.0
8	3.5	6.6	17.1	29.4

Table 4.4: Estimated scaling parameters for Sexbierum wind farm.

The table reveals the difference between the maximum and the turbulence intensity at  $\beta$  is small. The values of  $I_{add,\beta}$  and  $I_{add,max}$  are very similar at the distance 2.5D and at the distance 5.5D. Therefore the scaling of these profiles with both methods show nearly the same results. At a distance of 8.5 D the scaling parameters deviate by about 2.5 %. This profile contains the highest scatter of data points and has an asymmetric shape.

Due to the high scatter the comparison is limited to the values estimated and calculated at the wake half width  $\beta$ :  $I_{add,\beta}$ ,  $S_{zelaz}$  and  $S_{prandtl}$ . For this comparison, the ratio between the turbulence intensity at position  $I_{add(\beta)}$  and the scaling factor  $S$ , calculated according to the approach of Zelazny  $S_{zelaz}$  and Prandtl  $S_{prandtl}$  is plotted versus the distance in Fig. 4.20.

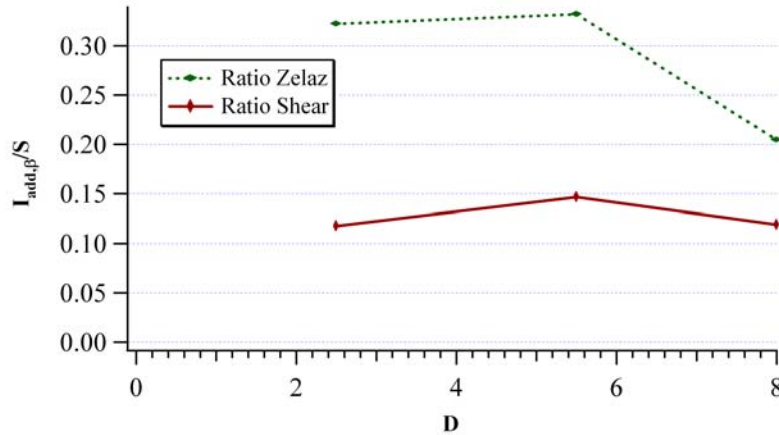


Figure 4.20: Ratio between the  $I_{add,\beta}$  and the scaling parameter  $S$  vs the distance for the approach from Zelazny and Prandtl approach.

The resulting values show the same order of magnitude as the values of the Nibe wind farm. The values  $S_{zelaz}$  are proportional to  $I_{add,\beta}$  at the distances  $2.5 D$  and  $5.5D$ . At  $8D$  the ratio deviates by a factor 0.5 from the previous points. The ratio with  $S_{prandtl}$  is nearly constant and therefore shows no trend. The mean values is  $L_{shear} = 0.13 \pm 0.02$

## Conclusion

The high scatter in the turbulence intensity profile prevented a precise estimation of the scaling parameters  $I_{add,\beta}$  and  $I_{add,max}$  from the turbulence intensity profiles.

The averaged ratio between  $I_{add,\beta}$  and  $S_{prandtl}$   $L_{shear}$  gives an average value of  $L_{shear} = 0.13 \pm 0.02$ . The value shows only small variations with distance to the wind turbine as has been observed in the results of Nibe wind farm as well.

## 4.6 Fit of double Gaussian profile to standard deviation profile

The standard deviation profiles estimated from the turbulence intensity profiles show a double peak structure as describe in section 4.2.5. The development of this structure with increasing distance is investigated at the example of the Nibe measurements.

Standard deviation profiles measured at the Sexbierum site have a very high scatter and could therefore not be used here.



#### 4.6. FIT OF DOUBLE GAUSSIAN PROFILE TO STANDARD DEVIATION PROFILE 81

Tower	Dist. [D]	$\sigma_{u,max}$	$\tilde{y}_{disp}$	$\tilde{\alpha}$	$\tilde{y}_{off}$	Chi-Square
1	2.5	$1.0 \pm 0.03$	$0.35 \pm 0.01$	$0.39 \pm 0.02$	$0.15 \pm 0.01$	0.12
2	4	$0.73 \pm 0.03$	$0.39 \pm 0.01$	$0.46 \pm 0.02$	$0.19 \pm 0.02$	0.03
3	6	$0.50 \pm 0.02$	$0.51 \pm 0.03$	$0.92 \pm 0.05$	$-0.03 \pm 0.03$	0.01
4	7.5	$0.41 \pm 0.04$	$0.42 \pm 0.09$	$0.81 \pm 0.13$	$-0.05 \pm 0.06$	0.04

Table 4.5: Resulting parameters from double Gaussian fit to wind speed standard deviation profiles from Nibe wind farm.

The equation (4.16) has been fitted with a least-square-method to the standard deviation profiles from Nibe. The development of the width  $\tilde{\alpha}$  and the displacement  $\tilde{y}_{disp}$  of the Gaussian profiles is discussed.

After subtracting the ambient turbulence intensity  $I_{amb}$  from the turbulence intensity profiles, the standard deviation profiles were calculated by multiplying the resulting difference profiles with the wind speed profile.

##### 4.6.1 Nibe wind farm

The double Gaussian function fitted to the standard deviation profiles measured at tower A and tower D are shown in fig. 4.21(a) and 4.21(b). The resulting parameters from the fit are listed in Table 4.5. The Chi-Square values are very low, so a good adjustment of the double Gaussian profile to the measured data is possible. With increasing distance to the wind turbine the double peak structure present at tower A and B evolves to a single peak structure at tower C and D. The results of the single peak fit show a larger width of the two Gaussian distributions  $\alpha$  compared to the width at the two nearer distances, whereas the distance of the peaks to the centerline  $\tilde{y}_{disp}$  is increased at the larger distances with regard the width at tower A and B.

The change of the double peak structure to a single peak could be well described with the double gaussian profile. Also, the fact that the maximum of the two Gaussian distributions are still separated from each other at the single peak situation, shows that the double Gaussian structure is still present at larger distances. Therefore it can be used to describe the shape of the turbulence intensity profiles in the intermediate and far wake of the wind turbine.

In fig. 4.22 the half width of the wake  $\tilde{\alpha}$  and the offset  $\tilde{y}_{disp}$  are plotted versus the distance. For comparison the development of the half width of the wind speed profile  $\tilde{\beta}$  is drawn. The half width  $\tilde{\alpha}$  of the double Gaussian profiles follow the half width of the wind speed profiles

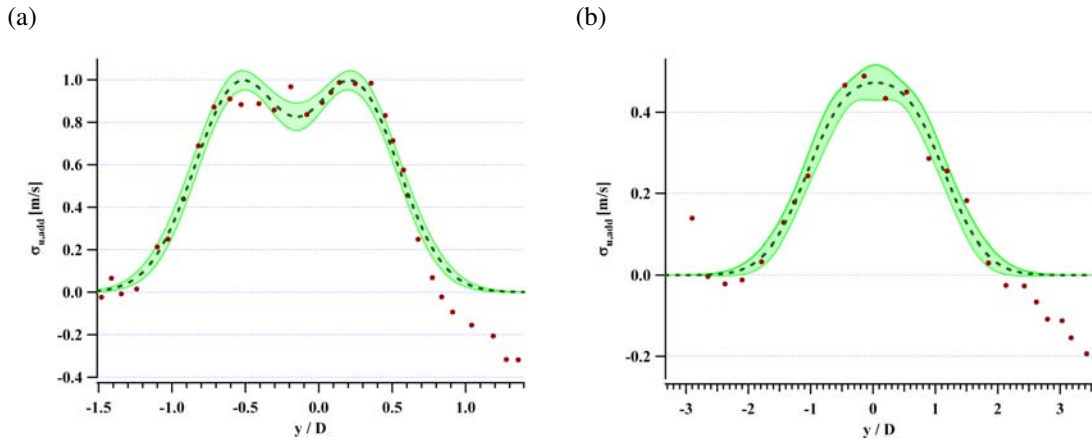


Figure 4.21: Double Gaussian fit to the profiles of standard deviation measured of the wind speed at tower A (a) and tower D (b). The measurement is shown as dots, the fit as broken-line.

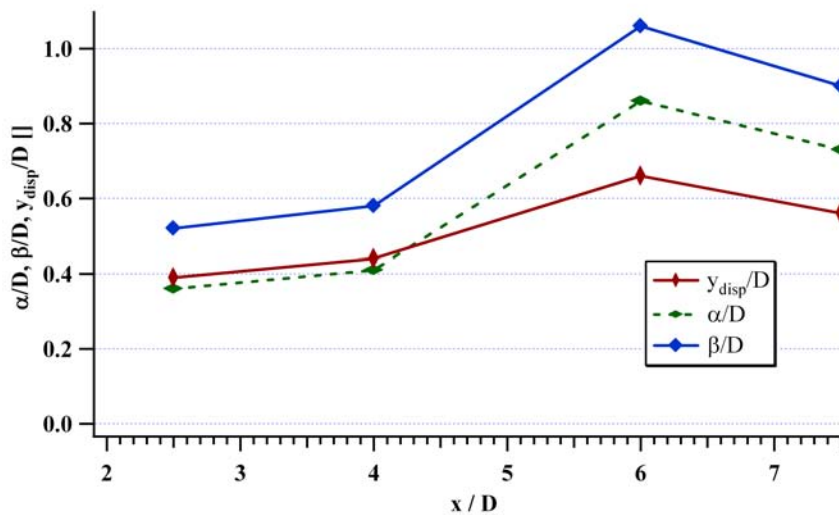


Figure 4.22: Development of the distant between the Gaussian profiles  $\tilde{y}_{disp}$  and the width  $\tilde{\alpha}$  with increasing distance. Additionally the wake half width of the wind speed profiles  $\tilde{\beta}$  is shown.

$\tilde{\beta}$  with a constant offset. The offset  $\tilde{y}_{disp}$  approximately shows a linear increase, if the data point at a distance of 6 D is excluded, where the turbulence intensity and wind speed profiles show an unusual behavior as described before.

The double Gaussian profile is able to reproduce the standard deviation profile of wind speed and therefore reproduces the turbulence intensity profiles in the wake for all four distances from the measurements at Nibe wind farm.

## 4.7 Conclusion

Wind speed profiles measured at single wake conditions behind wind turbines at Nibe and Sexbierum were investigated for similarity. The wind speed profiles were fitted to a Gaussian distribution and successfully scaled with the estimated wake half width and the wind speed centerline deficit.

The turbulence intensity profiles of the single wake measurements were scaled with different methods to prove similarity. The profiles can be scaled, but show only limited similarity as the turbulence intensity profile change from a broad shape with a plateau in the center to a Gaussian shaped profile.

In order to perform a scaling of the wake turbulence intensity, the ambient turbulence intensity had to be removed from the profiles. This was achieved by subtracting the ambient turbulence intensity directly from the profiles, giving good results.

The wake half width  $\tilde{\beta}$ , estimated from the wind speed profiles, was used successfully to scale the wake width of the turbulence intensity profiles. In combination with the scaling of the turbulence intensity estimated at  $\tilde{\beta}$ , the width of the profiles remain constant over the different distances behind the wind turbine and the changes of a plateau to a maximum occurs only in the center of the turbulence intensity profile. This was the best way to achieve a correct scaling since the turbulence is assumed to be generated at the border of the wake and then transported to the center of the wake with increasing distance. Therefore a decay of wake width in the turbulence intensity profile relative to the wind speed profile would therefore not be expected.

Good results in scaling of the turbulence intensity are achieved when using the approach from Prandtl to scale the turbulence intensity profiles at the wake half width. The ratio between estimated turbulence intensity at the wake half width and the calculated scaling factor is almost constant with a value of  $L_{shear} = 0.13 \pm 0.03$  observed for both wind farms.

The method by Zelazny, applying an eddy-viscosity approach to scale the turbulence intensity profiles gave highly scattered/varying results.

To scale the turbulence intensity profiles with an eddy-viscosity approach show high fluctuating results.

The parametrization of the wind speed standard deviation profiles with a double Gaussian profile shows that the width of the Gaussian profiles is related to the wake half width of the wind speed deficit profiles. The distance between the profiles indicate a linear increase with increasing distance.

The combination of scaling and the double peak feature of the profile is a good basis for developing a model for the description of the turbulence intensity in the wake. However due to the low number of measurements a parametrization could only be of preliminary nature.

The assumption of a double peak structure is able to describe the turbulence intensity profile in the near wake ( $2.5D$ ) and intermediate region ( $3-5D$ ), as it could reproduce the shape of the turbulence intensity profiles in all regions. These regions in the wake will be very important in the future for the siting of wind turbines onshore. The distance between wind turbines will decrease to the near or intermediate wake region due to an increasing exploitation of the sites onshore. The exact knowledge of the turbulence intensity is therefore quite important for the lifetime of the wind turbines.

# Chapter 5

## Describing the turbulence intensity in the wake of a wind turbine

### 5.1 Introduction

The turbulence intensity behind wind turbines is increased compared to the ambient flow, as already seen in the previous chapter. The present results show that the decay of the additional turbulence intensity in the wake is faster than the decay of the velocity deficit, so it is not proportional to the wind speed profile.

The calculation of the additional turbulence intensity in the wake was investigated in recent years by many researchers. The majority of the formulas describe the maximum turbulence intensity in the wake with an empirical formula estimated by fit from measured data.

The first approaches to calculate the turbulence intensity in a wake behind a wind turbine were made by Quarton and Ainslie [Quarton and Ainslie, 1989]. They proposed an empirical formula for the mean turbulence intensity, derived from wind tunnel measurements. A similar approach was presented by Crespo 1990 [Crespo et al., 1990]. Magnusson and Smedman [Magnusson and Smedman, 1999] developed a semi-empirical model, based on the wind speed profile in the wake. The main assumption was to use the traveling time of the wind in the wake as a main parameter. The most common used model is from Frandsen and Thogersen [Frandsen and Thogersen, 1999]). They developed an analytical model for the design turbulence, which includes the characteristics of the wind turbine material through the Wöhler factor in the calculation of the turbulence intensity. The model is part of the IEC international standards [IEC, 2005] and allow a fast calculation of turbulence intensity in a wind farm.

The aim of this thesis was to develop an analytical expression to describe the turbulence intensity profile in the wake of a wind turbine based on the parameters delivered by the wind speed profile.

In this scope, the approach from Magnusson and Smedman was investigated and improved. Therefore the analytical expression for the wind speed profile from Magnusson and Smedman and in addition the model from Ainslie [Ainslie, 1988] were used.

Also, an approach is presented, which is based on the results of the previous chapter. The profile is described by a function consisting of two Gaussian distributions and scaled with the derivation of the wind speed profile. For this purpose the results gained at the previous chapter were adapted to the wind speed profiles calculated with the model from Ainslie.

Magnusson uses an analytical formula for the calculation of the wind speed profile from the growth of smoke plumes in the free atmosphere. The travel time of the wind in the wake instead of the wind speed is recognized as the important parameter.

The well established wind layout softwares Windfarmer [Garrad and Hassan, 2004], Windpro [Energi- Og Miljødata (EMD), 2004], Wasp[Risø National Laboratory, 2004] and FLAP [Oldenburg, 2003] uses mainly two different models of wind speed deficits in the wake in order to calculate the farm efficiency: The analytical model after Jensen [Jensen, 1993] and the eddy viscosity solver after Ainslie [Ainslie, 1988].

The analytical approach from Jensen assumes a constant wind speed deficit over the whole wake area, but depending on the distance to the wind turbine. The wake width is growing linearly with increasing distance from the wind turbine and is estimated experimentally. The wind speed deficit is gained by solving the mass balance equation.

The eddy viscosity approach from Ainslie assumes an empirical inertial wind speed deficit profile in the near wake region, which is modeled with a numerical solver to farther distances. The model is steady state and works with an axisymmetric profile. This method is generally seen as the best model on the market and obtained best results in accuracy in the comparison of wind speed models in the ENDOW project [Schlez et al., 2001].

The chapter starts with a description of the calculation of wind speed profiles with the models from Magnusson et. al and Ainslie. Then a description of different ways of calculating the turbulence intensity in the wake of a wind turbine will be given. This is followed by the description of the improved approach based on the Magnusson et. al model and the description of the turbulence intensity profiles based on the derivation of the wind speed profile. The chapter concludes with a section about the superposition of wakes.

## **5.2 Wind speed wake models**

### **5.2.1 Analytical model after Magnusson**

Magnusson et. al. ([Magnusson and Smedman, 1996]) proposed a model to calculate the wind speed deficit in the wake of a wind turbine in dependence of the traveling time  $t$  of

the wind between the wind turbine and the measurement point instead of the distance  $x$ , as usually used. The traveling time is calculated from the ambient wind speed:  $t = x/u_{amb}$ . This time  $t$  is scaled with the time  $t_0$ , e. g. the point where the wind speed profile merges from a double peak structure to a single peak. The equation is estimated with measured data from Alsvik wind farm ([Magnusson and Smedman, 1996]):

$$t_0 = \frac{1}{f} \ln \left( \frac{H}{z_0} \right) \frac{R}{H}. \quad (5.1)$$

The equation includes the hub height  $H$ , the rotor radius  $R$ , the frequency  $f$  of the rotor rotation and the roughness length  $z_0$ . The maximum wake deficit  $A(t)$  was found to be based on the traveling time and the thrust coefficient  $C_t$ :

$$A(t) = 0.4 \ln \left( \frac{t_0}{t} \right) + C_t. \quad (5.2)$$

The wake is described with a Gaussian profile. The wake width, e.g. the standard deviation of the profile  $\sigma_y$  and  $\sigma_z$ , is again scaled with the transport time for both components  $y$  and  $z$ :

$$\sigma_{y,z} = 0.56 \sqrt{\frac{t}{t_0}}. \quad (5.3)$$

The wind speed deficit profiles are subsequently formulated as:

$$\frac{\delta u}{u}(t, y, z) = A(t) \exp \left( -\frac{(y/R)^2}{2\sigma_y^2} \right) \left( \exp \left( -\frac{(z/H)^2}{2\sigma_z^2} \right) + \exp \left( -\frac{(z+2H)^2}{2\sigma_z^2} \right) \right). \quad (5.4)$$

The last two terms should include the effects of the ground. Based on theories from air pollution dispersion a mirror image in the ground is assumed to produce the same wake and is superimposed to the first wake. The distances  $y$  and  $z$  are counted from the centerline of the wind turbine.

### 5.2.2 Model after Ainslie

After reviewing the analytical approach from Magnusson, the eddy viscosity model from Ainslie [Ainslie, 1988] is discussed. The model consists of an empirical set of formulas, which describes the mean wind speed profile at the end of the near wake and an axis-symmetric solver, which calculates the wind speed deficit profile at farer distances. The solver works with the Reynolds equation, with the boundary layer approximation and an eddy viscosity closure.

The distance between wind turbine and measurement point is  $x$  and the radial distance to the wake centerline is  $r$ .

For simplification, the wind speeds were normalized with the ambient wind speed  $u_{amb}$  and distances were normalized with the rotor diameter  $D$ . Normalized parameters were marked with a tilde over the letter.

The wind speed is named  $U$  in direction downwind of the wind turbine and  $V$  perpendicular to  $U$ , pointing from the centerline radial outwards. The wind speed components  $U$  and  $V$  are split into a stationary and a fluctuating part:  $U = u + u'$  and  $V = v + v'$ , where  $u$  and  $v$  are the stationary and  $u', v'$  are the fluctuating parts, respectively.

### Near wake profile

The near wake wind speed deficit profile is calculated for a distance of 2 diameters behind the wind turbine. The shape of the profile is assumed Gaussian, consisting of the centerline deficit  $\tilde{u}_{cent} = 1 - \tilde{u}(r=0)$  and a factor for the width of the wake  $\gamma$ :

$$\tilde{u}(\tilde{r}) = 1 - \tilde{u}_{cent} \exp(\gamma \tilde{r}^2). \quad (5.5)$$

The formula for the wind speed centerline deficit  $\tilde{u}_{center}$  was estimated from wind tunnel experiments and depends on the thrust coefficient  $c_t$ :

$$\tilde{u}_{cent} = c_t - 0.05 - (16c_t - 0.5)I_{amb}. \quad (5.6)$$

The factor  $\gamma$  is derived from the momentum deficit equation between the ambient flow and the flow in the wake. The momentum deficit caused by the rotor is calculated from the thrust coefficient. The resulting equation is:

$$\gamma = \frac{4\tilde{u}_{cent}(2 - \tilde{u}_{cent})}{D^2 c_t}. \quad (5.7)$$

### The differential equations

For the description of the stationary flow in the far wake, the Reynolds equation with the boundary layer approximation in cylindrical coordinates was used. This includes the following simplification of the Navier-Stokes-equation:

- The flow is incompressible
- The pressure gradient is zero
- No driving forces
- Gradients from the standard deviation of wind speed fluctuations  $\sigma_u, \sigma_v$  are neglected.



Then, the Reynolds equation for the velocity component  $u$  is written:

$$\tilde{u} \frac{\partial \tilde{u}}{\partial \tilde{x}} + \tilde{v} \frac{\partial \tilde{u}}{\partial \tilde{r}} = -\frac{1}{\tilde{r}} \frac{\partial}{\partial \tilde{r}} \overline{\tilde{r} \tilde{u}' \tilde{v}'}, \quad (5.8)$$

where the Reynolds stress term is already substituted by the eddy viscosity  $\varepsilon$  closure:

$$-\overline{u'v'} = \varepsilon \frac{\partial \tilde{u}}{\partial \tilde{r}}. \quad (5.9)$$

And the continuity equation for incompressible flows:

$$\frac{\partial \tilde{u}}{\partial \tilde{x}} + \frac{1}{\tilde{r}} \frac{\partial}{\partial \tilde{r}} (\tilde{r} \tilde{v}) = 0. \quad (5.10)$$

The boundary conditions for the wind speed are given by the wind speed deficit profiles at  $\tilde{x} = 0$  and at the upper, lower and  $\tilde{x} = \infty$  boundaries by the ambient wind speed  $u_{ambient}$ , e. g. normalized 1.

### Assumptions for the eddy viscosity

The eddy viscosity describes the turbulent convection between different layers in the flow. In the case of the wake flow, the main sources in the far wake are the ambient turbulence and the wind shear induced turbulence. The effects from rotor generated turbulence are neglected, due to the assumption that these flows are already dissipated in the far wake.

Ainslie constructed the total eddy viscosity with an ambient eddy viscosity term  $\varepsilon_{amb}$  and a wake induced eddy viscosity  $\varepsilon_{add}$ , which depends on the distance to the wind turbine and is independent of  $\tilde{r}$ :

$$\varepsilon_{wake}(\tilde{x}) = \varepsilon_{amb} + \varepsilon_{add}(\tilde{x}) \quad (5.11)$$

For the ambient eddy viscosity, Ainslie used an approach used by Monin [Monin and Yaglom, 1971]:

$$\varepsilon_{amb} = \frac{\kappa u^* h}{\phi_m(L, h)}, \quad (5.12)$$

based on the friction velocity  $u^*$ , the height above ground  $h$ , the von Kármán constant  $\kappa = 0.4$  and a function which includes the thermal stratification of the atmosphere  $\phi(L, h)$ .  $\phi(L, h)$  depends on the height and the Monin-Obukhov-length and could be set equal to one for neutral stratification. Together with the logarithmic wind profile and the empirical relation between the friction velocity and the standard deviation of wind speed  $\sigma_u = 2.4u^*$ , the following relationship for the eddy viscosity at hub height can be derived:

$$\varepsilon_{amb} = \kappa \frac{I_{amb} u_{amb}}{2.4} H, \quad (5.13)$$

where the standard deviation was directly substituted by the ambient turbulence intensity  $I_{amb}$  and  $H$  is the hub height of the wind turbine.

The added eddy viscosity should be proportional to the product of the typical length and the velocity scale. For the length the wake width  $r_w$  is chosen. According to Ainslie this definition is the radial distance from the centerline, where the wind speed deficit remains on 2.38 % of the ambient wind speed. The resulting equation is

$$\varepsilon_{add} = kr_w \left( \frac{\tilde{u}_{cent}}{\tilde{u}_{amb}} \right). \quad (5.14)$$

In case of a not fully developed turbulence in the wake, typically at distances of 3-5 rotor diameter, a filter function is used:

$$F(x) = \begin{cases} 0.65 + \sqrt[3]{\frac{x-4.5}{23.32}} & \text{for } \tilde{x} < 5.5 \\ 1 & \tilde{x} \geq 5.5 \end{cases} \quad (5.15)$$

The filter function is applied multiplicative to the added eddy viscosity.

### Meandering of the wind speed profile

In the wake model proposed by Ainslie an external stationary wind field has been assumed. In the case of a meandering of the wake, Ainslie developed an expression to correct the centerline deficit:

$$\tilde{u}_{cent,korr} = \tilde{u}_{cent} \sqrt{(1 + 7.12(\sigma_\theta \tilde{x} / \beta)^2)}, \quad (5.16)$$

where  $\tilde{x}$  is the axial distance behind the wind turbine,  $\sigma_\theta$  the standard deviation of wind direction fluctuations and  $\beta$  the wake width of the wind speed deficit profile.

### 5.2.3 Ainslie in the Farm Layout Program (FLaP)

The model from Ainslie is used within FLaP with a finite difference solver to calculate the axial-symmetric wind speed deficit profiles in the wake of a single wind turbine. For wind farm arrays the wind speed deficits are superimposed and rotor-averaged at the downwind wind turbines.

## 5.3 Models of turbulence intensity in the wake

Four different approaches to calculate the added turbulence intensity in the wake are described, namely the empirical equations from Quarton et. al and from Crespo et. al, the engineering approach from Frandsen et. al and the model from Magnusson, which describes a complete wake profile.

### 5.3.1 Quarton formula

Based on wind channel and field measurements, Quarton et. al. [Quarton and Ainslie, 1989] developed an empirical formula for the added turbulence intensity in the wake of wind turbines. The assumption was made, that the added turbulence intensity  $I_{add}$  is based on the thrust coefficient  $c_t$ , the ambient turbulence intensity  $I_{amb}$  as well as the ratio between the distance  $\tilde{x}$  from the rotor and the near wake length  $\tilde{x}_n$ . The near wake length is the distance behind the wind turbine, where the region of the near wake ends, thus the distance when the wind speed deficit changes from constant over the wake area to a Gaussian profile. For the three terms power exponents were estimated by fit from experimental data:

$$I_{add} = 4.8c_t^{0.7}I_{amb}^{0.68}\left(\frac{\tilde{x}}{\tilde{x}_n}\right)^{-0.57}. \quad (5.17)$$

The near wake length  $\tilde{x}_n$  could be set to  $2D$  as proposed by Ainslie [Ainslie, 1988] or calculated with an approach following Vermeulen [Vermeulen, 1980]. It is not clear from the paper, if Quarton calculated an average or a maximum turbulence intensity value in the wake of a wind turbine. The ambient turbulence intensity has to be given in percent.

An optimized version of the Quarton formula, based on newer measurements of the maximum turbulence intensity is described in the PhD thesis of Waldl [Waldl, 1997]:

$$I_{add,max} = 5.7c_t^{0.7}I_{amb}^{0.68}\left(\frac{\tilde{x}}{\tilde{x}_n}\right)^{-0.96}. \quad (5.18)$$

In the case of Quarton et. al. ([Quarton and Ainslie, 1989]), the added turbulence intensity is defined by:

$$I_{add} = \frac{\sqrt{\sigma_{u,w}^2 - \sigma_{u,amb}^2}}{u_{amb}} \quad (5.19)$$

where  $\sigma_{u,w}$  is the standard deviation of wind speed and  $\sigma_{u,amb}$  in the ambient conditions.  $u_{amb}$  is the wind speed in free flow conditions.

### 5.3.2 Empirical formula by Crespo

A similar approach was followed by Crespo et. al. [Crespo and Hernández, 1993], who used computer simulations based on his developed UPMWAKE code for deriving an empirical formula for the maximum added turbulence intensity.

Like the approach from Quarton it is based on the ambient turbulence intensity, the distance and either on the thrust coefficient or the wind speed deficit. The main difference is the scaling of the distance which is done with the rotor diameter  $D$  instead of the near wake length:

$$I_{add,max} = 0.73a^{0.8325}I_{amb}^{-0.0325}\left(\frac{x}{D}\right)^{-0.32}. \quad (5.20)$$

The induction factor  $a$  describes the state of the wind turbine and is defined by:

$$a = \frac{\Delta u}{2u_{amb}} \quad (5.21)$$

or alternatively with the thrust coefficient  $c_t$ :

$$a = 1 - \sqrt{1 - c_t}. \quad (5.22)$$

The formula was validated by comparison with experimental results from wind tunnel and field measurements.

For the calculation of the turbulence intensity Crespo normalizes the standard deviation according to Quarton with the ambient wind speed and adds the square of the turbulence intensities.

### 5.3.3 Approach from Frandsen and Thogersen

Frandsen and Thogersen [Frandsen and Thogersen, 1999] empirically estimated the maximum turbulence intensity in the wake, based on the thrust coefficient of the wind turbine. The formula should be valid for in-the-row closely spaced machines:

$$I_{add,max} = \frac{1}{c_1 + c_2 \frac{\bar{x}}{\sqrt{C_t}}}. \quad (5.23)$$

The equation was fitted to four data sets and the estimated constants are  $c_1=1.5$  and  $c_2=0.1$ .

Frandsen assumed the rotor generated wake turbulence intensity profile as Gaussian shaped. This is expressed in the following equation:

$$I_{wake} = I_{amb} \left( 1 + \alpha \exp \left( - \left[ \frac{\theta}{\theta_w} \right]^2 \right) \right). \quad (5.24)$$

where  $\theta$  is the angle between wind direction and direction of the downwind wind turbine. The constant  $\alpha$  describes the maximum turbulence intensity in the wake with the ratio of maximum added turbulence intensity and ambient turbulence intensity:

$$\alpha = \sqrt{\left( \frac{I_{add,max}}{I_{amb}} \right)^2 + 1} - 1. \quad (5.25)$$

Frandsen normalized the turbulence intensity with the ambient wind speed  $u_{amb}$  and used quadratic superposition of the ambient wind speed with the wake turbulence intensity. The model is presumed to be conservative.

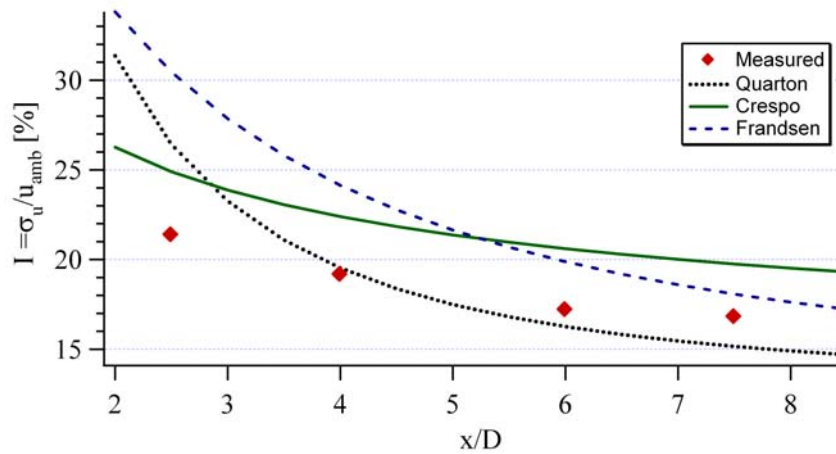


Figure 5.1: Development of the maximum turbulence intensity with increasing distance of the turbulence intensity profiles from the Nibe measurements. The maxima values are estimated from the TI-profiles in the wake of the wind turbine. The approaches from Quarton, Crespo and Frandsen are drawn in.

#### 5.3.4 Comparison of Quarton, Crespo and Frandsen model to Nibe measurements

Both approaches from Quarton and Crespo are compared to the measurements at the Nibe wind farm. The results are shown in fig. 5.1. The turbulence intensity estimated from the Quarton model decays fast with increasing distance, whereas the Crespo model acts conservative at all distances. The Frandsen model is a conservative approach and therefore overpredicts the turbulence intensity values at all distances. The different normalization methods of the models utilizing either the ambient wind speed or the wake wind speed, make it difficult to compare the anticipated results from the models. The maximum turbulence intensities of the different normalization methods could easily be estimated from measured profiles. There, the turbulence intensity profile and the wind speed profile are present and the turbulence intensity profiles can be transformed from one representation to the other: The maximum turbulence intensity can be estimated. In order to transform the models, a theoretical wind speed profile has to be assumed and the location of the maximum turbulence intensity in the wake profile must be known, since the location usually is not on the centerline of the profile and it changes slightly with the transformation. Then, the model can be transformed in order to allow a normalization based on the second approach.

### 5.3.5 Magnusson and the dependency on the traveling time

Magnusson et. al. [Magnusson and Smedman, 1996] described the added turbulence intensity  $I_{add}$  in the far wake of a wind turbine with two assumptions: the level of turbulence in the outer part of the wind turbine is induced by local turbulence production and in the core dominates transverse turbulence advection. These two processes are described by two terms, as argued by Magnusson: The first term assumes that the local turbulence is directly produced by the shear stress and is assumed to be proportional to the derivation of the stationary radial wind speed profile. The second term assumes that turbulence is advected from the outer region to the inner region and has its maximum in the centerline. These processes are taken to be proportional to the wind speed deficit. The resulting formula is:

$$I_{add}(r) = f_A(t_0/t) \frac{\partial(u(r/D)/u_{amb})}{\partial(r/D)} + f_B(t_0/t) \frac{u(r/D)}{u_{amb}} \quad (5.26)$$

Both factors  $f_A$  and  $f_B$  depend on the traveling time of the wind  $t$  between wind turbine and measurement point as well as on  $t_0$ , the time the wake needed to enter the far wake, e.g. when a Gaussian profile is developed. The assumption for  $t_0$  is based on an empirical formula equ. (5.1), which depends on the hub height, rotational frequency and roughness length. The relationships for  $f_A$  and  $f_B$ , estimated by a fit are:

$$f_A(t_0/t) = 0.76 \left( \frac{t_0}{t} \right) \quad (5.27)$$

$$f_B(t_0/t) = 0.6 \left( 1 - \frac{t_0}{t} \right). \quad (5.28)$$

The equations were adjusted to data from the Alsvik wind farm with situations of different traveling times, e.g. wind speeds in the wake, and different atmospheric stratification.

### 5.3.6 Calculation of turbulence intensity from the eddy viscosity

The eddy viscosity is describing the Reynolds stress from the derivation of the wind profile in radial direction. Therefore it could be used as a measure for the turbulence induced by the wind shear in the wake.

Assuming that the description of turbulence intensity in the far wake is nearly similar to the atmosphere turbulence intensity, the relation 5.13 for the estimation of the ambient eddy viscosity  $\epsilon_{amb}$  could be used in a reverse way: The turbulence intensity could be calculated from the eddy viscosity in the wake<sup>1</sup>. The rearranged equation is of the form:

$$I_{wake} = \epsilon \frac{2.4}{\kappa u_0 H} \quad (5.29)$$

Originally, Ainslie related  $\sigma_u^2$  directly to the shear stress  $\overline{u'v'}$  by a constant factor of 0.4 [Quarton and Ainslie, 1989].

<sup>1</sup>This way was used by Lange et. al. [Lange et al., 2003] to calculate the turbulence intensity with the Ainslie solver in FLAP.

## 5.4 The Shear-stress model

The presented model is a further development of the approach of Magnusson et. al. to describe the turbulence intensity in the wake of a wind turbine. The application of the assumptions of Magnusson et. al. to the measurements from Nibe do not give satisfying results, as described later in chapter 6 about the validation of the turbulence intensity models. The Magnusson et. al. approach was improved for the Nibe wind farm conditions (in the way to produce better results at the Nibe wind farm). The model from Magnusson et. al. was combined with the model from Ainslie and a calculation of turbulence intensity in the wake from the eddy viscosity was performed. In chapter 6 this model was validated with successfully at Nibe and two additional wind farms.

### 5.4.1 Description of the shear-stress model

The equation for describing the added turbulence intensity in the wake of a wind turbine consists of two terms:

$$I_{add}(r, x) = I_{shear}(\tilde{u}(\tilde{r}, \tilde{x})) + I_{conv}(\tilde{u}(\tilde{r}, \tilde{x})) \quad (5.30)$$

Both terms are based on the normalized wind deficit profiles  $\tilde{u}(\tilde{r}, \tilde{x}) = 1 - u(\tilde{r}, \tilde{x})/u_{amb}$ , which describe the radial wind speed deficit profile at a lateral distance  $x$  from the upwind turbine and radial distance  $r$  from the center of the wake.  $u_{amb}$  describes the incoming free wind speed.

#### First term: Shear generated turbulence

Wind shear generated turbulence is assumed to be highest at the steepest gradients of the wind speed profile as could be seen in the sketch from Townsend [Townsend, 1949] in fig. 5.2 (Shown here are the different terms of the turbulent kinetic energy equation in the wake of a circular cylinder in dependency of the distance from the centerline.) Therefore wind shear generated turbulence can be directly related to the derivative of the wind speed deficit profile. The wind speed deficit profile from the Ainslie model [Ainslie, 1988] is used to calculate the shear produced turbulence intensity. As in the empirical formulas from Quarton and Crespo, the added turbulence intensity in the wake is related to the ambient turbulence intensity  $I_{amb}$ . This relationship is considered by the turbulence intensity in the wake  $I_{mean}$ . The mean wake turbulence intensity  $I_{mean}$  resulting from ambient turbulence intensity and wind shear effects in the wake of a wind turbine is estimated according to the approach by Lange et al. as described in section 5.3.6.

$$I_{shear} = AI_{mean}(x) \frac{\partial \tilde{u}(\tilde{r}, \tilde{x})}{\partial \tilde{r}} \quad (5.31)$$

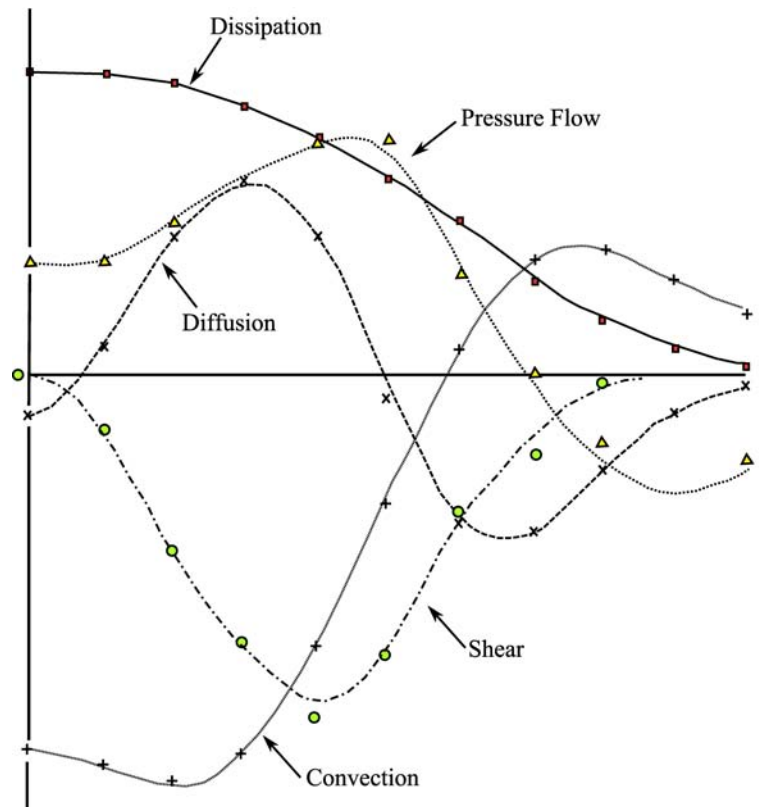


Figure 5.2: Terms of the turbulent energy balance of a circular cylinder in the self-similar regime. Redrawn from Townsend [Townsend, 1949]

$A$  is an empirical parameter, which has to be found by a fit.

The calculation of  $I_{mean}$  assumes that the turbulence intensity in the wake is proportional to the eddy viscosity. The eddy viscosity is a parameter to relate the Reynolds stress to the derivative of the wind speed profile. Therefore it is a direct measure of the turbulence generated by wind shear. The eddy viscosity in the wake is derived from the eddy viscosity approach used in the Ainslie model. The eddy viscosity depends only on the distance  $x$  from the wind turbine and represents therefore a mean value.

### Second Term: Convection dependent term

This term describes the convection processes inside the wake and the meandering, which cause a smoothing of the turbulence intensity profile. The convection of the turbulent kinetic energy is largest in the center region of the wake and low at the border as can be seen in fig. 5.2. The convection term is parameterized as a Gaussian distribution and is therefore assumed to be proportional to the Gaussian shaped wind speed deficit profile  $\tilde{u}_{def} = 1 -$



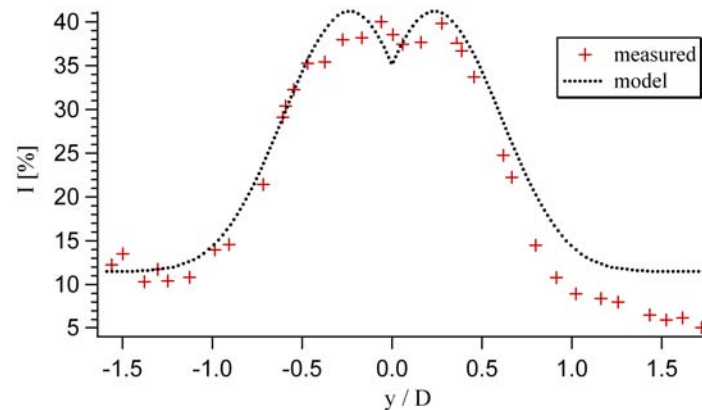


Figure 5.3: Measured and modeled horizontal turbulence intensity profile from Nibe wind farm at 2.5D distance versus horizontal distance normalized with the rotor diameter from the center of the wake

$\tilde{u}(\tilde{r}, \tilde{x})$ , following an approach from Magnusson [Magnusson and Smedman, 1999]:

$$I_{conv} = B(1 - \tilde{u}(\tilde{r}, \tilde{x})) \quad (5.32)$$

Like the parameter A, B defines the influence of the second term.

## 5.4.2 Model parameters

The empirical constants A and B of the model were obtained by a fit to the horizontal turbulence intensity profile from the Nibe measurements at a distance of 2.5D (see fig.(5.3)). The wind direction bins are in the range of  $2^\circ$  at all distances behind the wind turbine. Therefore, the profiles at nearer distances includes more data points than at further distances. For this reason the turbulence intensity profile at the nearest distance of 2.5 D was used.

The resulting values  $A=0.78$  and  $B=0.45$  are used for all subsequent calculations.

## 5.5 Scaling approach

### 5.5.1 Introduction

Based on the investigation of the previous chapter 4 an approach to model the turbulence intensity in the wake of a wind turbine with scaling is presented. The relationship consists of the description of the turbulence intensity profile by the superposition of two Gaussian distributions, scaled with the derivation of the wind speed profile at the wake half width  $\tilde{\beta}$ .

The parametrization is based on the results of the previous chapter. The values were adapted to the model from Ainslie, which is used to calculate the wind speed profiles in the wake.

## 5.5.2 Description of Scaling approach

The equations for the scaling approach consists of three terms: The scaling term  $I_{add,\tilde{\beta}}$ , the term for the shape of the profile of the wind speed standard deviation (including  $G$ ) and the wind speed profile  $u(\tilde{r})$ :

$$I_{add}(\tilde{r}) = I_{add,\tilde{\beta}} \frac{G(\tilde{r}, \tilde{r}_{disp}, \tilde{\alpha})}{G(\tilde{\beta})} \frac{u_{\tilde{\beta}}}{u(\tilde{r})}. \quad (5.33)$$

### Scaling term

In the previous chapter the turbulence intensity profiles from wake measurements at Nibe wind farms were successfully scaled with the derivation of the measured wind speed profile. The added turbulence intensity  $I_{add}$  at the position  $\beta$  is scaled with the derivation of the winds speed profile:

$$I_{add,\tilde{\beta}} = L_u \frac{\partial \tilde{u}}{\partial \tilde{r}}. \quad (5.34)$$

$L_u$  is a parameter for the ratio between the scaling and the turbulence intensity.

### Standard deviation term

The standard deviation profile of wind speed in the wake of a wind turbine is assumed to have a profile of two superimposed Gaussian profiles based on Eq. 4.16 with an axisymmetric approach with  $\tilde{r} = \tilde{y}$ :

$$G(\tilde{r}, \tilde{r}_{disp}, \tilde{\alpha}) = \left[ \exp\left(\ln(0.5) \frac{(\tilde{r} - \tilde{r}_{disp})^2}{\tilde{\alpha}(\tilde{x})^2}\right) + \exp\left(\ln(0.5) \frac{(\tilde{r} + \tilde{r}_{disp})^2}{\tilde{\alpha}(\tilde{x})^2}\right) \right]. \quad (5.35)$$

The profiles have the wake width  $\tilde{\alpha}$  and the distance  $\tilde{r}_{disp}$  from the centerline. The standard deviation profile is normalized to unity at the position  $\tilde{\beta}$ .

### The wind speed profile

The standard deviation of the wind speed has to be normalized with the wind speed profile, e.g. the local wind speed. This is done with the wind speed profile normalized to unity at the half width of the wake ( $\tilde{\beta}$ ).

$$u(r) = u_0 \left[ 1 - u_{cent} \exp\left(\ln(0.5) \frac{\tilde{r}^2}{\tilde{\beta}^2}\right) \right]. \quad (5.36)$$

### 5.5.3 Parametrization

Three parameters have to be estimated for the model: the scaling parameter  $L_u$ , the width of the double Gaussian profile  $\tilde{\alpha}$  and the distance to the centerline  $\tilde{r}_0$ .

The parametrization is done in accordance with the results of the previous chapter. The parameters are adjusted to the wind speed profiles calculated from the Ainslie model.

The parameter  $L_u$  is set constant with a value of 0.19. The wake width  $\tilde{\alpha}$  is assumed to be proportional to the wake width of the wind speed profile  $\tilde{\beta}$  with a constant offset of 0.12. The distance of the Gaussian profile to the wake centerline  $\tilde{r}_{disp}$  grows linearly with increasing distance  $\tilde{x}$ :  $y_0 = 0.37 + 0.018\tilde{x}$ . The parametrization was additionally done with the measured wind speed profiles from Nibe wind farm. These values are listed in parenthesis behind the values for the Ainslie mode in the following summary:

$$\begin{aligned} L_u &= 0.14(0.12) \\ \tilde{\alpha} &= \tilde{\beta} - 0.11(\tilde{\beta} - 0.15) \end{aligned} \quad (5.37)$$

$$\tilde{r}_{disp} = 0.33 + 0.03\tilde{x}(0.355 + 0.045\tilde{x}) \quad (5.38)$$

In the listed parameters it can be seen that the values based on the two origins: wind speed profiles from Ainslie model and measured wind speed profiles show large deviations. This results from the underestimation of the measured wind speed profiles by the Ainslie model, which is discussed more detailed in the following chapter.

In Fig. 5.4 the results of the parametrization for the Ainslie model and for the measured wind speed profiles can be seen. The turbulence intensity profiles can be modeled quite well with the parametrization with the measured wind speed profiles, as with the Ainslie model the turbulence intensity profiles decay to fast with increasing distance.

Unfortunately the data base for the parametrization, as seen in the previous chapter, is rather small. Therefore the proposed model is only a first step to describe the turbulence inside the wake of a wind turbine. It would be expected that the parametrization depends on additional environmental variables. For the optimization of the parametrization more measurements at different distances, different stability situations in the atmosphere and ambient turbulence intensity have to be done.

## 5.6 Superimposition of wakes

Inside a wind farm, a downwind turbine experiences the impact of multiple wakes from upwind turbines. The model superimposes the turbulence intensity profiles of these wakes. The incoming turbulence intensity has direct influence on the wake of a downwind turbine.

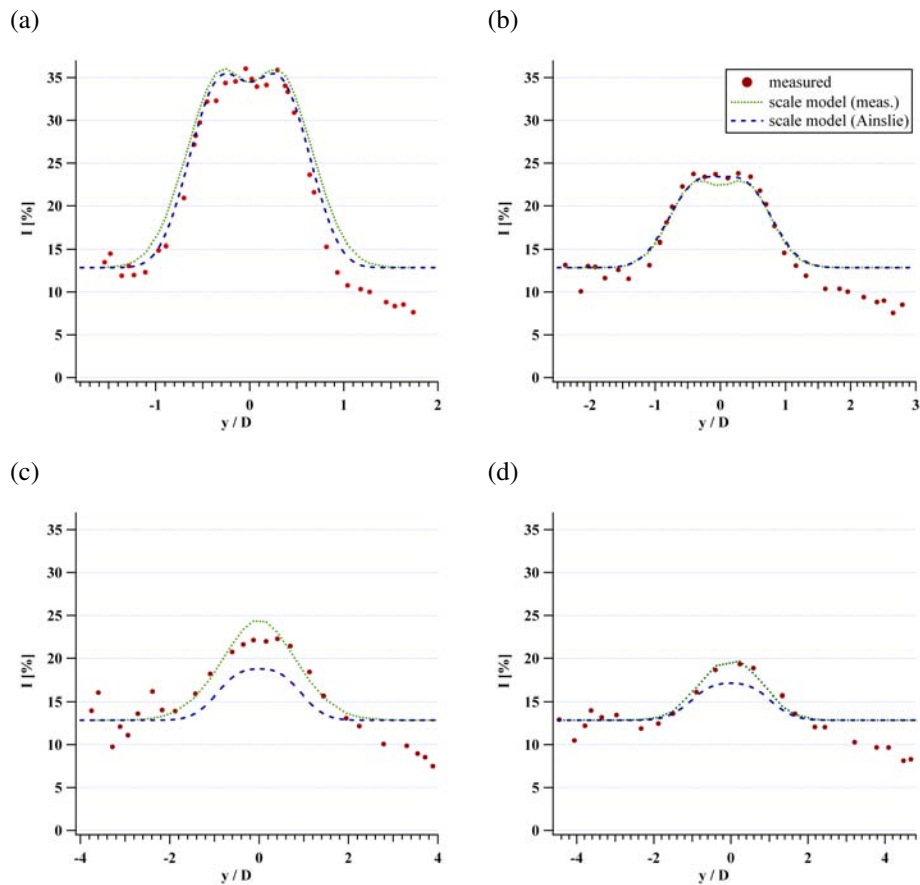


Figure 5.4: Turbulence intensity profiles calculated with the Scale model. Calculation and parametrization is based on the measured wind speed profiles from Nibe measurements and on the modeled wind speed profiles from the Ainslie model. The measured turbulence intensity profiles for the four different distances: 2.5D(a) 4D(b) 6D(c) and 7.5D(d) behind the wind turbine are also shown.

Two different approaches for the superimposition of the turbulence intensities in the wakes incident on the downwind turbine are used from the different authors for the calculation of the turbulence intensity in the wake. A quadratic superimposition:

$$I = \sqrt{I_{amb}^2 + \sum I_{add}^2}, \quad (5.39)$$

used from [Frandsen and Thogersen, 1999],[Quarton and Ainslie, 1989] and [Crespo and Hernández, 1993], as well as a superposition where the ambient turbulence intensity is directly added:

$$I = I_{amb} + \sqrt{\sum I_{add}^2} \quad (5.40)$$

proposed by [Magnusson and Smedman, 1996] were proposed.

In section 4.5.1, the influence from linear and quadratic adding of the ambient turbulence intensity was investigated at the example of the Nibe measurements. No significant differences in respect of the scaling were found between these two methods. The linear adding was used for the scaling of the turbulence intensity profiles and is therefore applied to the two model approaches.

The effect of the incoming turbulence intensity on the wake of a downwind turbine is taken into account by using the turbulence intensity incident on the downwind rotor as an input parameter  $I_{amb}$  for the Ainslie model. For this input parameter the superimposed turbulence intensity profiles from the upwind turbines are averaged quadratically over the area of the rotor of the downwind turbine and used as a parameter for the ambient turbulence intensity in the Ainslie model. A higher ambient turbulence intensity results in a faster growing wake width and a faster decay of the centerline deficit with increasing distance from the wind turbine. Apart from the ambient wind speed, this will effect the shape of the turbulence intensity profiles as well. The simulation of the wind farm with a changing ambient turbulence intensity at each wind turbine also influences the efficiency calculation.

## 5.7 Conclusion

The first approaches to describe the turbulence intensity in the wake are restricted to the maximum turbulence intensity in the wake as proposed by Crespo and Quarton. Frandsen described the turbulence intensity profile in the wake with a Gaussian profile, but does not include a change of the shape with the an increasing distance of the measurement to the wind turbine. Magnusson et al. were the first, who developed an analytical formula which includes this change of the shape of the profiles for describing the turbulence intensity profile in the wake of a wind turbine. This approach was further developed in this thesis to achieve better results with different wind farms, which is shown in the following chapter. Additionally a new approach, based on the results of the scaling from the previous chapter, was developed

here. This approach scales turbulence intensity profiles, which change the shape behind the wind turbine with increasing distance behind.

In table 5.1 an overview of the different models for the calculation of the turbulence intensity in a wind farm is given, including the different methods of normalization of the turbulence intensity as well as two approaches of superpositioning the ambient turbulence intensity: direct or quadratic adding.

model	normalization of turbulence intensity	superposition of $I_{amb}$	Calculated value
Quarton	$u_{amb}$	quadratic	max. turbulence intensity
Crespo	$u_{amb}$	quadratic	max. turbulence intensity
Frandsen	$u_{amb}$	quadratic	profile with distinct shape
Magnusson	$u_{wake}$	direct	profile with shape changing with dist.
Shear	$u_{wake}$	direct	profile with shape changing with dist.
Scale	$u_{wake}$	direct	profile with shape changing with dist.

Table 5.1: Overview of the different models to calculate the turbulence intensity in the wake of a wind turbine.

# Chapter 6

## Comparison of measured and modeled turbulence intensity in wakes

### 6.1 Introduction

Three different approaches to calculate the turbulence intensity in the wake of a wind turbine are compared to single and multiple wake measurements from three different wind farms. In addition it has been investigated, if the enhanced (Shear model) and the new developed approach (Scale model), previously described in chapter 5, yield to better results in estimating the turbulence intensity profiles in the wake of a wind turbine. The results are compared with the existing approach from Magnusson, which is the only existing approach which describes the change in the shape of the turbulence intensity profile with increasing distance.

Measurements of turbulence intensity in the wake of wind turbines are rare. In order to measure a wake profile, one measurement in front of and one behind the wind turbine is always needed: One in front to get the ambient turbulence, wind speed and wind direction and the other behind to obtain the wake conditions. To describe the development of the wake properties with increasing distance behind the rotor, measurement masts at different distances downwind of the wind turbine are needed.

The methods for measuring wakes from wind turbines range from qualitative methods with kites or smoke to cup and sonic anemometer measurements. Wake measurements behind a 2MW turbine with kites were done by Högström [Högström et al., 1988] in 1988. Measurement campaigns with two measurement masts started in 1990 at the Nibe wind farm [Taylor, 1990], followed by Sexbierum [Clijne, 1993] and other experimental sites (Horns Rev [Jensen, 2004], Vindeby [Barthelmie, 2002]). Vertical profiles were measured with SODAR within the scope of the ENDOW project at the wind farm Vindeby [Barthelmie, 2002].

In this study, single and multiple wake situations from three different wind farms are investigated. All include horizontal turbulence intensity profiles:

- Single wake measurements at four different distances from the Nibe wind farm.
- Single and double wake measurements from the wind farm Sexbierum.
- Double and quintuple wake measurements from the Vindeby wind farm.

The wake measurements from Nibe and Sexbierum are present as processed turbulence intensity profiles, whereas the Vindeby profiles are estimated from time series of 10min averaged data. The models are compared with the measured turbulence intensity profiles by calculating a Chi-Square value normalized with the number of data points:

$$\tilde{\chi}^2 = \frac{1}{N} \sum_{i=1}^N \frac{(I_{model} - I_{meas})^2}{I_{meas}}, \quad (6.1)$$

where  $N$  is the number of measurement points and  $I_{mod}$  and  $I_{meas}$  are the turbulence intensity values from the modeled and the measured profiles, respectively. The range of data points for the estimation of the Chi-Square values is derived from the points where the model with the broadest shape show an increase in turbulence intensity against the ambient turbulence intensity.

This chapter starts with a comparison of the models with the results from the Nibe wind farm, followed by a validation with the measurements from the Sexbierum wind farm. These models are then compared to the situation at the wind farm Vindeby. Finally, the results of this chapter are summarized.

## 6.2 Single wake measurements at Nibe wind farm

Turbulence intensity profiles of the single wake measurements at four different distances from the Nibe measurements are compared with the model approaches. The measurement setup is described in section 4.3.1. The turbulence intensity profiles available from Nibe wind farm are derived from 1 min averaged time series. For better comparison of the profiles to measurements from other sites, the profiles were transformed to an averaging time of 10 min, as described in chapter 2. For transformation an offset of 3.5 % was chosen, derived from the measurement of ambient turbulence intensity from the wind farm Elisenhof. It was not possible to derive a factor for transformation from the Nibe measurements, as there were no measurements of the turbulence intensity with different averaging times available.

A systematic offset occurs at all four distances between the center of the measured turbulence intensity profiles and the modeled ones. Therefore the centers of the turbulence intensity profiles are corrected from a wind direction of  $180^\circ$  to  $185^\circ$ , so that the center of the measured profiles agree with the modeled ones.



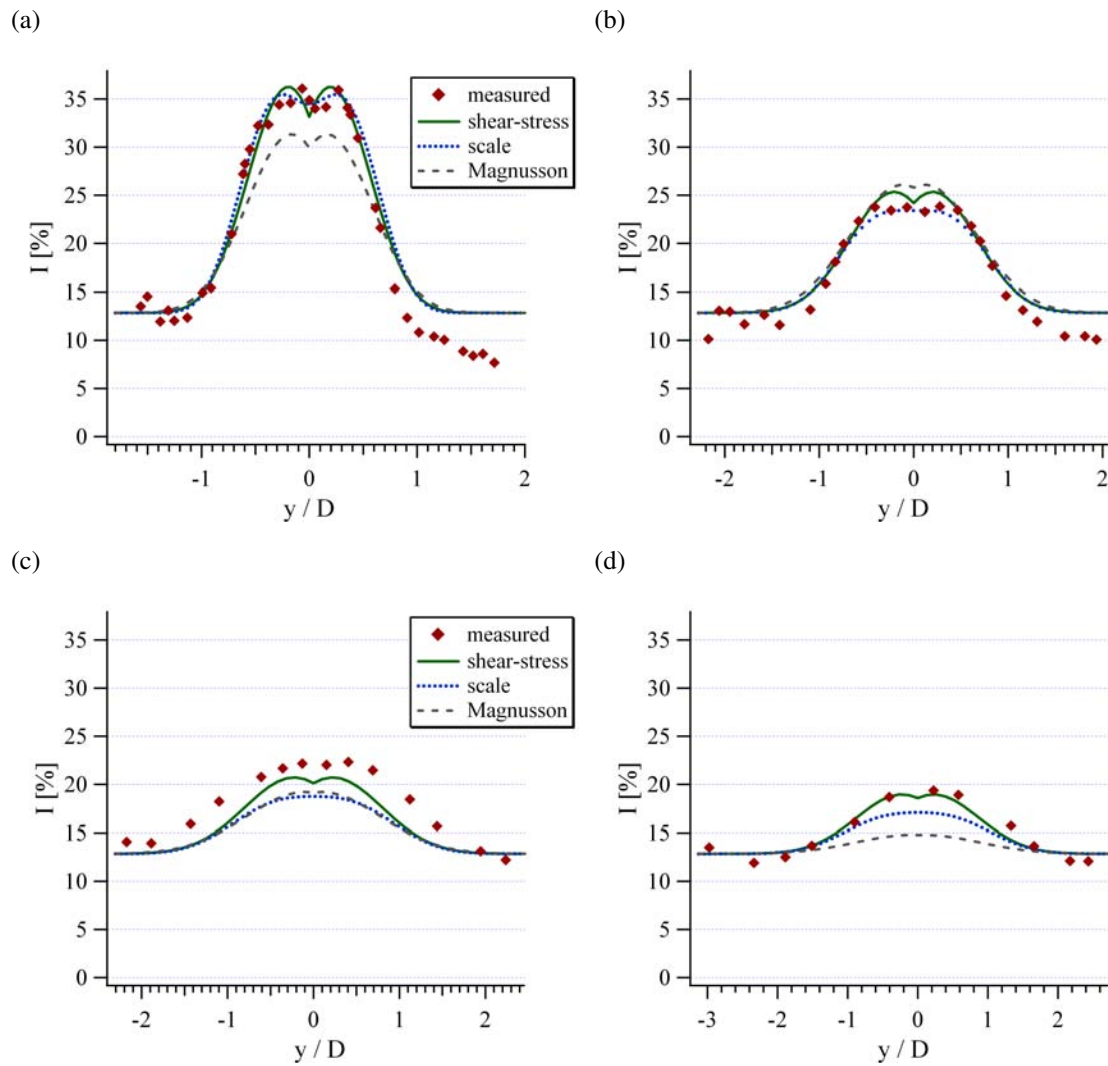


Figure 6.1: Measured and modeled horizontal turbulence intensity profiles versus normalized horizontal distance from the centerline. The profiles are measured at Nibe wind farm the four different distances: 2.5D(a) 4D(b) 6D(c) and 7.5D(d)

Figure 6.1 shows the modeled and measured turbulence intensity profiles at 2.5D, 4D, 6D and 7.5D at an ambient wind speed of 8 m/s and an ambient turbulence intensity of  $I_{amb}=11.5\%$ . The original profiles associate the turbulence intensity to the incoming wind directions. For a better comparison of the wake profiles at different distances and behind different wind turbines, the wind direction is transformed into distance relative to the centerline of the wake  $y$  and normalized with the rotor diameter  $D$ .

Regarding the measured turbulence intensity profiles in Fig. 6.1, at negative horizontal distances the measured values obviously fall below the assumed ambient turbulence intensity of 12.85%. This might result from a wind direction dependent ambient turbulence intensity. For the calculations an averaged ambient turbulence intensity for all wind directions is used, as there is no information of the ambient turbulence intensity for the different wind directions.

The turbulence intensity profiles from all three model approaches have nearly the same width at each distance behind the wind turbine, which corresponds well to the measured profiles at all four different distances. The Shear and Magnusson models show a spike in the middle at distances closer to the wind turbine. Such a discontinuity is not expected in the center of the wake, since the turbulent convection is strong (as observed in wind tunnel measurements behind a cylinder, see Fig. 5.2) and will smooth the turbulence intensity profile. The Scale model show a smoother and therefore more 'realistic' transition in the center.

In fig. 6.2 the maximum turbulence intensities of the profiles for all four distances are shown. For comparison the calculated maximum turbulence intensity levels from the three models are included. The maximum turbulence intensity of the model from Magnusson et. al at tower A has an estimated value of 30%, which is four-fifth of the measured value. At further distances, the maximum turbulence intensity of the Magnusson model decay too fast. The Shear model was adapted to the turbulence intensity profile at tower A, but estimates the maximum turbulence intensity at the other towers quite well. The Shear model uses only two constants, which specify the influence of the two terms of the model on the calculated turbulence intensity. Therefore the development of the maximum turbulence intensity with increasing distance is quite well modeled. The Scale model was developed, based on the analysis of the turbulence intensity profiles from the Nibe wind farm as described in chapter 4 and the parametrization in chapter 5. Therefore a good estimation of the maximum turbulence intensity is expected. Both models, the Shear and Scale show a similar development of the maximum turbulence intensity with increasing distance.

The main reason for the fast decay of the Magnusson model and the underestimation of turbulence intensity at tower C from the Shear and Scale model is the incorporation of wind speed models. The centerline deficit  $\tilde{u}_{def}$  of the wind speed profiles and the half width  $\tilde{\beta}$  of the wake from the wind speed measurements at different distances can be seen in fig. 6.3. The results of the two wind speed models Ainslie and Magnusson are plotted. It can be seen that the centerline deficit of the Magnusson model decreases too fast with increasing distance, whereas the Ainslie model underestimates the wind speed deficit at all four distances. The

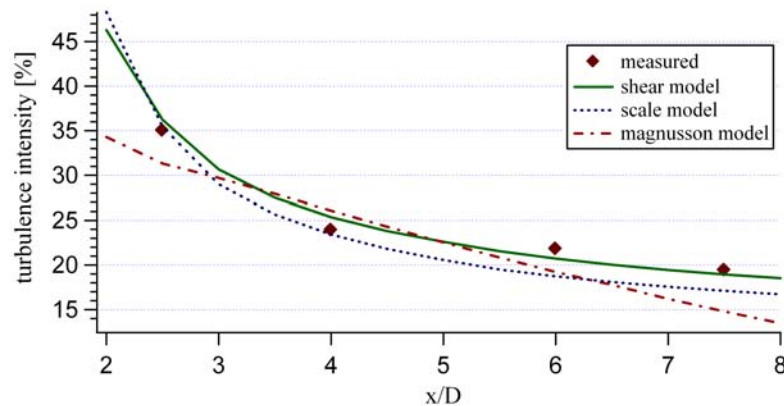


Figure 6.2: Maximum turbulence intensity (based on the results shown in table 4.3) in the wake plotted against the normalized distance behind the wind turbine for the Nibe measurements. Results from the three investigated models. The turbulence intensity values are composed of the added turbulence intensity  $I_{add}$  and turbulence intensity  $I_{amb}$ , which is corrected for an averaging time of 10 min..

decay of the wind speed deficit compared to the measurements, except for tower C, seems to be more reasonable than from the Magnusson model. The calculated half width of the wake underestimates the measured values slightly, except for tower C, and follows the measured values. At tower C the half width of the wake and the centerline deficit are completely underestimated by the model. The underestimation of the half width of the wake and the centerline deficit from the Ainslie model influence the calculation of the turbulence intensity profiles and lead to an underestimation of the width of the turbulence intensity profiles, which can be partly compensated with the chosen model parameters.

The shape of the modeled profiles is compared to the data points with the help of the normalized Chi-square value. The results can be seen in fig. 6.4 for all four distances and the three approaches. The Magnusson model shows the highest error at three from the four towers. Only at tower C a comparable error to the two other approaches is obvious. The error from the Shear and Scale model decrease continuously with increasing distance, except at tower C, where the two models underestimate the measured turbulence intensity profile. This results from the unusual behavior of the measured wind and turbulence intensity profiles at tower C, which is discussed in chapter 4.

### 6.3 Sexbierum single wake

Next, the models are compared to single wake measurements from Sexbierum wind farm. Single wake turbulence intensity profiles from three different distances behind the wind tur-

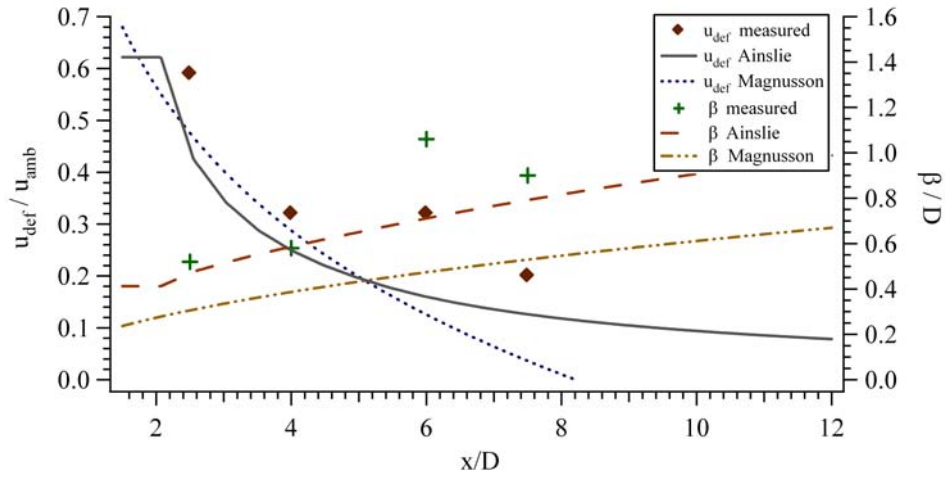


Figure 6.3: Centerline deficit of wind speed and wake width plotted versus the normalized distance for the single wake situation at Nibe wind farm. The measured values from 4 are plotted together with the model results from the wind speed models from Ainslie and Magnusson.

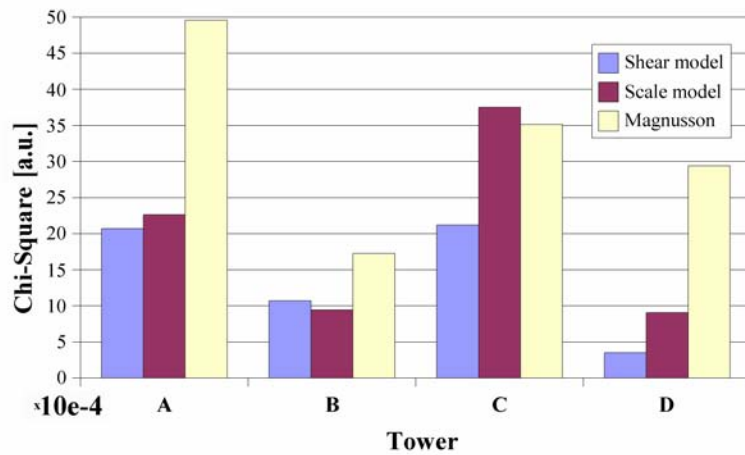


Figure 6.4: Calculated chi-square values from all four model approaches for the turbulence intensity profiles at all four towers.

bine of 2.5 D (Tower B), 5.5D (Tower A) and 8D(Tower C) are used to verify the models. The ambient wind speed for the turbulence intensity profiles is 9–10 m/s.

The turbulence intensity profiles are based on three minute averaged time series of wind speed. In order to make the turbulence intensity profiles comparable to other measurements, they were converted into a 10 min averaged turbulence intensity profile by a constant offset of 1.2 %. This offset was derived from the difference of ambient turbulence intensity measured with an average time of 10 min and 3min. The ambient turbulence intensity for the 10 min averaged profiles, which is also used as input for the three models, is 10.7 %. The turbulence intensity values of ambient turbulence intensity are taken from the Sexbierum report [Clijne, 1993].

In fig 6.5(a), 6.5(b), 6.5(c) the horizontal turbulence intensity profiles at the three distances can be seen. The data show very high scattering at all three distances. An increase in turbulence intensity is present, but a distinct shape can not be estimated. The profiles are used to compare the results from the turbulence intensity models qualitatively with measured data.

The turbulence intensity profile at a distance of 2.5D behind the wind turbine shows the lowest scattering of all profiles. The turbulence intensity increases fast from the outer parts to the center and between  $\tilde{y} = \pm 0.6$  the turbulence intensity scatters around 21% to 28% with one exception, where the turbulence intensity value has a maximum of 31.5 %. The Magnusson model has its maximum in this scatter, but the shape is smaller than the pattern of the scattered data points. The Shear and Scale model have both nearly the same maximum turbulence intensity, which overestimates the mean scatter of about 3 %. The width of the profiles from both models contribute to the measured turbulence intensity profile.

At 5.5D the measured turbulence intensity profile shows a very broad shape. A typical shape of the profile as in the measurements from Nibe can not be seen. All three models are smaller than the measured profile. The Magnusson model overestimates the maximum turbulence intensity in the wake. The turbulence intensity from the other models is in the order of the centerline scatter.

The turbulence intensity profile at 8D has an increase in turbulence intensity in the center, but shows a high scatter at the borders of the wake. The Scale model presents the lowest maximum, all the other models have their maximum near the measured values in the center. If a shape is assumed for the data, all three models are slightly too small in width.

The height of the turbulence intensity profiles from the Magnusson model depends strongly on the ambient wind speed. This can be seen, when a different ambient wind speed bin is analyzed. In Fig. 6.6 the turbulence intensity profiles at a distance of 8D with an ambient wind speed of 6-7 m/s are shown. The measured profile has turbulence intensity values similar to the wind speed bin of 9–10 m/s. The Shear and Scale model have nearly the same height, however the maximum of the turbulence intensity Magnusson model is only at 12%. The Magnusson model depends mainly on the travel time between wind turbine and

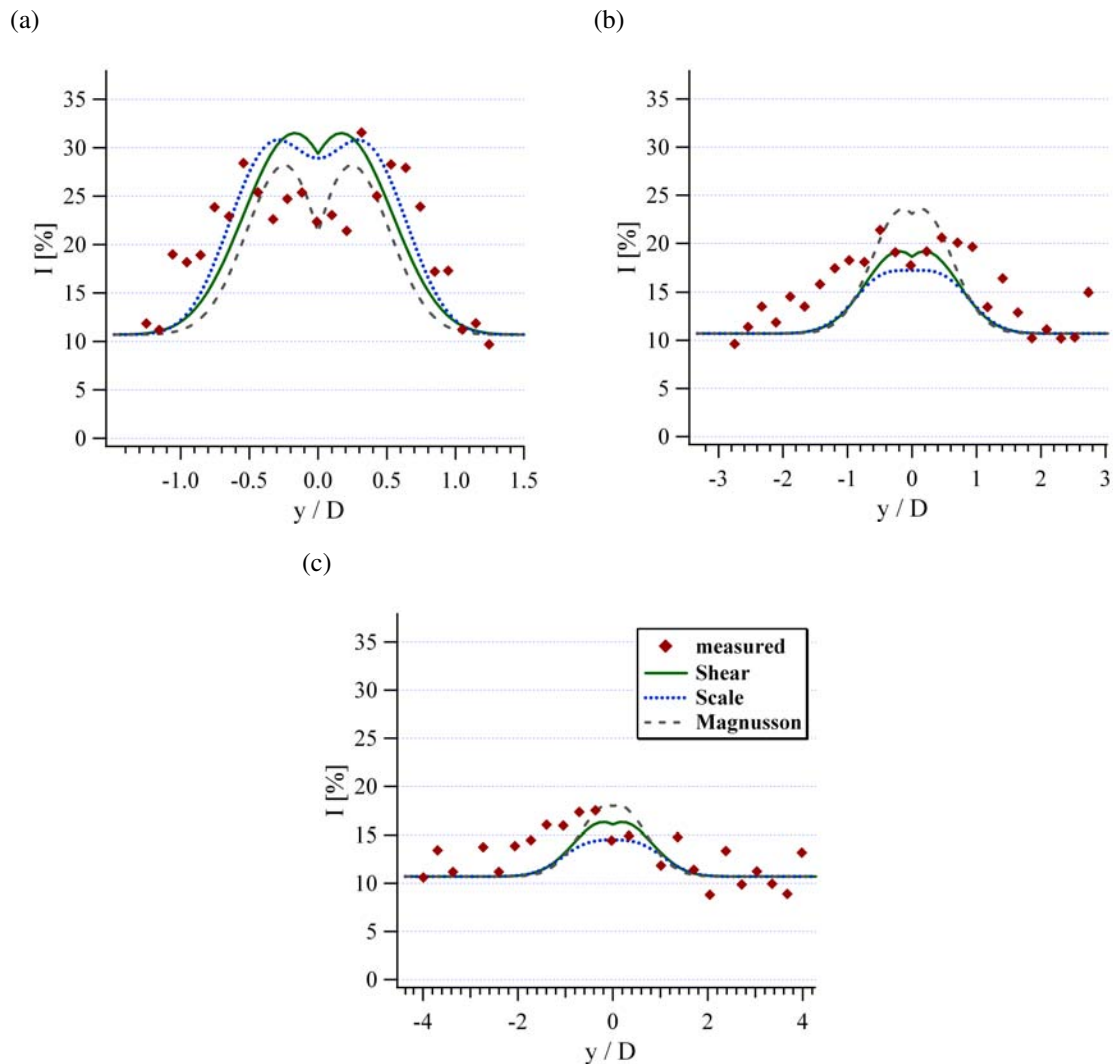


Figure 6.5: Measured and modeled turbulence intensity profiles from single wake measurements at Sexbierum wind farm at the distances of  $2.5D$  (a),  $5.5D$  (b) and  $8D$  (c).

measuring point. According to the different ambient wind speeds, the travel time changes. The change in ambient wind speed does not show the expected influence on the turbulence intensity profiles, as expected by Magnusson. The dependence of the turbulence intensity profiles on ambient wind speed is sometimes small. This can be verified by measurements from the wind farm Elisenhof, described in chapter 2.

The Chi-square values for the models at all three distances can be seen in fig. 6.7. The Chi-square values at tower B are much higher than results from the models at the Nibe wind farm. At tower A and C the values are moderate and are similar values to the results from the Nibe measurements. A statement of the quality of the models with the Chi-Square values is hardly be possible, because the difference between the result of the models is small compared to the

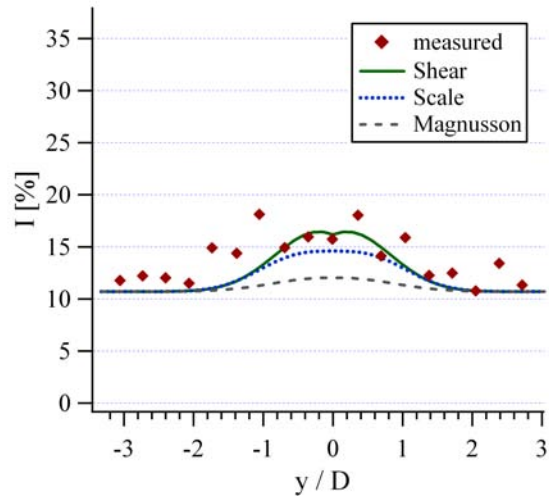


Figure 6.6: Turbulence intensity profile measured at tower C. The ambient wind speed bin is 6-7 m/s. The model from Magnusson show a very low turbulence level resulting from the low ambient wind speed.

total Chi-square values.

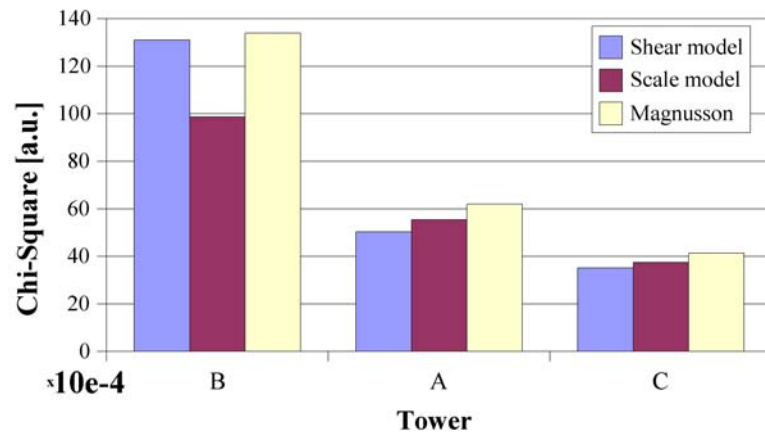


Figure 6.7: Normalized chi-square values estimated from the models compared to the measured data for the single wake measurement at wind farm Sexbierum.

## 6.4 Sexbierum double wake

A double wake situation measured at Sexbierum wind farm is compared with the model. The configuration of the wake measurement can be seen in figures 4.3 and 4.5. The double wake profile from an ambient wind speed bin of 6–7 m/s is used in this case, as the turbulence intensity profile from the wind speed bin of 9–10 m/s has not enough data points to show a complete profile. The turbulence intensity profile is shown in Fig. (6.8).

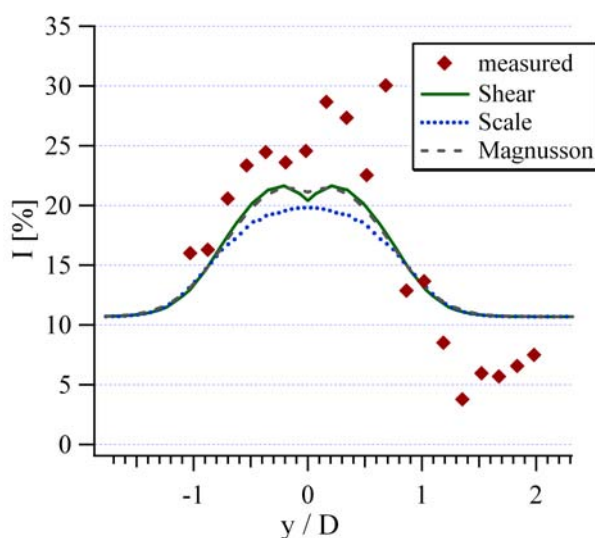


Figure 6.8: Double wake measurement of turbulence intensity from Sexbierum wind farm.

The measured profile shows an asymmetric behavior. At negative distances from the centerline the shape of the turbulence intensity profile shows a similar shape compared to the Nibe measurements. At positive distances the turbulence intensity becomes higher and drops outside the wake to values lower than 5%. The source of this different behavior of the turbulence intensity values on both sides of the profile is not documented in the report 4.5.

The Shear model follows the turbulence intensity values at negative distances very well, but underestimates the maximum values slightly and the asymmetric shape of the complete profile can not be reproduced. The Scale model has a more narrow shape and a smaller maximum. The profile has only a single peak, in contrast to the Shear model. The shape of the Magnusson model is nearly identical to the shape of the Shear model. None of the models could follow the measured turbulence intensity values at positive distances.

The Chi-Square errors are estimated to assess the deviations of the profiles from the measured values. The errors are plotted in Fig. 6.9. The errors of all models are even higher than the errors from Tower B at the single wake measurements, which is assumed to result from the strange behavior of the profile at positive distances from the centerline, where the turbulence



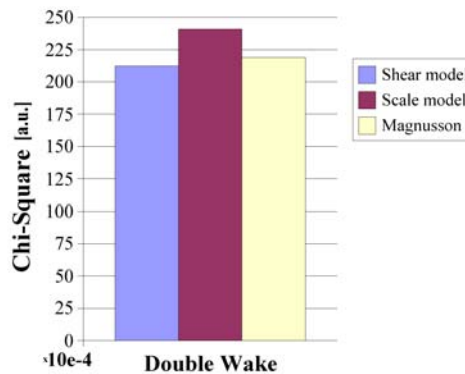


Figure 6.9: Chi-square values for the double wake measurement from Sexbierum wind farm.

intensity first increase on values over 30% and then drops down to values below ambient turbulence intensity of 5%. Compared to the absolute error, the error values of the models merely differ.

## 6.5 Vindeby double and quintuple wake

The models are compared with the offshore situation at the Vindeby wind farm with double and quintuple wake measurements (see fig. 6.10(a) and 6.10(b)). The wind speed profiles are shown together with the standard deviations of the measured turbulence intensities in each bin. A sketch of the layout of the wind farm is presented in fig. 3.1 and the wind farm is described in section 3.2.

The data were provided as time series measured at two meteorological masts. For the double and quintuple wake situation, one of the mast was always in free stream conditions. Therefore the ambient wind speed and the ambient turbulence intensity could be measured. A wind speed class from 8.5 and 10.5 m/s was selected for the measured wind speed profiles, providing a good statistics. The ambient turbulence intensity was binned for the different wind directions and used as input for the models. Thus the influence of the wind direction dependent ambient turbulence intensity on the turbulence intensity in the wake can be accounted for in the models. The mean ambient turbulence intensity for the double wake is 5.8% and for the quintuple wake 7.2%.

The shapes of the measured turbulence intensity profiles for double and quintuple wake situations are nearly symmetric, resulting from a nearly uniform turbulence intensity over specific wind directions due to the homogenous roughness of the surrounding water surface.

The Shear model underestimates the measured values slightly. At the double wake the ambient turbulence intensity is too high, for larger positive distance. This might result from

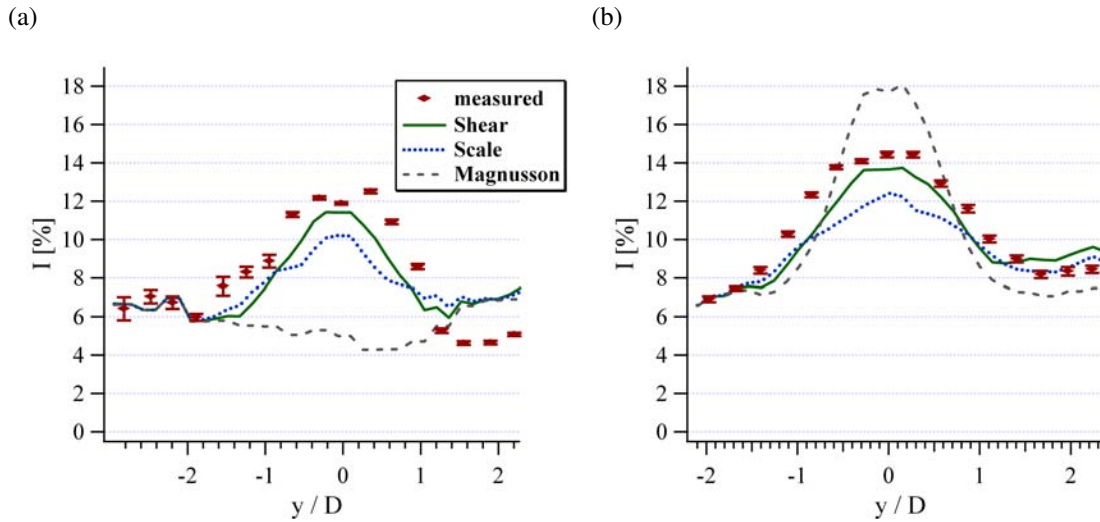


Figure 6.10: Double (a) and quintuple (b) wake situation measured at Vindeby wind farm. Results of all four models are shown. The error bars at the measured values show the standard deviation from each bin.

the different measurement conditions for the ambient turbulence intensity at the meteorological and the turbulence intensity which influences the wake. For the double wake situation the southern cup anemometer of the mast SMS is used for the free stream conditions. At wind directions for the distances  $y/D$  in the wake  $> 1$  the cup at mast SMS is influenced by the shadowing effects of the mast itself and therefore measures a higher ambient turbulence intensity.

At the border of the wake, hence, at distances to the centerline larger than one, the modeled wake width (Scale model) fits well at double and quintuple wake situation. At lower distances, the values of the modeled wake are smaller than the measured values. The maximum turbulence intensity is slightly underestimated in both situations.

The parametrization of the wind speed profile calculated from the Magnusson model is strongly influenced by the roughness length. Roughness lengths of 0.03m and  $z_0 = 2 \cdot 10^{-6}m$  were calculated for the double wake situation and the quintuple wake situation, respectively, by fitting the measured wind speed profile as described in the report from the Vindeby campaign [Barthelmie et al., 1994]. The Magnusson assumes at higher roughness lengths a higher ambient turbulence intensity and therefore a faster decrease with increasing distance from the wind speed centerline deficit in the wake. This results in combination with the far distance of more than  $9D$  to no resulting wind speed deficit in the wake from the wind speed model inside the Magnusson model and therefore no added turbulence intensity. Only the level of ambient turbulence intensity can be seen in fig. 6.10(a). In contrast to the very low roughness length in quintuple wake situation, a low ambient turbulence intensity is calculated by the model which yields at the centerline a slower decrease in wind speed deficit

with increasing distance behind the wind turbine. As a result, the turbulence intensity profile has a very high maximum, which overestimates the measured turbulence intensity profile in quintuple wake situation (see Fig. 6.10(b)).

The comparison of the Chi-Square values of the three models (fig. 6.11) show good results for the Shear and Scale model. The values of the quintuple wake are the lowest from all compared wakes. The Magnusson model shows very high Chi-square values for the double wake situation, as the model results reflect only the ambient turbulence intensity. For the quintuple wake the overestimation of the turbulence intensity yield a higher Chi-square compared to the other two models.

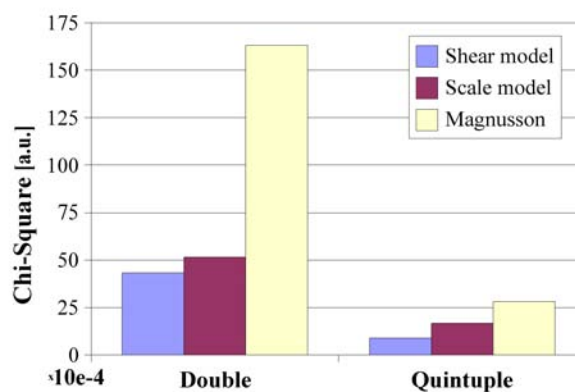


Figure 6.11: Normalized chi-square values for the double and quintuple wake measurement from Vindeby offshore wind farm.

## 6.6 Conclusion

The three model approaches were compared to turbulence intensity profiles from three different wind farms. The Shear model showed good results at the onshore and offshore wind farms. The maximum turbulence intensity was slightly underestimated, but the wake widths were estimated well. The Scale model showed an underestimation of the maximum turbulence intensity in the profiles, present at all measurements. Compared to the offshore measurements, the calculated turbulence intensity profiles were too narrow. The parametrization has to be improved by including more wind farms measurement data.

The maximum turbulence intensity from the Magnusson model decayed too quickly with increasing distance. Due to the combination of long distances in the order of  $9D$  and low roughness lengths, the output of the Magnusson model overestimates the maximum turbulence intensity in the wake at the offshore wind farm. On the other hand at higher roughness

lengths, the turbulence intensity decays too fast with increasing distance and is already zero while an increased turbulence intensity could be still measured in the wake. Additionally, the ambient wind speed has a strong influence on the predicted  $ti$  profiles, which can not be observed in the measurements. The strong dependency on roughness length and ambient wind speed yields high errors in the model, compared to the actual measurements.

The models require wind speed profile data as input. Therefore the models depend strongly on the calculated wind speed profiles. For the Nibe wind farm it has been shown that the wind speed deficits are too small at all distances computed with the Ainslie model. The wind speed model from Magnusson decays too fast with increasing distance. This effect is reflected in the turbulence intensity profiles, e.g. the turbulence intensity from the Magnusson model decay also too fast with increasing distance. Therefore, an exact calculation of the heights and widths of the wind speed profiles is very important and will improve the turbulence intensity profiles as well.

The Chi-Square values of both the Shear as well as the Scale model were low at the Nibe wind farm at all towers, since they were adapted to this data. Despite the high scattering of the measurement data at Sexbierum, both model exhibit low values at the measurements at tower A and C. At tower B and in the double wake situation the Chi-Square values are higher than the double of the other towers. The comparison of the Vindeby multiple wake situation data results in satisfying low values. The Magnusson model tends to higher Chi-Square values at nearly all measurements. Extreme high values are achieved at the offshore situation at Vindeby wind farm, exceeding the results of the other two models more than a factor of three.

# Chapter 7

## Application of the model

In this chapter, the two new models called 'Shear model' and 'Scale model' were compared with the turbulence intensity measurements at the wind turbines of an entire wind farm. Direct measurement of turbulence intensity over the entire rotor area at each wind turbine in a wind farm is with present stage technically not possible. Jørgensen [Jørgensen et al., 2003] used an indirect way: The turbulence intensity is calculated on the measured power fluctuations of the single wind turbines. Thus, the turbulence intensities can be determined for different wind directions and consequently for different shading situations.

These calculations were done by Jørgensen for the offshore wind farm Middelgrund. The wind farm consists of twenty wind turbines, which are erected along a single line with a slight bow. In that way, data from nearly complete shading, as well as partly shading, could be measured.

For comparing the measured values with the turbulence models, the modeled turbulence intensity profiles were averaged over the rotor area for certain wind directions.

The chapter is organized as follows: At the start of the chapter a short description of the wind farm is given, followed by an explanation of the estimation of turbulence intensity from power fluctuations. In the subsequent section, the models were compared with the measured values. The estimation of turbulence intensity from the power fluctuations of the wind turbine is tested with our measurements from the wind farm Elisenhof. The chapter will close with a conclusion.

### 7.1 Description of the wind farm Middelgrund

The wind farm Middelgrund is a near shore wind farm, i.e. the distance to the coast is less than 2 km. The wind farm consists of twenty wind turbines, which are arranged within a

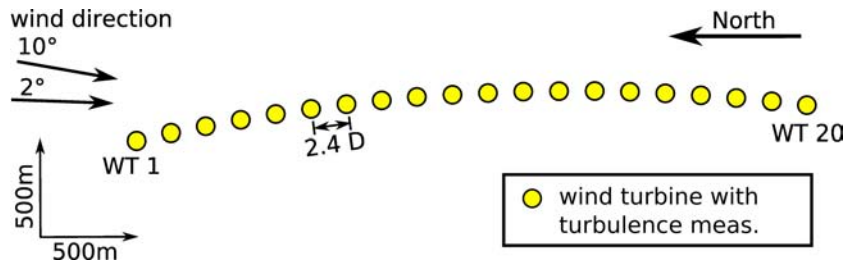


Figure 7.1: Layout of Middelgrund wind farm with incoming wind directions used

distance of 2.4 rotor diameters, in a bow of approximately 12km in the north-south direction (see Fig. 7.1). Middelgrund is sited in the Oresund near Copenhagen.

The installed wind turbines are of the type Bonus 2MW with a rotor diameter of 76m and a hub height of 64m. The power and thrust coefficient curve used for the model calculations can be found in the appendix D.2. The power and its standard deviation was measured at each wind turbine. The averaging time was 10min. The wind direction was estimated from the direction control of the wind turbines.

## 7.2 Turbulence intensity estimated from power fluctuations

Thomsen and Markkilde-Petersen [Thomsen and Markkilde-Petersen, 1992] presented a way to estimate the standard deviation of the wind speed at the rotor from power fluctuations of the wind turbine. The standard deviation of the wind speed is assumed to be proportional to the standard deviation of the power. The impact of the wind speed fluctuations influence on the power fluctuations is determined by the derivation of the power curve:

$$\sigma_u(u) = \frac{\sigma_P}{B} \cdot \left( \frac{dP}{du} \right)_u^{-1}, \quad (7.1)$$

where  $\sigma_u$  is the standard deviation of the wind speed,  $\sigma_P$  the standard deviation of the power,  $P$  the mean power and  $u$  the mean wind speed.  $B$  is a constant factor, which is empirically estimated and is usually ranging from 0.8–0.9.

The wind speed can be estimated from the inverse power curve  $u(P)$  of the measured mean power. From the standard deviation of the wind speed  $\sigma_u$  and the mean wind speed  $u$ , the turbulence intensity can be calculated as  $I = \sigma_u / u$ .

### 7.3 Comparison of the wind turbine estimated turbulence intensity with measurements

For comparison, our measurements from the wind farm Elisenhof were used to validate the approach from Kenneth et. al. The incoming turbulence intensity on the wind turbine was measured with an ultrasonic anemometer 2.49 rotor diameter in front of an Enercon E-66 wind turbine as described in chapter 2. Wind and power measurements were recorded simultaneously with subsequent calculations of and mean and standard deviations of wind and power. The averaging time was chosen to be 1min for both values in order to achieve a higher number of measurement values. The incoming wind direction bin comprises angles from  $240^\circ$  to  $280^\circ$  with an average wind direction of  $263^\circ$ .

The mean wind speed was measured with the ultrasonic anemometer and estimated from the mean power from the wind turbine. The power curve from the manufacturer (taken from the database in the software WindPro [Energi- Og Miljødata (EMD), 2004]) was used to estimate the wind speed. The mean wind speed values from the two measurements provided nearly the same results over a wind speed range of 4 to 14 m/s with only little scatter. A linear fit gives the equation:  $u_{USA} = (0.97 \pm 0.003)u_P + (0.28 \pm 0.02)$ , where  $u_{USA}$  is the wind speed measured with ultrasonic anemometer and  $u_P$  the wind speed estimated from the power measurement.

For the verification of equ. (7.1), the derivation of the power curve has to be proportional to the ratio of the standard deviation of power and the standard deviation of wind speed. In Fig. 7.2 this ratio as well as the derivation are shown in dependence of the mean wind speed  $u$ . The values are bin averaged with a bin size of 1 m/s. The derivation of the power curve was scaled with a factor of  $1/B = 0.45$  in order to fit the measured values. The error bars show the standard deviation of the values in the corresponding wind speed bins. Both curves agree well together at wind speeds from 4 m/s to 10 m/s. At higher wind speeds in excess of 12 m/s, the derivation of the power curve exhibits a faster decrease with higher wind speeds. Above wind speeds of 14 m/s the wind turbine runs with constant power and an estimation of the power fluctuations is not possible at values larger than 14 m/s.

Jørgensen recommended to use the formula not at low wind speeds and sets the upper limit of its validity to 13 m/s. In the present measurements the upper wind speed limit is 10 m/s. Apart from the similar shape of the ratio of standard deviations and the derivation of the power curve, the error bars indicate a high scatter of the measured values, which add a high error to the estimation of the turbulence intensity.

At the present site a value of  $B=2.2$  is estimated. This is more than a factor of two higher, than the specified range of  $B=0.8..0.9$  from Jørgensen. The reason could be the different averaging time and different ambient conditions. The ambient conditions are quite different, as Middelgrund is a near shore wind farm and the wind farm Elisenhof is an onshore wind

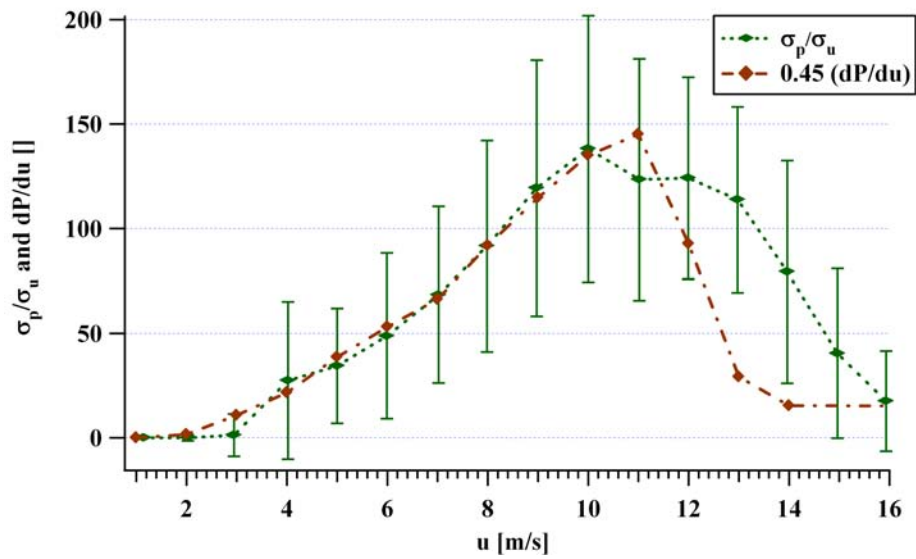


Figure 7.2: Ratio of the standard deviations of power and wind speed versus the wind speed and the derivation of the power curve with a factor 0.45. The values are binned for wind speed steps of 1 m/s.

farm. Therefore the orography, the ambient turbulence intensity and the thermal structure of the boundary layer would be quite different as well. The origin of the higher B could not be clarified. Since it is not clear if Jørgensen used the nearby meteorological mast to calibrate his measurements, the turbulence intensity at the wind turbines could be underestimated.

The wind turbine averages the turbulence intensity over the complete rotor area and might not be sensitive to eddies smaller than the rotor diameter, which contribute to the turbulence intensity measured with the ultrasonic anemometer.

Additional factors can contribute to an underestimation of the turbulence intensity with this method. It is known that the power curve depends on the incoming turbulence intensity. At higher turbulence intensity, the power production increases at lower wind speeds and decreases at higher wind speeds [Kaiser et al., 2003]. The used power curve is therefore not valid at different ambient turbulence intensities. The change in turbulence intensity between ambient and wake situation would affect the power curve and therefore the measurement of the turbulence intensity via the wind turbine.



## 7.4 Application of the turbulence models to the wind farm Middelgrund

The estimated rotor averaged turbulence intensities at Middelgrund are compared to the Shear and Scale models for two selected wind directions. The data was taken from the publication of Jørgensen [Jørgensen et al., 2003]. The wind direction classes  $1^\circ$ - $3^\circ$  and  $9^\circ$ - $11^\circ$  were chosen. The first arrangement induces a nearly complete shadowing of the wind turbines in the middle of the farm and the second induces a partial shading. The ambient wind speed lies in the range of 6–7 m/s. The results are shown in Fig. 7.3(a) and Fig. 7.3(b) in conjunction with the measured values. The turbulence intensity at the turbines are plotted in dependency of the wind turbine number. The numbering starts with the most northern turbine. For the two cases, different ambient turbulence intensities were used as input pa-

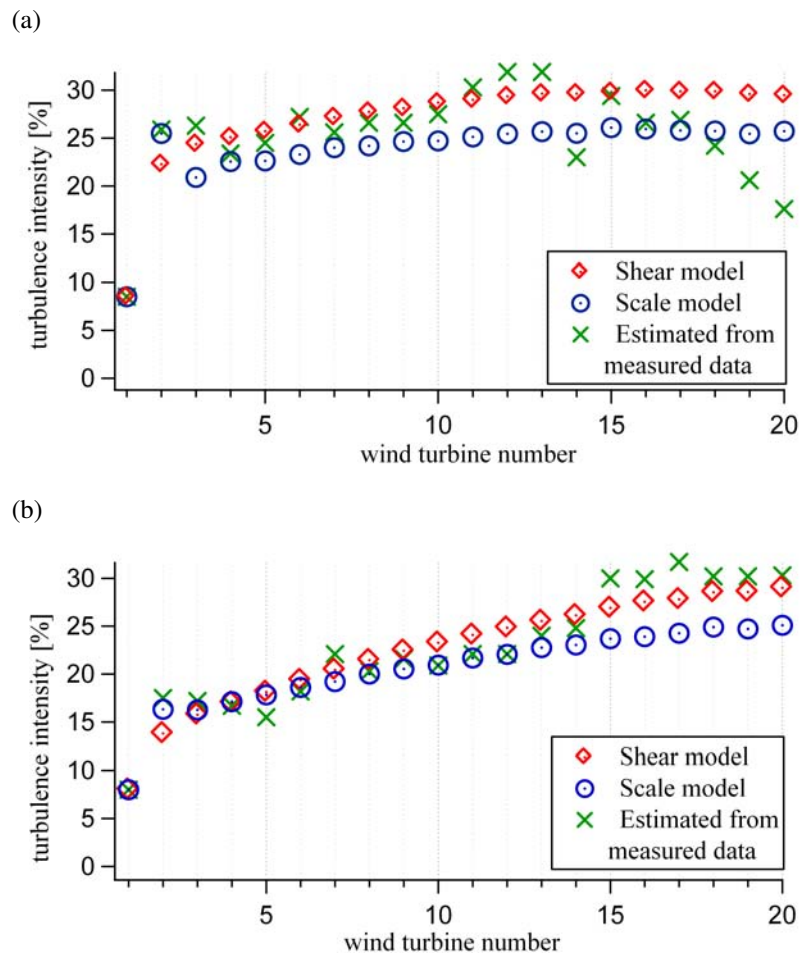


Figure 7.3: Rotor averaged turbulence intensities versus the wind turbine number at Middelgrund wind farm for the wind directions of:  $1^\circ$ - $3^\circ$ (a) and  $9^\circ$ - $11^\circ$ (b).

rameters:  $I_{amb}=8.5\%$  for the direction of  $1^\circ-3^\circ$  and  $I_{amb}=8\%$  for the direction of  $9^\circ-11^\circ$ . This turbulence intensities correspond to the measured turbulence intensity at the wind turbine 1, which is in free stream condition.

The turbulence intensity measured at the first wind turbine gives directly the ambient turbulence intensity. At the second wind turbine the turbulence intensity increases to 25% in the nearly full wake situation ( $1^\circ-3^\circ$ ) and to 18% in the partial wake situation ( $9^\circ-11^\circ$ ). At the two, respectively three wind turbines further downwind the turbulence intensity decreases slightly before it increases again slowly at the following turbines. This continuous for all turbines for the partial wake situation, whereas in the full wake situation the turbulence intensity decreases again from the wind turbine 13. Wind turbine 13 shows unusually low turbulence intensity.

For both wind directions the turbulence intensities at the first and second wind turbine in partial wake situation are underestimated by the Shear model. For the full wake situation the turbulence intensity modeled with the Shear model increases with turbine number up to 30 % at wind turbine 16. Until wind turbine 15 the results from the model follow roughly the slope of the estimated turbulence intensity values. After wind turbine 15, the measured values drop down, which is not reflected in the model. The turbulence intensity of the model decreases slightly to 29.5 %, where as the estimated values drop off to 17.6 %. In case of the partial wake situation the turbulence intensity increases slowly up to a value of 29 %. In the nearly full and partial wake situations, the model overestimates the turbulence intensity at 13 wind turbines and at 11 of 20 wind turbines, respectively.

The Scale model estimates the turbulence intensity of the first wind turbine in wake situation at  $1^\circ-3^\circ$  well and then drops off at the second wind turbine in wake situation, where the turbulence intensity is underestimated. This effect can also be observed at the second wind direction class, but the difference is smaller and follows the estimated values at wind turbine 2 and 3. From wind turbine 3 at the full wake situation the turbulence intensity increases up to 26.1 % but underestimates the turbulence intensity in general. From wind turbine 15 onwards the turbulence intensity decreases very slightly, but does not follow the steep decrease of the measured turbulence intensity values. For the second wind direction class the model shows the increase of turbulence intensity at the first wind turbine in the wake and the small decrease down at the second wind turbine in the wake situation. The measured decrease up to wind turbine 5, can not be reproduced by the model. Instead, the modeled turbulence intensity increase from wind turbine 4 to wind turbine 20 and reach maximum value of 25.1 %. Despite the scatter of the estimated values the Scale model follows the slope of the estimated values, but does not include the large turbulence intensity step change at wind turbine 15. The model underestimates 16 of 20 measured turbulence intensity values in the nearly full wake situation and 14 of 20 in the partial wake situation.

The method from Jørgensen has the disadvantage that turbulent structures in the order of the rotor diameter might exert a larger influence on the power fluctuations than smaller turbulent

structures, that is, the wind turbine acts as a low pass filter. Added turbulence from the wake, however, is known to consist of smaller eddies than turbulence in the ambient flow. Results, presented in chapter 2, showed the increased energy of smaller eddies as well as the absence of large scale eddies (while they are present in free stream condition).

While the turbulence intensity increases with the wind turbine number, the modeled turbulence intensity values from the models does not increase monotonically, but fluctuates about an increasing mean value. This effect results from the quantization of the ambient turbulence intensity for the Ainslie solver. To reduce calculation time inside FLaP, the wind speed profiles were calculated with the Ainslie solver in advance. Calculations were performed for different ambient wind speeds and turbulence intensities. Therefore the values from ambient turbulence intensity are quantized and produces this effect.

## 7.5 Conclusion

The Thomsen and Markilde-Petersen approach for the calculation of the turbulence intensity agrees well with the estimated mean value of turbulence intensity, measured at the wind farm Elisenhof. The measurement values show a high scatter, but this might be reduced at offshore situations due to the more homogeneous wind flow. As proposed by Jørgensen at Elisenhof the approach is only valid for a wind speed range from 4 m/s to 10 m/s. This result does not interfere with the results from Middelgrund because of the selected wind speed range of 6-7 m/s. The measurements from Elisenhof shows that the constant B is site specific and is higher than the assumed value of Jørgensen for Middelgrund. Since it was not clear if the meteorological mast at Middelgrund wind farm was used for verification of the turbulence intensity, estimated from the power fluctuation. It is possible that the turbulence intensity have been underestimated by the Middelgrund measurements.

The approach by Thomsen and Markilde-Petersen is a good method to estimate the turbulence intensity at all the wind turbines in a wind farm. An alternative procedure is the use of nacelle anemometer. However, these anemometers have the disadvantage, that the air flow is disturbed by the nacelle and the rotor themselves, generating additional measurement uncertainties.

The results from the two models are different. The turbulence intensity of the first wind turbine in wake situation has been underestimated, while the Shear model overestimates the turbulence intensity at the majority of the wind turbines further downwind. Therefore the model acts conservative for nearly all values in the wake. Values predicted by the Scale model are slightly underestimated by a turbulence intensity of about 3 %. Comparisons with measurements at wind farm Elisenhof indicate that the estimated turbulence intensity values from Middelgrund are underestimated. In this case the Shear model gives the more reliable results, based on the conservative turbulence intensity calculation.

The turbulence intensity from the Shear model and the Scale model decay at wind turbines further downwind at an ambient wind direction of  $1^\circ$ - $3^\circ$ , where complete shadowing of nearly all wind turbines occurs. A continuous increase of turbulence intensity at the wind turbines further downwind was observed at Horns Rev wind farm by Jensen [Jensen, 2004], where the wind turbines are placed in a straight line. The model should therefore be compared with large wind farms like the offshore wind farm Horns Rev in the future.

# Chapter 8

## Conclusion

The turbulence in the wake is commonly described with the parameter turbulence intensity. It could be shown that the turbulence intensity is as first approximation an adequate way for measuring the amount of turbulence in the wake, as the turbulence in the wake compared to the free stream has similar structures.

The choice of sampling frequency has nearly no influence on the turbulence intensity profiles. The removing of a linear trend effects the profiles at an averaging time of 1min significant, at higher averaging times the difference is negligible. The use of the absolute wind speed vector instead of the fluctuations in the directions of the mean wind speed, which is the one of the main differences between cup and ultrasonic anemometer, show only small differences. Significant change in the measured values occur with different averaging times, where the increase in measured turbulence intensity goes logarithmic with increasing averaging time. Generally it is possible to convert the turbulence intensity profiles between different averaging times as long, as the time does not exceed 10 minutes.

It is possible to scale the wind speed profiles from different distances behind the wind turbine from the two investigated wind farms. An assumed Gaussian shape agrees well with the profiles. The turbulence intensity profiles are not simply to scale, because they exhibit a Gaussian profile at further distance and at nearer a plateau in the center of the profile. Nevertheless the width can be scaled with the wake width of the wind speed profiles and good results were estimated in scaling the height of the profiles with the derivation of the wind speed profile at the wake half width. The shape of the turbulence intensity profiles can be described well with the superposition of two Gaussian profiles. Before scaling, the ambient turbulence intensity has to be subtracted from the profiles.

Based on this results a method was developed which base on the model for the wind speed profile developed by Ainslie to scale and calculate the shape of the turbulence intensity profile (Scale model). Following another way, the model from Magnusson was developed further on: It was combined with the wind speed profile from the Ainslie model and the influence of the different terms was formulated different (Shear model).

The new methods were validated with success with three wind farms. They can predict the turbulence intensity at the different distances and in case of multiple wake situations well. The model based on the scaling approach tends to under predict the turbulence intensity profiles, the enhanced Magnusson shows only a slight under prediction. At the comparison with the whole wind farm Middelgrund, the shear model predicts the turbulence intensity at the wind turbines well. The scale model tends to too low predicted values of the turbulence intensity.

Both models show good results, the accuracy of the predictions depends i.e. on the wind speed profile. A better calculation of the wind speed profiles can enhance the accuracy of the turbulence intensity profiles.

For the parametrization of the Scale model, more measurements are needed in future. In the past only few measurements behind wind turbines at different distances were published. There is further need.

# Appendix A

## Technical data of the Metek Ultrasonic Anemometer

The high resolution measurement at wind farm Elisenhof was done with the ultrasonic anemometer USA-1 from Metek. The ultrasonic anemometer consists of three ultrasonic transponder pairs mounted around a single bar. 3d flows could be measured with a sampling frequency of 50 Hz. The signal is transferred to the data logger via RS422 digital port.

### A.1 Offline head correction for Metek anemometers

The Metek ultrasonic anemometer consists of a middle bar surrounded by three transponder pairs for the measurement of all three velocity components of the wind. The middle bar causes a flow distortion, which has to be corrected in the measured data.

The Metek ultrasonic anemometer at the wind farm Elisenhof logged the wind speed data as raw time series with a sampling frequency of 50 Hz. No internal correction for the sensor head was applied.

A correction algorithm for the influence of the middle bar was applied according to [Met, 2004] for 2d-flows. The 2d correction is suggested for flows with a vertical deflection of the wind stream, which does not extend  $\pm 15^\circ$ . At the current investigation the angle are smaller with a maximum value around  $10^\circ$ .

With the components of the undisturbed flow  $x_c, y_c$  and  $z_c$  and the measured components  $x_m, y_m$  and  $z_m$  the flow will be corrected using a linear corrective factor  $\Delta$ . The equation for the corrected wind speed are:

$$x_c = x_m \cdot \Delta \quad (\text{A.1})$$

$$y_c = y_m \cdot \Delta \quad (\text{A.2})$$

$$z_c = z_m \cdot +0.031v_c(\sin(3\alpha) + 30^\circ), \quad (\text{A.3})$$

where  $\alpha$  the azimuth angle of the incoming flow and  $v_c$  is the absolute wind speed in the horizontal plane:

$$v_m = \sqrt{x_m^2 + y_m^2} \quad (\text{A.4})$$

The corrective factor  $\delta$  is formulated as:

$$\Delta = 1 + 0.015 \sin(3\alpha + 30^\circ) \quad (\text{A.5})$$

The correction could also be applied directly to the absolute horizontal wind speed:

$$v_c = v_m \cdot \Delta \quad (\text{A.6})$$



# Appendix B

## Conversion of Averaging time

It is not unusual that time series from measurements at wind farms are already averaged values. How to convert the averaged wind speed and standard deviation to longer averaging periods is described in the following.

The mean values of wind speed could be directly converted by averaging over the values in the new averaging period, e.g. for converting from 1 min to N min average wind speed:

$$u_N = \frac{1}{N} \sum_{i=1}^N u_i \quad (\text{B.1})$$

Converting the turbulence intensity from 1 min values could be done with the following expression:

$$I_N = \frac{\sqrt{\frac{1}{N} [\sum_{i=1}^N \sigma_i^2 + u_i^2]} - u_N^2}{u_N^2} \quad (\text{B.2})$$



## Appendix C

### Calculation of angle to horizontal distance

The measured data at the meteorological mast always declared with angle. The model use the radial distance from the centerline to calculate their values. To compare both data: Measured and modeled, a conversion is necessary. This is done with simple trigonometry

$$y = x \sin(\theta), \quad (\text{C.1})$$

where  $x$  is the distance between wind turbine center and meteorological mast, e.g. other wind turbine and  $\theta$  the angle between the connection line wind turbine– meteorological mast and the wind direction. A schematic sketch could be seen in fig. C.1.

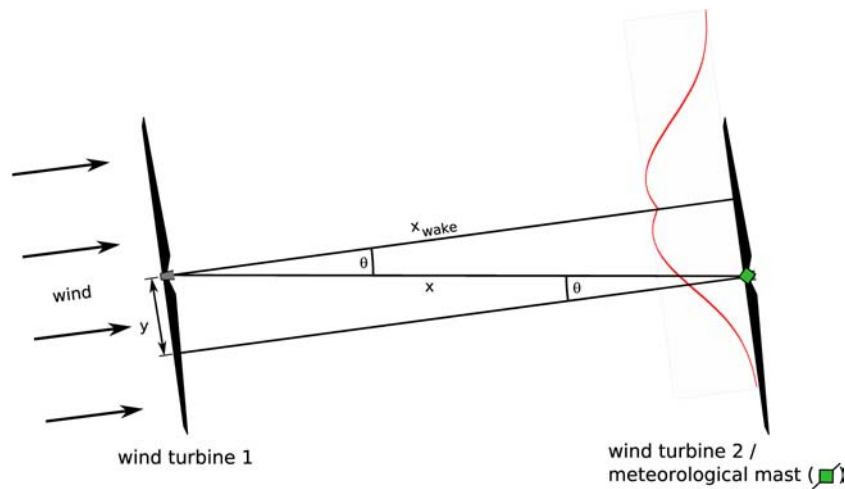


Figure C.1: Relation between the measured angle and the expansion of the wake. A schematic turbulence intensity profile was drawn in red color.



# **Appendix D**

## **Additional information about the wind farms**

Overview over the power and thrust curve of the wind turbines used in the investigated wind farms and additional information about layout, measurement masts and measured data.

## D.1 Elisenhof wind farm

The instrumentation of the mast at the different heights is shown in fig. D.1. In Fig. D.2 the complete layout of the wind farm Elisenhof could be seen and in Fig. D.3 the power and the thrust curve of the nearest wind turbine 17, an Enercon E-66.

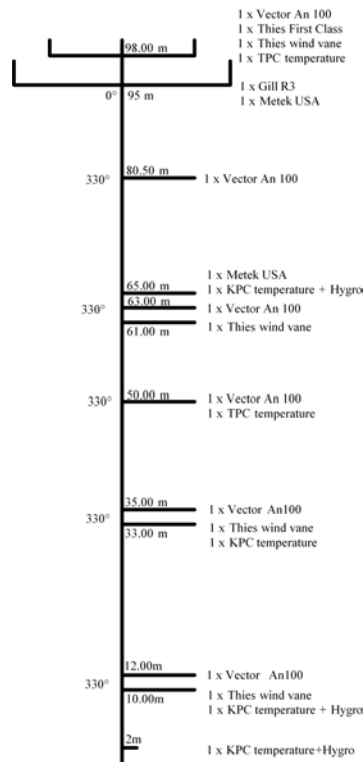


Figure D.1: Sketch of the instrumentation of the meteorological mast at wind farm Elisenhof. The heights are the heights of the booms, not of the measurement instruments

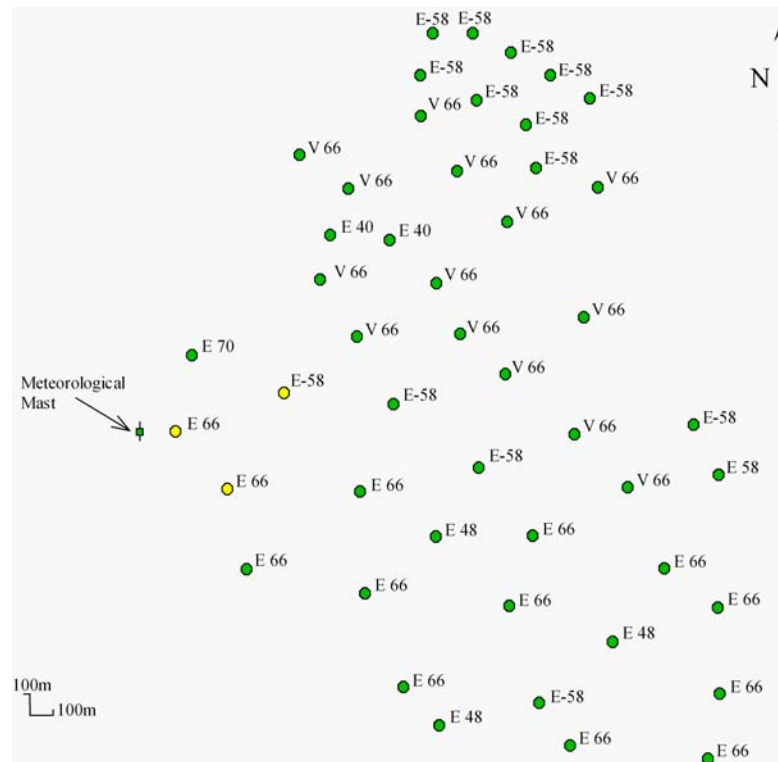


Figure D.2: Layout of the wind farm Elisenhof. The yellow marked wind turbines influence the measurement at the meteorological mast directly.

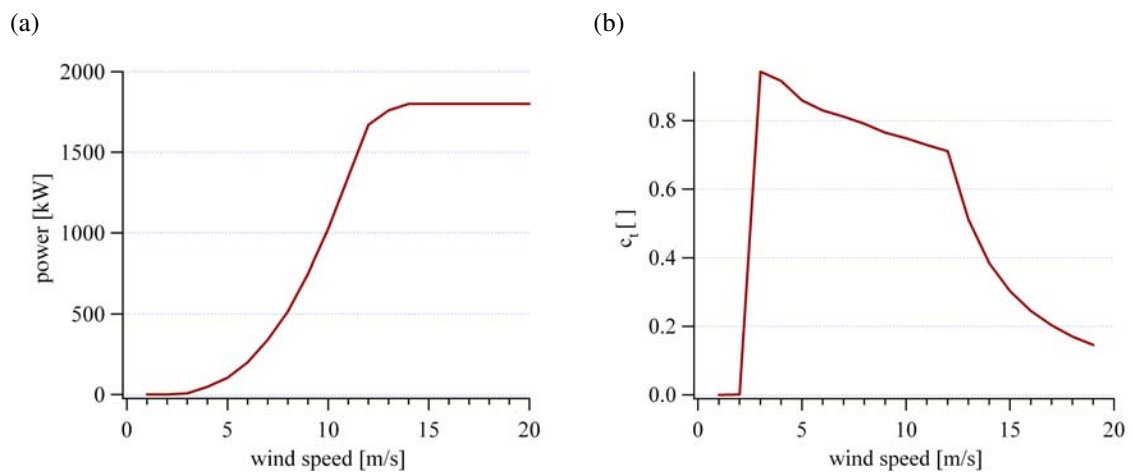


Figure D.3: Power and thrust curve from the wind turbine Enercon E-66 at wind farm Elisenhof. The power curve and the thrust curve are from manufacturer information from the database in the software WindPro [Energi- Og Miljødata (EMD), 2004]

## D.2 Middelgrund

Power and thrust curve as applied by the publication from [Jørgensen et al., 2003] are shown in Fig. D.4.

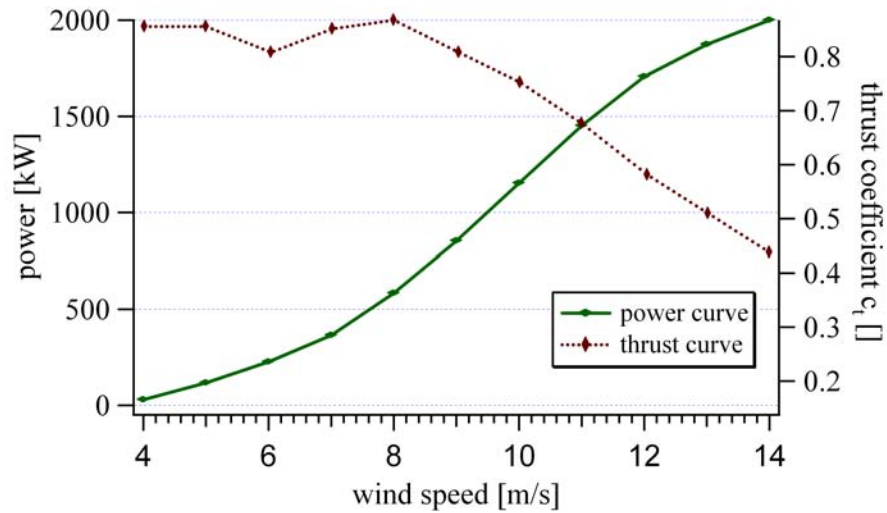


Figure D.4: Power and thrust curve from the Bonus wind turbine at Middelgrund wind farm [Jørgensen et al., 2003].



## D.3 Nibe wind farm

The section includes the wind speed deficit and turbulence intensity profiles measured at Nibe wind farm (D.6(a) and D.6(b)), a table of the technical data of the Nibe wind turbine and the graphics of the power curve and the thrust curve D.5. All data are taken from [Taylor, 1990].

turbine type:	Nibe
power:	630 kW
rotor diameter:	40m
hub height:	45m
rotor blades:	3
control:	stall-control (turbine A) pitch-control (turbine B)
RPM:	34 rpm

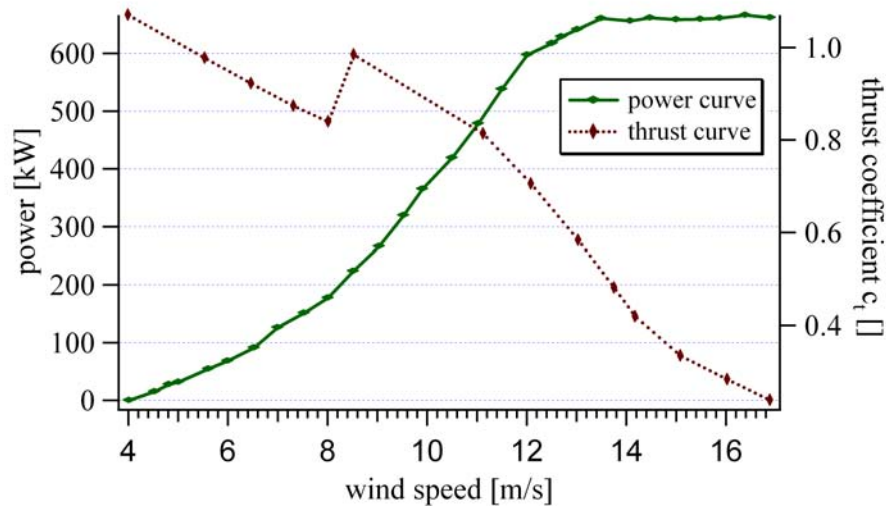


Figure D.5: Power and thrust curve from Nibe experimental wind turbines at Nibe wind farm [Taylor, 1990].

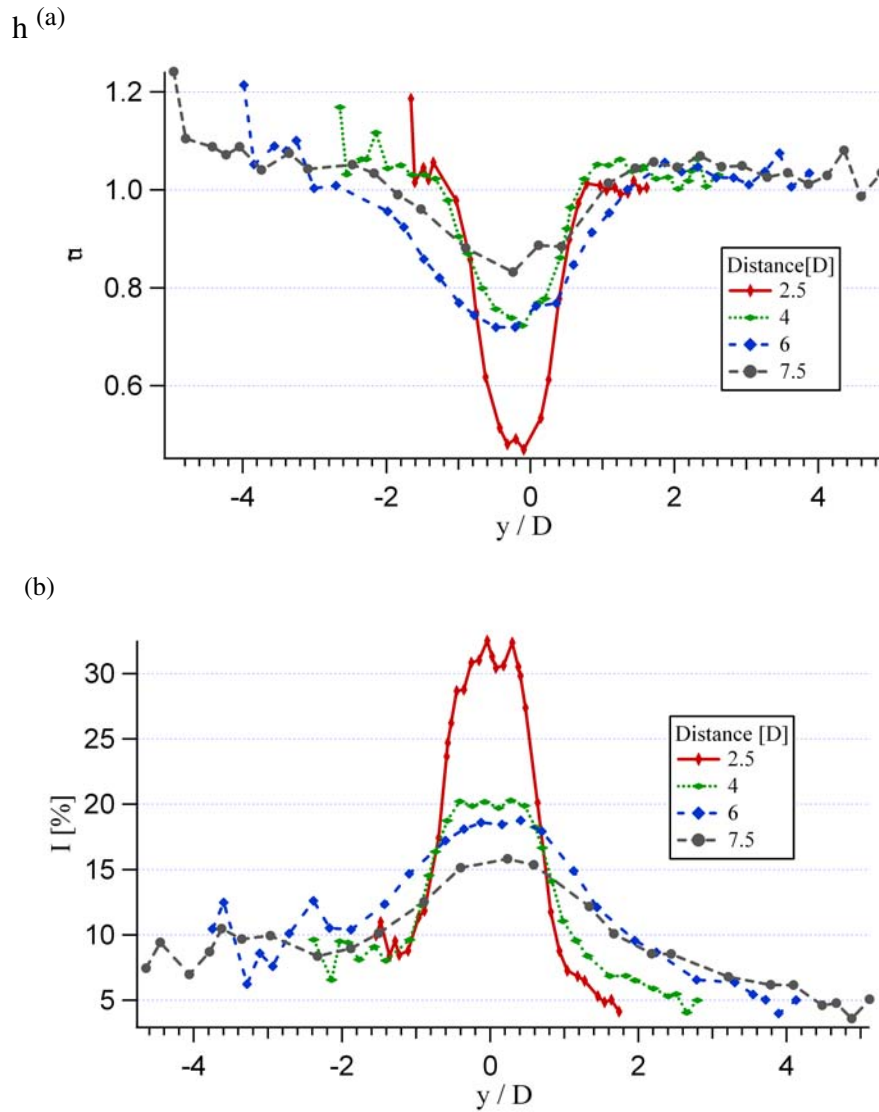


Figure D.6: Wind speed deficit(a) and turbulence intensity profiles(b) measured at Nibe wind farm at an ambient wind speed of 8.0 to 9.1 m/s [Taylor, 1990].

## D.4 Sexbierum wind farm

Technical data of wind turbines at Sexbierum wind farm ([Clijne, 1993])

turbine type	Holec WPS-30
power	310 kW
hub height	35 m
rotor diameter	30.1 m
rotor speed	30 rpm
Number of blades	3

The power and thrust curve are shown in Fig. D.7 and the unprocessed wind speed and turbulence intensity profiles in Fig. D.8(b) and D.8(a).

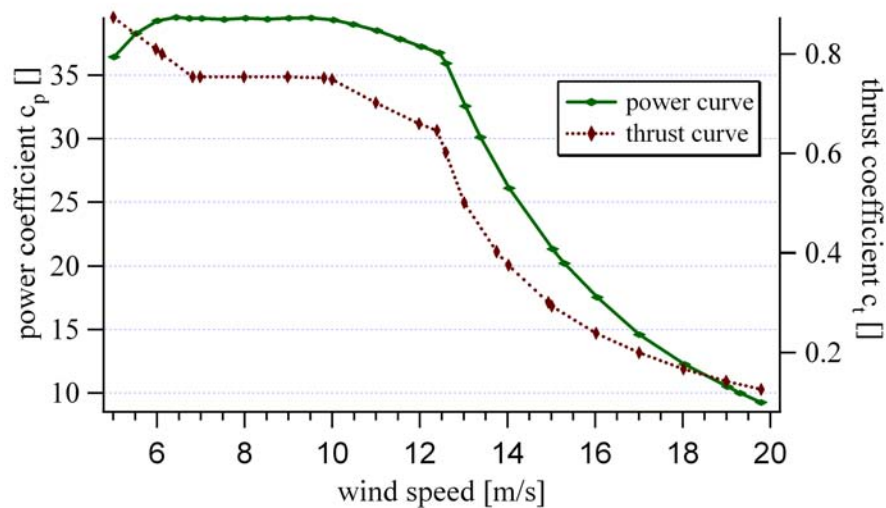


Figure D.7: Power coefficient and thrust curve from HOLEC wind turbines at Sexbierum wind farm [Clijne, 1993].

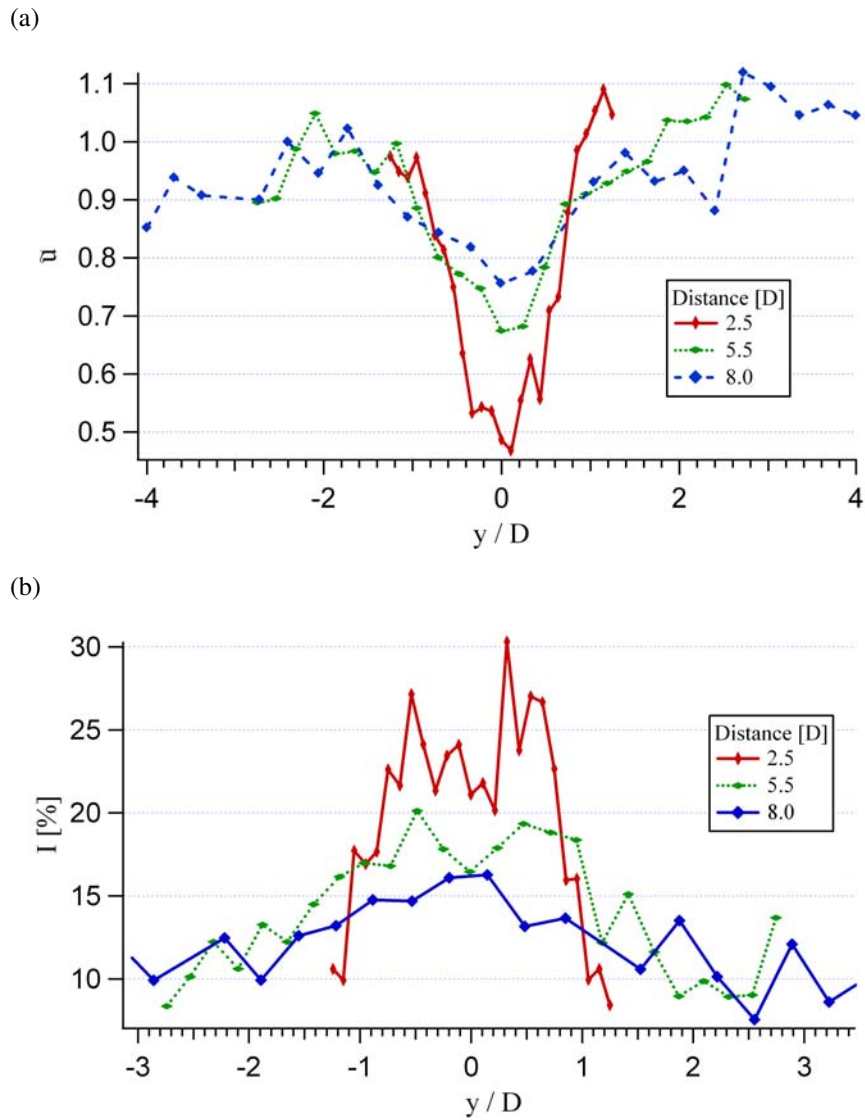


Figure D.8: Wind speed deficit(a) and turbulence intensity profiles(b) measured at Sexbierum wind farm at an ambient wind speed of 9.0 to 10.0 m/s.

## D.5 Vindeby

Power curve and thrust curve from the 450kW Bonus wind turbines are shown in Fig. D.9. Information taken from [Barthelmie et al., 1994].

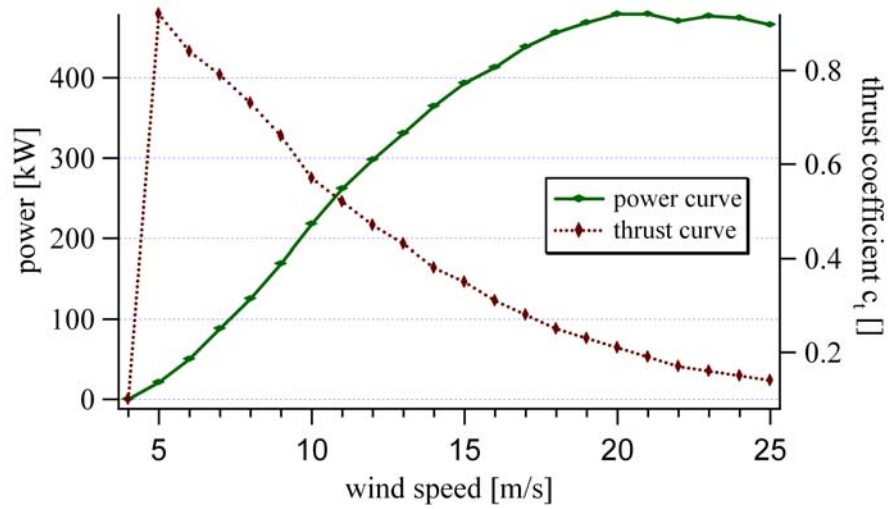


Figure D.9: Power and thrust curve from 450kW Bonus wind turbines at wind farm Vindeby [Barthelmie et al., 1994].



# Bibliography

- [Vin, 2004] (2004). <http://www.windpower.org/de/pictures/offshore.htm>.
- [Met, 2004] (2004). Flow distortion for 3-d flows as measured by metek's ultrasonic anemometer usa-1. Technical report, METEK GmbH.
- [IEC, 2005] (2005). IEC 61400-1 (2005) wind turbines, part 1: Design requirements, 188/184/cdv. Technical Report Third Edition, International Electrotechnical Commission.
- [Abramovich, 1963] Abramovich, G. N. (1963). *The theory of turbulent jets*. The M.I.T. Press.
- [Ainslie, 1988] Ainslie, J. F. (1988). Calculating the flowfield in the wake of wind turbines. *Journal of Wind Engineering and Industrial Aerodynamics*, 27:213–224.
- [Barthelmie, 2002] Barthelmie, R. (2002). Proceedings of the endow workshop 'offshore wakes: measurements and modelling'. Technical Report Risø-R-1326(EN), Risø National Laboratory, Roskilde.
- [Barthelmie et al., 1994] Barthelmie, R. J., Courtney, M., Højstrup, J., and Sanderhoff, P. (1994). The Vindeby project: A description. Technical Report Risø-R-741(EN), RISØ.
- [Bendat and Piersol, 1971] Bendat, J. S. and Piersol, A. G. (1971). *Random Data: Analysis and Measurements Procedures*. Wiley-Interscience.
- [Castaing et al., 1990] Castaing, B., Gagne, Y., and Hopfinger, E. (1990). Velocity probability density functions of high reynolds number turbulence. *Physica D*, 46:177–200.
- [Clijne, 1993] Clijne, J. W. (1993). Results of sexbierum wind farm; single wake measurements. Technical Report 93-082, TNO Environmental and Energy Research.
- [Crespo and Hernández, 1993] Crespo, A. and Hernández, J. (1993). Analytical correlations for turbulence characteristics in the wakes of wind turbines. In *European Community Wind Energy Conference*, pages 436–439.

- [Crespo et al., 1990] Crespo, A., Manuel, F., and Hernandez, J. (1990). Numerical modelling of wind turbine wakes. In *Proceedings EWEC Madrid 1990*.
- [Deiss et al., 2001] Deiss, O., Lackmann, F., Hilling, C., and Kameier, F. (2001). Turbulenzeinflüsse bei der messung der windgeschwindigkeit. *Erneuerbare Energien*.
- [Energi- Og Miljødata (EMD), 2004] Energi- Og Miljødata (EMD) (2004). *WindPro [Computerprogramm] Version 2.3*.
- [Frandsen and Thogersen, 1999] Frandsen, S. and Thogersen, M. L. (1999). Integrated fatigue loading for wind turbines in wind farms by combining ambient turbulence and wakes. *Wind Engineering*, 23(7):327–340.
- [Garrad and Hassan, 2004] Garrad and Hassan (2004). *Windfarmer [Computerprogramm] Version 3.2*.
- [Hansen and Larsen, 2003] Hansen, K. S. and Larsen, G. C. (2003). Parameterisation of turbulence intensity. In *EWEC*.
- [Harsha and Lee, 1970] Harsha, P. T. and Lee, S. C. (1970). Correlation between turbulent shear stress and turbulent kinetic energy. *American Institute of Aeronautics and Astronautics*, 8(8):1508–1510.
- [Högström et al., 1988] Högström, U., Asimakopoulos, D. N., Kambezidis, H., Helmis, C., and Smedman, A. (1988). A field study of the wake behind a 2 MW wind turbine. *Atmospheric Environment*, 22(4):803–820.
- [Jensen, 2004] Jensen, L. E. (2004). Wake measurements from the horns rev wind farm. In *Proceedings of the European Wind Energy Conference*.
- [Jensen, 1993] Jensen, N. (1993). A note on wind generator interaction. Technical Report M-2411, Risø National Laboratory, DK-400 Roskilde.
- [Jørgensen et al., 2003] Jørgensen, H. E., Frandsen, S., and Vølund, P. (2003). Wake effects on Middelgrunden windfarm. Technical Report Risø-R-1415(EN), Risø National Laboratory, Roskilde, Denmark.
- [Kaimal and Finnigan, 1994] Kaimal, J. C. and Finnigan, J. J. (1994). *Atmospheric Boundary Layer Flows: their structure and measurement*. Oxford University Press.
- [Kaiser et al., 2003] Kaiser, K., Hohlen, H., and Langreder, W. (2003). Turbulence correction for power curves. In *EWEC Madrid*.
- [Lange et al., 2003] Lange, B., Waldl, H.-P., Guerrero, A. G., Heinemann, D., and Barthelmie, R. J. (2003). Modelling of Offshore Wind turbine wakes with the wind farm program FLaP. *WIND ENERGY*, 6:87–104.



- [Magnusson, 1996] Magnusson, M. (1996). *Wind Turbine "Wakes"*. PhD thesis, Acta Universitatis Upsaliensis.
- [Magnusson and Smedman, 1996] Magnusson, M. and Smedman, A.-S. (1996). A practical method to estimate wind turbine wake characteristics from turbine data and routine wind measurements. *Wind Engineering*, 20:73–92.
- [Magnusson and Smedman, 1999] Magnusson, M. and Smedman, A.-S. (1999). Air flow behind wind turbines. *Journal of Wind Engineering and Industrial Aerodynamics*, 80:169–189.
- [Medici, 2004] Medici, D. (2004). *Wind Turbine Wakes - Control and Vortex Shedding*. PhD thesis, KTH Mechanics – Royal Institute of Technology.
- [Monin and Yaglom, 1971] Monin, A. and Yaglom, A. (1971). *Statistical Fluid Mechanics*. MIT Press, Cambridge, Massachusetts.
- [Oldenburg, 2003] Oldenburg, U. (2003). *FLaP (Farm Layout Program) [Computerprogramm] Version 2.1*.
- [Quarton and Ainslie, 1989] Quarton, D. and Ainslie, J. (1989). Turbulence in wind turbine wakes. *Wind Engineering*, 14:15–23.
- [Risø National Laboratory, 2004] Risø National Laboratory (2004). *WAsP [Computerprogramm] version 8.1*.
- [Schetz, 1968] Schetz, J. A. (1968). Turbulent mixing of a jet in a cowflowing stream. *AIAA journal*, 6:2008 – 2010.
- [Schlez et al., 2001] Schlez, W., Umaña, A., Barthelmie, R., Larsen, G., Rados, K., Lange, B., Schepers, G., and Hegberg, T. (2001). ENDOW: Improvement of wake models within offshore wind farms. *Wind Engineering*, 25(5):281–287.
- [Sforza et al., 1979] Sforza, P. M., Stasi, W., M.Smorto, and Sheerin, P. (1979). Wind turbine generator wakes. In *17th Aerospace Sciences Meeting*.
- [Taylor, 1990] Taylor, G. J. (1990). Wake measurements on the nibe wind turbines in denmark. Technical report, Risø National Laboratory.
- [Thomsen and Markkilde-Petersen, 1992] Thomsen, K. and Markkilde-Petersen, S. (1992). Experimental investigation of gear box duration loadings on stall and pitch controlled wind turbines. Technical Report Ris/o-R-653(EN), Risø.
- [Townsend, 1949] Townsend, A. A. (1949). The fully developed wake of a circular cylinder. *Australian journal of scientific research*, 2:451–468.

- [Troldborg et al., 2006] Troldborg, N., Sørensen, J. N., and Mikkelsen, R. (2006). Numerical simulations of wakes of wind turbines in wind farms. In *EWEC*.
- [Vermeulen, 1980] Vermeulen, P. E. J. (1980). An experimental analysis of wind turbine wakes. In *Proceedings of the 3rd International Symposium on Wind Energy Systems*, pages 431–450, Lyngby, Denmark.
- [Waldl, 1997] Waldl, H.-P. (1997). *Modellierung der Leistungsabgabe Von Windparks und Optimierung der Aufstellungsgeometrie*. PhD thesis, Carl von Ossietzky Universität Oldenburg.
- [Zelazny, 1972] Zelazny, S. W. (1972). *Modeling of turbulent axisymmetric coflowing streams and quiescent jets: A review and extension*. PhD thesis, Faculty of the Graduate School of the State University of New York at Buffalo.

**Lebenslauf Arne Henning Wessel**

- 25.06.1975 Geburt in Bremen, Staatsangehörigkeit: deutsch
- 1991-1994 Besuch der Sekundarstufe II Gymnasium des Schulzentrums im Holter Feld; Abitur in den Fächern Mathematik, Physik, Geschichte und Deutsch
- 1994-1998 Grundstudium der Geophysik an der Universität Bremen; Abschluß: Vordiplom
- 1998-2002 Hauptstudium der Physik an der Carl von Ossietzky Universität Oldenburg; Diplomarbeit zu dem Thema: Transiente Störstellenspektroskopie an  $\text{Cu}(\text{In,Ga})(\text{S,Se})_2$ -Dünnschichtsolarzellen
- seit 2003 Doktorandenstudium an der Carl von Ossietzky Universität Oldenburg

## **Eidesstattliche Erklärungen**

Hiermit erkläre ich, dass ich diese Arbeit selbständig verfasst und nur die angegebenen Hilfsmittel benutzt habe. Die Dissertation wurde weder in Teilen noch in Gänze veröffentlicht.

Kassel, den 30.04.2008

(Arne Wessel)